

Studying the Meander Bend Migration of the Arial Khan River

Jannatul Ferdoush

Roll No.: 0416282035

MASTER OF SCIENCE IN WATER RESOURCES DEVELOPMENT



INSTITUTE OF WATER AND FLOOD MANAGEMENT

BANGLADESH UNIVERSITY OF ENGINEERING AND TECHNOLOGY

March, 2022

**INSTITUTE OF WATER AND FLOOD MANAGEMENT
BANGLADESH UNIVERSITY OF ENGINEERING AND TECHNOLOGY**

The thesis titled ‘**Studying the Meander Bend Migration of the Arial Khan River**’ submitted by Jannatul Ferdoush, Roll No. 0416282035P, Session April 2016, has been accepted as satisfactory in partial fulfillment of the requirement for the degree of M. Sc. in Water Resource Development on 20 March, 2022.

BOARD OF EXAMINERS



.....
Dr. Mohammad Shahjahan Mondal
Professor
Institute of Water and Flood Management
Bangladesh University of Engineering and Technology, Dhaka

Chairman
(Supervisor)



.....
Dr. A.K.M. Saiful Islam
Professor
Institute of Water and Flood Management
Bangladesh University of Engineering and Technology, Dhaka

Member
(Ex-Officio)



.....
Dr. G.M. Tarekul Islam
Professor
Institute of Water and Flood Management
Bangladesh University of Engineering and Technology, Dhaka

Member



.....
Dr. Shampa
Assistant Professor
Institute of Water and Flood Management
Bangladesh University of Engineering and Technology, Dhaka

Member

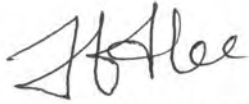


.....
Dr. Rabin Kumar Biswas
Superintending Engineer
Directorate of Planning 3
Bangladesh Water Development Board, Dhaka

Member
(External)

CANDIDATE'S DECLARATION

It is hereby declared that this thesis or any part of it has not been submitted elsewhere for the award of any degree or diploma.



.....

Jannatul Ferdoush

Dedicated to

My mom and sons: my inspiration and strength

Acknowledgement

First and foremost, all praises are to the Almighty Allah, for His shower of graces and blessing throughout the long journey of this study.

I would like to express my sincere gratitude to my thesis supervisor, Dr. Mohammad Shahjahan Mondal, Professor, Institute of Water and Flood Management (IWFM), Bangladesh University of Engineering and Technology (BUET), for giving me the opportunity to do this study with him and providing continuous support, advice, and guidance all through the research. His dynamism, sincerity, and way of teaching have inspired me to learn each and every new thing in my research works.

I would like to thank the members of the Board of Examiners: Dr. G.M. Tarekul Islam, Professor, Dr. A.K.M. Saiful Islam, Professor and Director, Dr. Shampa, Assistant Professor from IWFM, BUET and Dr. Robin Kumar Biswas, Superintending Engineer, Directorate of Planning from Bangladesh Water Development Board (BWDB), Dhaka for their useful comments and suggestions.

Special thanks to the officials of the BWDB and the local people for providing facilities during the field visit and helping me with the collection of the field data and necessary documents for the research.

I am extremely grateful to my family members, especially to my mother for her prayers, sacrifices, and caring for my education. I want to remember my late father, who always inspired me and was very optimistic about my higher education and research.

Finally, I would like to mention my two lovely kids, the sources of all happiness in my life. They provide me with continuous encouragement and faith to resolve all hard times. They also had lots of sacrifices behind finishing my study.

Abstract

The Arial Khan is a meandering river, flowing in a south-eastward direction after bifurcating from the right bank of the Padma River. Incessant channel shifting and bend migration are very common phenomena for this river. This study investigates multiple time- and bend-scale morphological characteristics of the river. The river planform analysis and bend geometry estimation from remotely sensed satellite images have been conducted by GIS and CAD software. The time-series analysis is based on selected seven years of image processing for a period of 49 years: 1972, 1980, 1988, 1999, 2007, 2017, and 2021. Among these seven years, 1972, 1980, 1999, 2007, and 2021 are represented as the years when the offtake of the river arrives at the ultimate downward (southwest) and upward (northeast) points alternately, and 1988 and 2017 are the interim years. Thus, the river takes 19 years on an average to shift the offtake at the ultimate downward and 8 years at the ultimate upward position. The shifting of the offtake with time is correlated with the morphological changes of the offtake, i.e., alteration of the offtake bed elevation and in-front bar formation, which control the diversion of flow from the parent river into the Arial Khan. Thus, the offtake influences the dynamic behavior of the river morphology in terms of sinuosity, bend geometry, and bend migration. During downward shifting of the offtake, the sinuosity so as the length of the river increases, though the 4-6 km linear path of the river gets subtracted due to this shifting. Again, the reduction of sinuosity and length occurs during upward shifting of the offtake, even though an extra 5-7 km linear distance of the river path is added due to this shifting. The average sinuosity of the river is 1.78, the highest and lowest values of it have been found as 1.62 and 1.95 in the years 2021 and 1980 respectively. The river is divided into the three reaches: upper, middle, and lower based on the spatial variability of floodplain, morphology, and bend migration pattern and direction. The upper reach has a comparatively wide active floodplain and valley, having loosely compacted soil. The average water depth and thalweg elevation of the river increase towards downstream; currently the bed slope of the river is 0.037 m/km. The river width increases successively from the upper reach to the lower reach with the average value of 237 m, 277 m, and 320 m respectively. The sinuosities of the upper two reaches are lower compared to the lower reach, with values of 1.60, 1.55, and 2.11 respectively. A total of 37 characteristics bends from the three consecutive reaches have been selected from different study periods. In the upper reach, downstream migration

dominates where four out of six cutoffs have occurred during the study period. The lateral migration dominates in the middle and lower reaches; each of the reaches contains only one cutoff. The migration direction of the upper two reaches is not consistent but it is unidirectional in the lower reach. Among the six significant bend cutoffs, the chute and neck cutoffs are equal in the number of three. Before cutoff, the bends adopt a shape of curvature with an average radius of 501 m and all radii range between 218m and 817m. The average lifetime of bends before cutoff or channel straightening is 24 years, though reach-wise the lifetime successively increased towards downstream to 18 years, 25years, and 32 years respectively in the three reaches. All modes of migrations: expansion, rotation, translation, and extension persist in the river. In most cases, newly generated simple symmetrical bends are converted to asymmetrical, elongated, or compound shapes. The average radius of the bends of the Arial Khan River is 921m, though reach-wise the radii vary as 775m, 1127m, and 883m respectively for the upper, middle, and lower reaches. The upper reach is more migration prone; here the average migration rate is more than double of the other two reaches, which are 108 m/y, 42 m/y, and 46 m/y respectively. The higher migration rate of 70-80 m/y was found during the time period of 1981-1999, and for the rest of the periods, the rates were within the value of 45-50 m/y. The Arial Khan River sustains a particular relationship between migration rate and relative curvature; maximum migration rate prevails for the bends with relative curvature of 1.5-3.5 and having a peak value of around 3.0. The average values of relative curvature for the bends of the upper and lower reaches are 3.5 and 3.1 respectively, which fall within the estimated range. But for the middle reach, the value is 4.8, which is beyond the range. In time-scale, the relative curvatures are within the estimated range of 1.5-3.5 during the time period of 1972-1999, and the values are beyond this range during 2000-2021. Chronologically the change of morphology in terms of bend migration of the Arial Khan has been found as upper reach > lower reach > middle reach and in time-scale as 1972-1999 > 2000-2021. The overall feature of the river from 1972 to 2021 reveals that a significant increase in sinuosity and reduction in river width and aspect ratio have occurred. The migration rate of the river fluctuates from time to time, but the trend has declined slightly. The frequency of bend cutoff has reduced notably, the last cutoff occurred in 2004 in the Arial Khan River. The absence of local sediment and discharge data are the major limitations of this study. Otherwise, this study can be considered as a good attempt toward multiple time- and bend-scale analyses of a meander river of Bangladesh.

Table of Content

CHAPTER ONE: INTRODUCTION	1
1.1 Background of the Study.....	1
1.2 Objectives.....	3
1.3 Scope and Limitations of the Study	3
1.4 Organization of the Thesis	4
CHAPTER TWO: REVIEW OF LITERATURE	6
2.1 Introduction.....	6
2.2 Studies on River Bend Migration in the World	6
2.3 Studies on River Bend Migration in Bangladesh.....	14
2.3.1 Study on the Padma River.....	14
2.3.2 Study on the Gorai, Madhumati and Dhaleshwari Rivers	15
2.3.3 Study on the Arial Khan River.....	16
2.3.4 Study on other Meander Rivers.....	18
CHAPTER THREE: STUDY AREA.....	19
3.1 Introduction.....	19
3.2 Arial Khan River System	19
3.3 General Hydrology of the River.....	20
3.4 General Morphology of the River.....	22
3.5 Arial Khan Offtake.....	24
CHAPTER FOUR: METHODOLOGY AND DATA COLLECTION	27
4.1 Introduction.....	27
4.2 Time-series Remotely-sensed Data.....	27
4.3 Ground-Truthing	29
4.4 Data for Offtake Hydro-morphology	30
4.4.1 Development of rating curve for the offtake station	30
4.4.2 Determination of bed level change at the offtake	32
4.4.3 Evaluation of the offtake shifting.....	32
4.5 Assessment of River Planform.....	32
4.5.1 Bankline delineation.....	32

4.5.2	Selection of river reach	33
4.5.3	Existing river sections	34
4.5.4	Measurement of river width	35
4.5.5	Measurement of river depth and slope	35
4.5.6	Estimation of river thalweg	35
4.6	Determination of meander geometry	35
4.6.1	Selection of meander bend	36
4.6.2	Identification of crossings/ inflection point and bend apex	36
4.6.3	Estimation of radius of curvature	38
4.6.4	Selection of meander belt	38
4.6.5	Measurement of meander length and meander width	39
4.6.6	Assessment of mode of bend migration	40
4.6.7	Calculation of rate of bend migration	40
4.7	Bend Migration Prediction	41
4.7.1	Time-sequence maps and extrapolation method	42
4.7.2	Radius of curvature	42
4.7.3	Angle of migration	43
4.7.4	Magnitude of centroid of the arc migration	43
4.8	Field Assessment	43
4.8.1	B3 bend from R1 reach	44
4.8.2	B17 bend from R2 reach	44
4.8.3	B22 bend from R3 reach	44
CHAPTER FIVE: RESULTS AND DISCUSSION		46
5.1	Padma River near the Offtake of Arial Khan River	46
5.2	Diversion of Discharge into the Arial Khan River	48
5.3	Temporal Change of the Offtake Hydro-morphology	49
5.3.1	Offtake shifting	49
5.3.2	Thalweg position of the offtake	50
5.3.3	Discharge at the offtake station	50
5.3.4	Tidal influence on river width near offtake station	52
5.4	Arial Khan Channel Geometry	53
5.5.1	General stability of river reach	53
5.5.2	Length of river	54

5.5.3	Width of river.....	55
5.5.4	Depth and slope of river in a recent year	58
5.5.5	River thalweg	59
5.5.6	Sinuosity of the river.....	60
5.5.7	Channel aspect ratio and river migration	62
5.6	Arial Khan Bend Geometry	64
5.6.1	Bend Generation.....	65
5.6.2	Modes of migration of different bends.....	67
5.6.3	Radius of curvature of bend	70
5.6.4	Bend cutoff.....	70
5.6.5	Relative curvature of bend and reach.....	72
5.6.6	Bend migration and migration rate	73
5.7	Some Developed Relationships	76
5.7.1	Width, depth, and flow velocity vs. discharge	76
5.7.2	Migration rate vs. relative curvature	77
5.7.3	Relationship between meander length and river width.....	79
5.7.4	Relationship between meander length and discharge	80
5.7.5	Relationship between meander width and river width.....	81
5.7.6	Relationship between meander width and discharge	82
5.8	Prediction of Bend Migration.....	82
5.8.1	Bend B3 of reach R1	83
5.8.2	Bend B17 of reach R2.....	85
5.8.3	Bend B27 of reach R3	87
5.9	Observations on Existing Conditions of Bends Based on Field Visit.....	88
5.9.1	Bend B3 of reach R1	88
5.9.2	Bend B17 of reach R2.....	89
5.9.3	Bend B22 of reach R3	90
5.10	Discussion	90
5.10.1	Offtake shifting and change of river planform.....	91
5.10.2	Spatial variability of planform and morphology.....	93
5.10.3	Temporal variation in the planform and morphology.....	95
5.10.4	Natural and anthropogenic impact on bend-scale change of river.....	97
5.10.5	Bend migration prediction.....	98

CHAPTER SIX: CONCLUSIONS AND RECOMMENDATIONS99

6.1 Conclusions 99

6.2 Recommendations 102

REFERENCES..... 104

APPENDIX A 114

APPENDIX B 124

APPENDIX C 127

APPENDIX D 129

List of Tables

Table 3.1:	Existing bank protection work of the Arial Khan River.....	20
Table 4.1:	Landsat images used for the analysis	28
Table 5.1:	The Padma River section near the Arial Khan River offtake during the study period.....	46
Table 5.2:	Offtake morphology, (-) sign indicates downward shifting of the offtake.....	49
Table 5.3:	Rating curve equation (2008-2019).....	51
Table 5.4:	Generation of the bends in the Arial Khan River in different time periods.	66
Table 5.5:	Shape of different bends and their modes of migration.	68
Table 5.6:	Types of cutoff and radii of curvatures at the cutoff bends.....	71
Table 5.7:	Average migration in different time period.....	73
Table 5.8:	Actual and predicted R_c , θ_c and D_c for bend B3	84
Table 5.9:	Actual and predicted R_c , θ_c and D_c for bend B17	86
Table 5.10:	Actual and predicted R_c , θ_c and D_c for bend B27	87
Table 5.11:	Values of the parameters from three reaches: upper, middle and lower reach...	94
Table 5.12:	Values of the parameters for the years of 1972, 1980, 1988, 1999, 2007, 2017 and 2021.	96

List of Figures

Figure 2.1:	Modified Brice classification of meandering channels (Lagasse et al., 2004).....	9
Figure 3.1:	Daily water level of the Arial Khan of years (a) 1991 and (b) 2011.....	21
Figure 3.2:	Daily discharge of the Arial Khan of years (a) 1991 and (b) 2011.	22
Figure 3.3:	The Arial Khan River system.....	23
Figure 3.4:	Oxbow lake and meander scars of the Arial Khan River floodplain [Google Earth].....	24
Figure 3.5:	Offtake shifting of the Arial Khan River in different time intervals, (→) indicates direction of previous to next location of offtake.	25
Figure 4.1:	Ground truthing of image from the identified locations of bend B3.	29
Figure 4.2:	Stage (G) vs. discharge (Q) plot for the gauge reading at offtake of the Arial Khan River.	31
Figure 4.3:	The Arial Khan River divided into three reaches: R1, R2 and R3.	33
Figure 4.4:	BWDB sections of the Arial Khan River.	34
Figure 4.5:	Some characteristics bends of the Arial Khan River from the years of 1972 and 2021.....	37
Figure 4.6:	Inflection points and apex of a selected bend of the Arial Khan River.....	38
Figure 4.7:	Typical meander belt with meander geometry (Lagasse et al., 2004).....	39
Figure 4.8:	Migration of bend from initial year (Y1) to final year (Y2).....	41
Figure 4.9:	Field visit in three bends B3, B17 and B22 at R1, R2 and R3 reaches	45
Figure 5.1:	The meandering channel and mid-channel bar formation of the Padma and the downward shifting of the offtake in (a), (c), (e) and (f); straight channel and upward shifting of the offtake in (b) and (d).	47
Figure 5.2:	The concentration of total suspended matters in the Padma River in the period 1991–2019, and the red area represents the duration of La Niña (Zheng et al., 2021).	48
Figure 5.3:	Temporal change of bed elevation at Offtake-AKU1	50
Figure 5.4:	Maximum discharges (Q_{max}), average discharges (Q_{avg}) and minimum discharges (Q_{min}) of the Arial Khan River at Offtake.	52
Figure 5.5:	River water width for measured water level (W) and tidal water level (W' and W'').	53
Figure 5.6:	The changes of lengths of three reaches - R1, R2 and R3, and the entire river during different periods.	54
Figure 5.7:	The relationship of offtake shifting and change of river length.	55

Figure 5.8:	Temporal change of river width of (a) entire river and (b) different reaches - R1, R2 and R3.....	56
Figure 5.9:	River width measured along (a) the entire length and (b) at 37 bend crossings and apex points from upstream to downstream.	57
Figure 5.10:	The average water depth at the sections corresponding to the three river reaches: R1, R2 and R3 in 2019.....	58
Figure 5.11:	Change of maximum depth/ thalweg at different sections of the R1 reach.	59
Figure 5.12:	Change of maximum depth/ thalweg at different sections of the R2 reach.	60
Figure 5.13:	Average thalweg elevation at all the sections, estimated from 1972 to 2019.....	60
Figure 5.14:	The change of sinuosity (SI) in three reaches R1, R2 and R3 and in entire river in different time periods.....	61
Figure 5.15:	The relationship of offtake shifting and change of river sinuosity.....	62
Figure 5.16:	Time-scale change of the average aspect ratio and migration rate of the Arial Khan River.	63
Figure 5.17:	The dimensionless aspect ratio (W/D) and average migration rate at different sections and reaches of the Arial Khan River.....	64
Figure 5.18:	Bend geometry of the Arial Khan River.....	65
Figure 5.19:	Age of each bend and reach-wise average age of the bends.	67
Figure 5.20:	R_C value for different bends of the Arial Khan River.....	70
Figure 5.21:	Different modes of migration in the Arial Khan River; (a) translation, (b) rotation, (c) extension, (d) expansion, (e) neck cutoff, (f) chute cutoff, (g) straight and (h) downward shifting.	71
Figure 5.22:	The relative curvature (R_C/W) of the three reaches and the consecutive bends of the Arial Khan River.....	72
Figure 5.23:	The migration rate (M_r) of different bends of different river reaches of the Arial Khan River (1972-2021).	74
Figure 5.24:	The migration rate (M_r) of the Arial Khan River and three reaches R1, R2 and R3 of the river in different time periods.	75
Figure 5.25:	The relationship of W, D and U to changing Q at the station of the Arial Khan River offtake.	77
Figure 5.26:	Migration rate (M_r) and relative curvature (R_C/W) along the Arial Khan River of heterogeneous floodplains. Maximum M_r occurs at $R_C/W= 1.5$ to 3.5 with the peak at ~ 3.0	78
Figure 5.27:	Average R_C/W of the Arial Khan River in selected years. The R_C/W values within the range 1.5-3.5, indicating higher migration rate... ..	79

Figure 5.28:	Relationship between M_L and W of the Arial Khan River.....	80
Figure 5.29:	Relationship between M_L and Q of the Arial Khan River.....	81
Figure 5.30:	The relationship between Mw and W of the Arial Khan River.....	82
Figure 5.31:	The relationship between Mw and Q of the Arial Khan River.....	83
Figure 5.32:	Actual and predicted migration of bend B3... ..	85
Figure 5.33:	Migration prediction for bend B17.....	86
Figure 5.34:	Migration prediction for bend B27.....	88
Figure 5.35:	Shape of the bend before and after the Madaripur town protection project in 1987.....	89

Abbreviations and Acronyms

CAD	Automatic Computer Aided Design
BFC	Best-fitting Circle
BUET	Bangladesh University of Engineering and Technology
BWDB	Bangladesh Water Development Board
D	River Water Depth
D _c	Magnitude of Centroid of the Arc Migration
D/W	Channel Aspect Ratio
G	River Stage
GBM	Ganges Brahmaputra Meghna
GIS	Geographic Information System
IWFM	Institute of Water and Flood Management
LM	Landsat Multispectral Scanner
L _r	River Length
L _v	Valley Length
MSS	Multispectral Scanner
M _L	Meander Length/Wavelength
M _r	Migration Rate
M _w	Meander Width
MNDWI	Modified Normalized Difference Water Index
NDWI	Normalized Difference Water Index
NIR	Near-Infrared
OLI	Operational Land Imager
PWD	Public Works Department
Q	River Discharge
Q _{avg}	Average Discharge
Q _{max}	River Maximum Discharge
Q _{min}	River Minimum Discharge
R1	Upper Reach
R2	Middle Reach
R3	Lower Reach
R _c	Radius of the Curvature
R _c /W	Relative Curvature
θ _c	Angle of Migration
SI	River Sinuosity

TM	Thematic Mapper
TSM	Total Suspended Matter
U	Flow Velocity
W	River width
WL	Water Level
USGS	United States Geological Survey

CHAPTER ONE

INTRODUCTION

1.1 Background of the Study

The dynamic behavior of any natural river system is an inherent and common phenomenon for a region. The continuous evolvement and adjustment of this system are articulated to the change of the earth-atmosphere system. When a single-thread channel of any river system is winding across its floodplain or landscapes as a series of different sizes and shapes of reversing curves, it leaves a footprint of a course with a zigzag pattern known as a meander river.

When water is allowed to flow freely over a plain alluvial soil surface having a certain slope, it advances by posing an oscillatory path, which is the base of a bend formation of the meander river. As a result of super-elevation in a curve path, lateral slope and lateral pressure gradient develop in the bend. On the other hand, the flow of water through a bend produces centrifugal acceleration, resulting relatively high velocity flow field towards the outer bank. These two mechanisms are responsible to develop secondary circulation along the cross-section of the bend, which is near the bed towards the inner bank and near the free surface towards the outer bank. Thus, in a typical meander river, the flow field is responsible for erosion to take place in the outer/concave bank of a bend, transportation of this eroded sediment, and then deposition of sediment near the next inner/convex banks where the stream power is low enough to be settled down the sediment. The whole process governs the migration of bends of a meander river, which can be said otherwise that migration of the bend is strongly co-related with the curvature of the bend. Bend migration is a continuous process where erosion and deposition take place simultaneously at the bed and bank of the alluvial meander rivers. Through the migration process, the natural meander river tends to freely adjust its course within the entire valley width.

The people living alongside the meandering rivers like the Arial Khan and any other rivers of Bangladesh have experienced river migration over time. The magnitude of this migration is excessive near river bends which leads to loss of land and property and may sometimes be the cause of hazards to infrastructure in the vicinity of the river. Hence, a

bend-scale migration study of the river is very important in connection with the riverbank stabilization, navigation, flood control, and the development of water resources projects.

The Arial Khan River exhibits a great extent of spatial and temporal variability in meander intensity. The spatial variability is largely attributed to the non-uniform distribution of the bank materials and changes in flow conditions due to the several entrances and exits of tributaries and distributaries along the entire length of the river (Winkley et al., 1994). As an active meandering river, bank erosion, channel shifting, and bend migration are very common phenomena for this river, especially in the upper reach, directly influenced by the parent River Padma. But the lower reach has the influence of tidal flow and is relatively stable, homogeneous, and less complex in terms of bend characteristics. Though there have been a few studies on morphological characteristics of the Arial Khan River (Biswas et al., 2018; Akter et al., 2013; Mamun, 2008; Hossain et al., 2007; Winkley et al., 1994; Ashrafuzzaman, 1992), the meander bends characterization and migration did not receive due attention. The controlling factors involved in the bend migration process were not also investigated thoroughly and systematically. Meandering in a river appears due to bank instability, which is the result of bend migration (Ikeda et al., 1981). This bend migration depends on a number of factors including discharge, water-surface slope, channel width, and depth, bend geometry, and large floods (Nicoll and Hickin, 2010; Heo et al., 2009; Hooke, 2006). On the other hand, for the Arial Khan River, the river training works have imparted bank stability and thus influenced the meandering nature to some extent. It is necessary to investigate the linkage of these factors to bend migration in terms of lateral and downstream migration of the river.

The Ganges, Brahmaputra, and Meghna Rivers exhibit year-to-year extreme variation in discharge and sediment load, which often bring changes into planform and the offtake morphology of its distributaries as well. Thus, the hydro-morphology of a distributary river is not only dependent on the discharge of the parent river but also on the flow features which are controlled by the offtake morphology of the river.

The satellite image analysis revealed that the Padma River near the Arial Khan Offtake had changed its course a number of times from meandering to straight and again from straight to meandering during the period of 1960-2003 (Nippon Koei Co., 2005). Though the temporal changes in the offtake morphology of the river were studied (Mamun, 2008),

the reasons for such changes were not investigated. Moreover, it is anticipated that the change in course of the Padma River will have certain influences on the position of the Arial Khan Offtake and planform geometry within this river. Thus, it would also be interesting to investigate the role of the Padma River on the evolution of offtake morphology and meander bend migration in the Arial Khan River.

1.2 Objectives

The explanation and interpretation of morpho-dynamics of an alluvial meander river is involved with the migration of progressive bends, which is the resultant of interaction between eroding force from flow (water and sediment) and resisting force from bed and bank of the river. In simple words the study focuses on the morphological responses of the river in terms of bend migration against the disparity of hydrology and offtake morphology of the river.

The specific objectives of this study are:

- i. To analyze planform of the Arial Khan River using open-source satellite images and to assess its meander bend pattern and migration; and
- ii. To investigate the relationships of meander bend migration with flow, bed and bank characteristics, and offtake shifting of the river.

1.3 Scope and Limitations of the Study

The main focus of the study is to understand the river morpho-dynamics in time- and bend-scale, i.e., the change of migration mode and rate of different bends with time and establish relationships of bend geometries for the Arial Khan River inspired and followed by different well-known empirical relationships. The morphological responses with respect to river flow are also investigated in this study. The controlling factors of temporal change of morphology are correlated with the offtake shifting, which is very common for most of the meandering tributaries of the main rivers of Bangladesh. Therefore, the analysis procedure of this study is applicable to any other meandering river in Bangladesh.

Sometimes the studies on the braided river in some particular cases involve the existence of bend features and bank migration/ shifting, where this study may give a good guideline. Hence, this study will help in better planning and designing of structural interventions on and around the Arial Khan and other rivers of Bangladesh as well.

The study has some limitations which are listed as follows:

- The morpho-dynamics of a river are associated with the morphology and hydraulics of the river and some geological parameters as well. The geological parameters are not considered in this study.
- The satellite images of the monsoon season all through the study period were not possible to incorporate in this study due to the unavailability of good quality and cloud-free images.
- Access to the intended location of the bank was not possible during the field visit.
- The discharge variations due to internal tributaries and distributaries were not considered in this study.

1.4 Organization of the Thesis

This thesis is organized into six chapters which are described in the following:

Chapter One contains the state of condition as background and specific objective of the study. It also contains scope by means of prospects and possibilities are described and the limitation: different constraints are mentioned.

Chapter Two provides the related literature on the meander study. This chapter has two sections; the first section presents the literature on bend migration of the meander river in a world context and the second section covers the same topic but in the Bangladesh context.

Chapter Three is the overview of the study area. It consists of a brief description of the Arial Khan River system along with the river offtake, general hydrological condition, and morphology.

Chapter Four states the step-by-step method and technique applied in the study. The data collection and its interpretation, some calculation procedure, and the plan and purpose of the field survey are depicted.

Chapter Five contains the results and discussions on the time- and bend-scale migration analysis of the river. The factors which control the characteristics of the river on bend-scale are also explained in this chapter.

Chapter Six the last chapter of this study contains the conclusion and recommendation, where the ending is drawn through mentioning the key findings of the study and some suggestions and advice for the further proceeding of the research.

CHAPTER TWO

REVIEW OF LITERATURE

2.1 Introduction

Bend-scale analysis of meander rivers has been attaining great appeal to researchers, as the dynamic behaviors of meander rivers are largely dependent on the nature of the successive bends. For example, the study of channel property characterization, change of river planform, quantification of lateral and downstream migration, and its future prediction, all are accomplished with the help of local and time-scale bend analysis. Meander river exists all over the world in different geology and hydro-morphological settings, among which a significant number of rivers are flowing through alluvial floodplains. As a result, in the world context a good number of literatures on bend analysis of meandering rivers are found and every year new studies with innovative ideas have enriched this number. Bangladesh is a riverine country, where the meander rivers flow almost every part of this country. As a result, the literatures on the meander river within Bangladesh territory cover significant numbers. The studies from the world and Bangladesh perspectives, relevant to this thesis are discussed separately in the next two sections.

2.2 Studies on River Bend Migration in the World

The initiation of bend generation in a straight channel and its evolution involved in the physical processes of energy dissipation, least work by river, and minimization of the variability of essential properties, i.e., depth, velocity, and local slope (Langbein and Leopold, 1966). Thus, the meander river is the most stable form among all other types of the river where the erosion and deposition processes are resulting to occur the bend and bend migration. The concept of bend migration, very popular as the “bend theory”, was first proposed by Ikeda et al. (1981). The theory has described that the bend instability is resulting from the erosion at the outer bank by relatively high flow velocity and conversely deposition at the inner bank by deflected flow velocity. Based on this theory, researchers of different branches have carried out an in-depth study of the meander river system.

In literature two types of bend analysis have been found: qualitative and quantitative, both are important to develop a concept on temporal characteristics changes and migration of bend, assessment of different controlling factors behind these changes, and establishment of correlations among the factors. Though, the study has suggested that all correlations are not equally applicable to all meander rivers (Schumm and Thorne 1989), especially for large rivers flowing in alluvial floodplains. Because these types of floodplains generally develop with horizontal and vertical heterogeneity of sedimentation in a relatively long geological time-scale. Again, migration is a discontinuous process (Chang, 1992); it takes place at individual bends for a specific time and rate. Thus, the response of all bends against the controlling factors along the entire river reach may not be the same.

However, several controlling factors have been discussed in different studies. Shen (1971) and Callander (1969) have summarized some of the basic factors which influence the bend formation, change of shape with time, and migration as well, which are: the presence of secondary current, hydrologic and topographic conditions, lateral disturbance - caused by differences between the materials of left and right banks, and erosion and deposition processes along the banks at different rates in different times. When one or more factors get changed spatially or temporally, the river receives these changes by continuous adjustment of its course to maintain a state of equilibrium between controlling factors and river planform. Thus, the adjustment renders a configuration to the river planform in such a way that it maximizes the efficiency or conveyance capacity of the river and minimizes the works of the river during downstream conveyance of flow (Parish, 2004).

The study by Schumm (1977) has described that the planform changes of a river occur in two different ways: by (a) intrinsic factors, where the river works itself for these types of inherent changes, i.e., cutoffs, channel migration, and avulsion and (b) extrinsic factors, when external factors are imposed, i.e., changes in sediment supplies from water-shade of the entire river system and human intervention. The discharge is considered the most influencing factor to provide the shape of a bend and thus the alteration of the planform geometry. A simple and homogeneous type bend configuration generally occurs when there exists only one influencing discharge; whereas more than one influencing discharges are responsible to provide a configuration of compound bend (Parish, 2004). The erosion of the outer bank depends on the resisting strength of the bank provided by the bank material. According to Hickin and Nanson, (1984) fine sediment has high cohesive

strength and gravel has high inertia force; the existence of both materials at the outer bank of the channel gives higher resistance to erosion compared to the resistance from the material of fine-sand range. A similar statement was given by Schumm (1977): the channels of fine sediment are narrow, deep, and sinuous and the sandy channels are wide, shallow, and relatively straight. Again, the channel having flow with reduced sediment load also tends to erode and increase sinuosity with time (Shen et al., 1979).

The study of Lagasse et al. (2004) suggested that, before analysis of bend migration, the meandering channel should be classified according to meander classification approaches which have been proposed in different literatures. Because the channel classification provides basic insights about the bend instability from aerial photo, geometric maps, or remote-sensing imagery, it does not require excessive field data and observation. There are three planimetric properties: wavelength, sinuosity, and degree of irregularity, which are used to characterize the planform of the meander river (Ferguson, 1975).

A good number of meander river classifications are found in literatures. The most popular way to classify the meander river is by its sinuosity. According to Brice (1975), rivers with sinuosity values of 1-1.05 are described as straight, of 1.06-1.5 as sinuous and the sinuosity values greater than 1.5 are referred to as meandering. Again, the author classified the meander river into nine major categories (from A to G) considering the phase of the flow, channel width at the bend, the existence of a point bar, and chute channel. Several studies (Thorne, 1992; Lagasse et al., 2004) separately have adapted the Brice classification, which is termed as modified Brice classification. One modified Brice classification proposed by Lagasse et al. (2004) is given in Figure 2.1. Here, two more channel classes B2 and G2 are added. In this classification scheme in Figure 2.1, equal-width rivers are in classes B1 and G1, which are relatively stable. Class A consists of equal-width, deep, or incised channels. Class F is a class of compound “wandering” low-water channels, with wide bars. The channels B1, G1, and F are either stable or migration is highly unpredictable. Except for these three classes of the channel, the rest of the channel classes are generally considered in the channel migration study.

The meander river patterns are again classified depending on the shape of the bend as regular or irregular, and simple or compound (Chitale, 1970). In a regular meander pattern, all bends are in a series of similar shapes, frequencies, and radii. But when bends are

deformed in shape, amplitude, and wavelength, then the meander patterns are called irregular. Non-homogeneous alluvium, variable discharges from tributaries, and water loss to permeable strata are responsible for the meander irregularity. Free meander occurs when the channel does not face any constraints from valley walls to be migrated laterally, whereas the confine meanders are those that are unable to fully develop the planform geometry, as parallel valley walls obstruct channel migration.

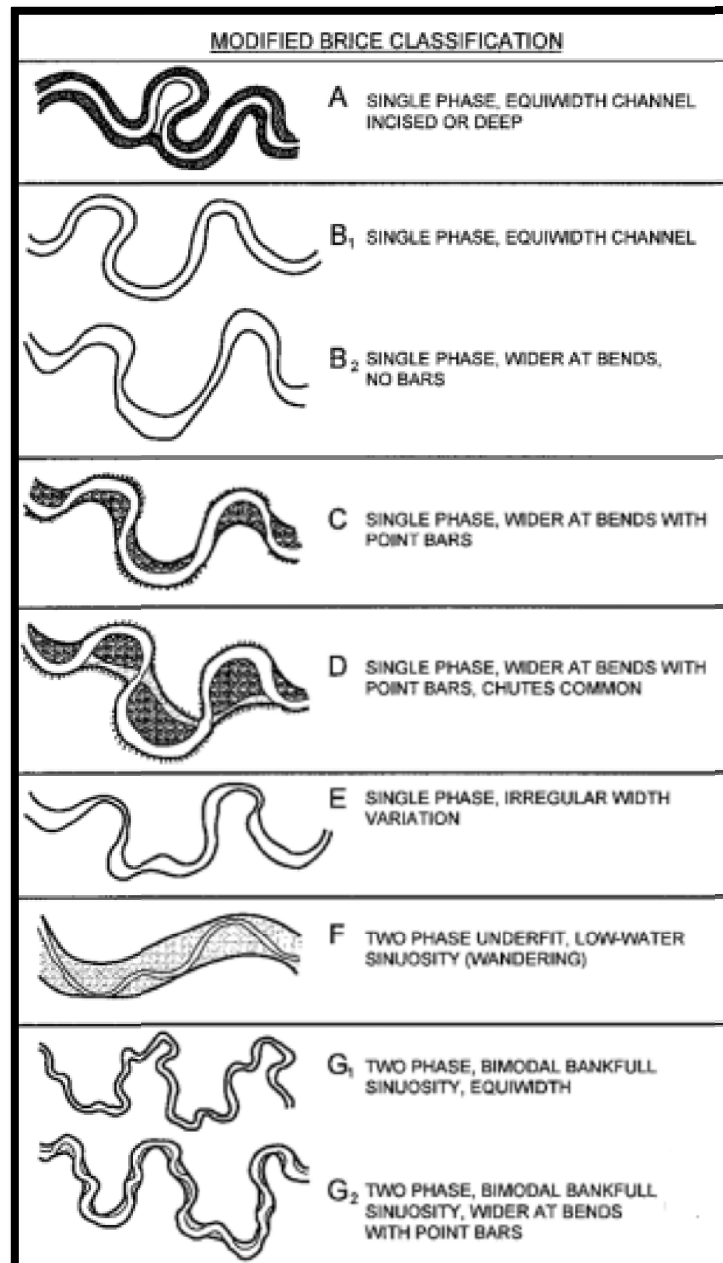


Figure 2.1: Modified Brice classification of meandering channels (Lagasse et al., 2004).

The bends of the natural meander river in the alluvial flood plain always evolve and change their shape with time during three stages of bend formation: initiation, growth, and end-stage of bend before final abandonment through different modes of cutoff. The ultimate result is the temporal migration of bend. Thus, at the field level, bends are not in idealized simple symmetrical shape and form sine-generated curves, but mostly asymmetrical with varying wavelength; best fitted circular arcs are frequently used to define their shape during analysis. Asymmetrical shape develops in bend when the flow of discharge from upstream attacks to the location slightly downstream of the bend apex in a newly developed symmetrical bend, resulting in bend erosion and sometimes deepest scour at toe also occurs and which causes mass failure of the bank. Thus, that bend gets distorted from a symmetrical shape and forms a skewed shape in the down-valley direction.

The above meander classification, which is described in Figure 2.1, reveals that active meander rivers have point bars, which play an important role in giving the shape of consecutive bends. The study of Dietrich and Smith (1983) supports this statement, where authors have used a mechanism term as “bar push”. When the sediment supply is sufficient, the inner bank point bar accumulates more sediment, which pushes the path of high-velocity flow towards the outer bank and increases the shear stress, which triggers the erosion along with the outer bank and bend migration as well, which is called “bar push”. Contrarily, lack of sediment flow causes a rate of faster erosion at the outer bank than the rate of inner bank deposition. In this case, the river migrates such a way it seems that the outer bank influences pull the inner bank, termed as “bank pull”. Another study (Constantine et al., 2014) has pointed out that the river migration rate increases with the increase of sediment supply in the flow.

After classification of the channel, bend-scale analysis of individual bend is performed using different analysis techniques, depending on the aim and outcome of the studies. Some studies (Yousefi et al., 2021; Bag et al., 2019) have used a single bend, whereas others (Guo et al., 2021; Mason and Mohrig, 2019; Mirzaee et al., 2018) have dealt with several characteristics of bends of a particular river reach to understand morphological characteristics changes and to explore the impact of sudden natural events or man-made intervention on a river. When the empirical relationships among the parameters are intended to establish in the bend study, some authors (Hudson and Kesel, 2000) have used

a single river with long-term data or multiple rivers (Donovan et al., 2021; Sylvester et al., 2019; Nicoll and Hickin, 2010; Hickin and Nanson, 1984) within similar geomorphological settings. Though, other studies have suggested (Hudson and Kesel, 2000; Hooke, 1987), rivers in a wide range of geomorphological settings should be incorporated to establish a general meander theorem. Long-term historical data, images from remotely sensed and aerial photographs, topographic maps, and the geographic information system (GIS) are very common and have been frequently used in most the studies.

One of the important studies on lateral migration of river bends is by Hickin and Nanson (1984), where 189 bends of different rivers with different sediment characteristics were studied. The authors used 23 sets of field data and aerial photographs from 23 different rivers of similar hydro-morphological characteristics and some common parameters such as stream power per unit bed area, the resisting force for migration per unit boundary area, bank height, the radius of curvature of bend, and channel width to establish a relationship between migration rate per unit river width (relative migration, M/W) and bend curvature ratio (radius of curvature of bend / river width). Their findings were remarkable, which suggested that the maximum migration rate occurs in the bend when the value of bend curvature ratio is between 2 and 3; beyond this range, the migration rate decreased significantly. Again, the lateral migration of sand bed and the bank was maximum, and it was minimum in the material of gravel and clay, as the co-efficient of resistance to lateral erosion was found maximum in gravel and clay and minimum in the sand. The study has suggested that for non-cohesive sediment (from coarse to fine sand), both cohesive force and inertial force give a minimum resistance against lateral erosion, but these combined forces for cohesive material are comparatively high and give more resistance.

The relation between migration and channel curvature was first proposed by Bagnold (1960). Here, the author set up a laboratory experiment with pipe flow and found that a minimum resistance of pipe appeared within bend curvature ratio between 2 to 3.

Recent years' studies (Donovan et al., 2021; Sylvester et al., 2019) have shown that the bend with high curvature migrates at a high rate, which has deviated from the previously well-established concept: maximum rate of migration is associated with the bend of intermediate curvature (Hickin and Nanson, 1984; Bagnold, 1960).

The migration rate has been predicted for the Sabine River and compared with the observed value. A satisfactory result has been found through the analysis of 12 bends (Heo et al., 2009). The study has shown that the migration rate was maximum for the bend when the bend curvature ratio was 2.5 and when the value was below 1.6, the secondary flow was still active and scoured the outer bank.

Hudson and Kesel (2000) have studied the migration of 125 bends from long-term old historical data and made a relation between migration rates and bend curvature for the Mississippi River, where no hydrological entity was incorporated. The authors concluded that the relationship, which was originally established from the model study of homogeneous floodplain with free meander river, generally deviated from natural meander rivers of a heterogeneous complex floodplain. They found that when the bend curvature ratio was between 1.0 and 2.0, the bend migration was the maximum for the heterogeneous floodplain with locally varying resistance to erosion. Again, in the reaches where the number of clay plugs was low, the bend migration rate was comparatively higher than in the reaches with a higher number of clay plugs.

In the study of Guo et al. (2021), data set of two different characteristics rivers with 290 bends was used and compared the pattern of morphological changes in terms of migration between the two rivers. The authors explored that the river with stronger stream power migrated faster than the weaker one. Again, a faster migration rate happened in translation mode and moderate bend curvature. They also found that, when the migration rate in a river was comparatively slow, simple bend geometry was deformed to a shape of complex form.

Bend cutoff has been analyzed by Hooke (2004) on the Bollin River. The river had undergone several cutoffs within shorter periods and based on that evidence the author has given a set of hypotheses and its explanation about the occurrence of cutoffs. Most of the cutoffs were neck cutoff and before the ultimate cutoff, bends were migrated downstream and tightened its shape by decreasing wavelength, increasing amplitude, and a complex formation of the apex. The findings from the study: a river with an erodible bank and large discharge may cause the short-term bank adjustment; short-term high flow when frequently associated, channel undergoes cutoffs in different bends with different rates;

upstream disturbances like urbanization and artificial cutoff influence the river adjustment at a downstream section through the cutoff.

A total of 30 river bends of the Trinity River, Texas have been used by Mason and Mohrig (2019) and proposed that a constant river width at the bend is sustained by counterbalancing the erosion and deposition during the migration process. Thus, the small change in width was compensated within 2-3 years. Tight bends exhibited a small amount of temporary change of width, but for the larger bends, the width changes were comparatively high.

The bending analysis in the study of Nicoll and Hickin (2010) has covered confined meander rivers within similar geomorphological settings. The authors have suggested that the parameters of bends related to the migration of confined meander rivers have consisted of those of the free meander rivers, and they also have proposed, that a confined meander river is not a unique river but a different trajectory from a free meander river.

Among many other studies on the meander river, lateral migration in flood season and thus reach and time-scale change of meander geometry of the Bhagirathi River has been studied in Ghosh and Mukhopadhyay (2021). Again, a single bend has been analyzed in Yousefi et al. (2021) to identify the change of the meander loop by the sudden extended flood.

The bend-scale analysis is important for the development of a proper understanding of the morphological behavior of a meander river. These types of analysis on meander rivers from all corners of the world have addressed different theories, hypotheses, arguments, and anomalies as well. Sometimes the well-established empirical relationships may attitude unlikely in different regions of homogeneous and heterogeneous floodplains with different sizes of a drainage area and sediment characteristics of bank bend and flow. Still, there have huge scopes to incorporate innovative ideas with more precise analysis tools and techniques that would be accepted unanimously and thus the researchers of different branches have great interests in the meander river.

2.3 Studies on River Bend Migration in Bangladesh

The meander rivers, bifurcated from the right and left banks of the Brahmaputra-Jamuna, the Ganges and from the right bank of the Padma River of Bangladesh, generally flow through alluvial flood plains of the same/similar characteristics. A single parent river, in some cases, conveys more than one distributary meander river with alike sediment characteristics and hydrological variation. Thus, the literatures on different meander rivers of Bangladesh may sources of common and basic ideas about the hydro-morphological processes of the meander river of the specific river system. So far, most studies have been on the Padma River; being treated as a meander-like channel. Besides this, significant studies have come from both the Arial Khan and Modhumati Rivers and some others from different meander rivers i.e., the Kushiara, Manu, etc.

2.3.1 Study on the Padma River

Researchers (Arefin et al., 2021; Chowdhury, 2021; Hussain et al., 2021; Ophra et al., 2018; Dewan et al., 2017; Islam, 2016) have paid great attention to the morphological study of the Padma River. Hydro-morphological processes of the Padma have a great impact on the entire river system of the south-western region, as it is a feeder river for several meander rivers of this region. Though the Padma River is not a typical meander river, the wider channel of the river has curved banks in several locations, which are spatially treated as a meander-like channel and flow dynamics.

Like some other meander river studies, meander parameters, i.e., sinuosity, erosion, and accretion and the relation of these parameters with the hydrology of the Padma River have been studied by Dewan et al. (2017). The study has revealed that, for bank erosion of the Padma River, average discharge played an important role, though flood discharge had an insignificant contribution. Analysis from 1973 has also explored that, a good number of concave (inner) banks experienced more accretion and less erosion, and a similarly opposite scenario had occurred for convex (outer) banks, which were not following the typical meander theory. It was due to mass bank failure in different locations and distribution and deposition of that sediment along different bends randomly.

Another study on the Padma River is by Chowdhury (2021), where it has been revealed that the deep channel of the river has moved in such a way that the flow path has turned from straight to meander over 40 years from 1979 to 2019. In some cross-sections of the river, the meander belt has developed, and the sinuosity has increased to a range from 1.06 to 1.11, which was an average of 1.04 in 1979. An increasing trend of island bar size in different locations of the river has also been found.

Other important studies on the Padma River are (Arefin et al., 2021; Hussain et al., 2021; Ophra et al., 2018; Islam, 2016), the majority of these studies deal with the time-scale analysis of erosion deposition and riverbank shifting.

2.3.2 Study on the Gorai, Madhumati and Dhaleshwari Rivers

Spatiotemporal Variation of the Gorai-Madhumati River morphology in terms of point bar, river width, bend migration rate, and river sinuosity of the pre-and post-Farakka era from 1972 to 2018 has been studied in Gazi et al. (2020) using RS-GIS technique. The river was divided into two segments and some characteristic bends of each segment were identified and analyzed in different timeframes. The authors have suggested that the Farakka barrage is the main entity for the hydro-morphological changes of the river. As discharge in the river has decreased over time, the local controlling factors have shifted from flood plain topographic factors to hydraulic factors. The overall sinuosity of the river has increased with the increase of erosion and deposition and the river has shifted to a more meandering pattern. Growth and decay of the sand bars have been found in the different timeframes, though accretion was predominated in all bars in recent years.

Another study is by Biswas et al. (2021) on the Gorai-Madhumati River has described the change of channel geometry where the same parameters are used as the previous study has done. The authors suggested that seasonal variation of discharge, extreme flood events: like the floods of 1988 and 1998, and human interventions are responsible for hydro-morphological changes of the river.

The influence of discharge on morphological variation of the Dhaleshwari River is studied in Banda and Meon (2018) to analyze the change of bend geometry. A migration model

has been used to simulate bend scouring and compared the simulated result with investigated field data.

The meander characteristics and the controlling parameters are not properly addressed in the above studies, which are important for meander river analysis, though few meander parameters are used in some studies. In fact, in the Bangladesh context, empirical and theoretical researches on the meander river have some bounds due to data limitations to incorporate all environmental variables. But there have been scopes to investigate the meander river by following established empirical relationships and using historical images and measured secondary data.

2.3.3 Study on the Arial Khan River

Several literatures have been found on the Arial Khan River, an important river flowing before the Padma Bridge site. Among them, the studies related to hydro-morphology and channel shifting/migration are Biswas et al. (2018), Akter et al. (2013), Mamun (2008), Hossain et al. (2007), Winkley et al. (1994), Ashrafuzzaman (1992), etc.

The morphological process of the upper Arial Khan River has been analyzed from historical hydro-morphological data. Based on this analysis, effective river erosion management techniques have been suggested by Akter et al. (2013). The study has found that, though the river had some specific nodal points, the locations of erosion were not fixed. As an alluvial meander river, the channel possessed typical erosion-prone bends. The study has quantified some bend characteristics, i.e., average meander length and amplitude were four and one respectively, the sinuosity of the river showed a decreasing trend with an average value of 1.5, the migration modes of the bends were rotation, translation, and expansion; each mode of migration have existed in a specific section of the river. The average time required to change the location of erosion was around 2-5 years. According to the erosion and accretion rate, the upstream part was very dynamic, whereas the middle and downstream parts had a reduction in the rate. The study has suggested that morphological parameters of the river were highly influenced by discharge, water level, type of sediment flow (suspended sediment), nature of floodplain (active Ganges), and recently accomplished river training work for the Arial Khan bridge.

Another study on the upper Arial Khan River is by Biswas et al. (2018), where the morphological variability and some related hydrological parameters are the main focus. This is a reach scale study, where it is supposed that high sediment entrainment into the river system during monsoon and human activity and intervention are responsible to channel pattern changes, i.e., sinuosity, river width, and river area.

An important study on channel instability analysis of the Arial Khan River is by Winkley et al. (1994), where highly unpredictable meandering characteristics of the river and the reasons behind it have been identified with necessary explanation through field data and observation. To do so, the hydrology (discharge, sediment) of the Arial Khan and of the parent river the Padma, the morphology (pools, crossings, and bars) of the Padma near the Arial Khan, and the morphology of the Arial Khan Offtake have been considered and suggested that all of these have imparted in the morphological development of the river.

Among other literatures on the Arial Khan River, Mamun (2008) has discussed the change of the Arial Khan Offtake morphology through continuous accretion and formation of the sand bar in front of the river mouth which is influencing the declination of river discharge with time; Hossain et al. (2007) have identified morphological changes of the river near the Arial Khan bridge, and Ashrafuzzaman (1992) has used hydrological and bathymetric data of the Arial Khan River to identify the spatio-temporal changes of different hydro-morphological features of the river.

A typical meander river morphology study based on meander bends has been accomplished in several literatures, where the bend-wise spatio-temporal variation of morphological parameters has been analyzed. But no analysis has ever been done in Bangladesh to establish meander characteristics of a specific river addressing the associated controlling factors of meander parameters. This is particularly due to the insufficient hydro-morphological and geological data of floodplain and entire river system of Bangladesh, as bend-scale detail analysis requires adequate data availability, long-term field data collection, and historical records of natural events and anthropogenic disturbance as well of the river.

2.3.4 Study on other Meander Rivers

From Bangladesh's perspective, an important bend-scale study is (Uddin et al., 2012), where the authors have chosen the Kushiyara River. Some common meander parameters, i.e., meander wavelength, the radius of curvature; sinuosity, meander width, meander ratio, and bend migration have been analyzed for the selected critical bends to explore the meander characteristics of the river and its changing pattern with time. Some well-established correlations among these parameters have been found in different literatures, which have been ignored in this study. The other controlling factors of the morphological changes of this river are not properly addressed here.

Another similar type of study on channel shifting in critical bend locations by Deb and Ferreira (2015), where the Manu River migration phenomenon has been interpreted by several sections of the river, containing critical bends. Morphological changes have been analyzed in terms of spatio-temporal changes of sinuosity, river width, left/rightward shifting of channel mid-line, and finally area of erosion and accretion of the river. Huge seasonal variations of discharge and sudden flash floods have great impacts on morphological alteration of the river with clay deposited banks.

Using GIS and prediction model, the future prediction of morphological changes in selected river reach of the Teesta has focused on Akhter et al. (2019). The authors have correlated the increase of sediment load with the morphological changes of this river, as the river width has contracted in recent years with the formation of some mid-channel bars. Local and temporal differences in channel migration rate have been found. It has also been found that the decreasing trend of the annual discharge, channel narrowing, and mid-channel bars, all have triggered to form of partial new channels. Besides this, according to the result of the prediction model up to 2031, both left and right banks individually have seen to shifting.

CHAPTER THREE

STUDY AREA

3.1 Introduction

The study river is the Arial Khan River, a part of the Ganges-Padma River system. The river is one of the meander rivers of Bangladesh, the meandering pattern of this river is governed by the geological and topographic condition of the entire region and the in-stream hydrological and sedimentological response of the river.

3.2 Arial Khan River System

The Arial Khan is one of the right-bank distributaries of the Padma; it branches off almost the middle of the Padma River at Chowdhuri Char of Faridpur district. The upstream river basins of the Ganges and Brahmaputra receive one of the highest rainfalls in the world and to its downstream; the combined flow passes through the Padma. As a connecting river, the Arial Khan carries out a partial discharge of the Padma and disperses the flow into the Bay of Bengal through the Tetulia River.

The average length of this reach is 108 km, though yearly stretching and shortening of the length have been seen at regular intervals, depending on the fluvial processes within the Arial Khan and the upstream river system. A total of 90 % of the course of the upper Arial Khan flows within the Madaripur district and falls into the lower Arial Khan River in the Barishal district.

Historically the Arial Khan River course and the surrounding geological location are important as it has been conveying tremendous discharges from Ganges Brahmaputra Meghna (GBM) basin. Before the massive earthquake in 1762, the present Arial Khan course was the main course of the Padma River and directly transmits the Ganges and Brahmaputra River discharge to the Bay of Bengal. Later, the Padma River incised the floodplain near Mawa to form a new channel, the present course, a 100 km length of downfall channel located at the very end of the vast Ganges-Brahmaputra River system. Since then, the Arial Khan has been flowing as a right bank confluence of the Padma

River. Lateral shifting of these two rivers has been occurring repeatedly within the adjacent floodplain, some of which have still existed as a meander scar.

According to wetlands classification (Prosoil, 2016), the Arial Khan is defined as a semi-major, second-order river of the Ganges-Padma River system. There are several tributaries, distributaries, and small excavated canals, which receive and contribute to discharge to the Arial Khan River. Among them, the Moinakata, Beel Padma, and Palong are tributary rivers and connected to the Padma River, though the offtake of The Moinacata and Beel Padma Rivers are silted up. The Kumar, Lower Kumar, and Palordi are distributary rivers. Several permanent river training works have been made along the river; guide bank near the Haji Shariatullah Bridge, Madaripur town protection work, and bank protection work against severe erosion near Mollarhat Bazar under Kalkiniupazila of Madaripur district are prominent. The information on the permanent bank protection works in detail are presented in table 3.1.

Table 3.1: Existing bank protection work of the Arial Khan River.

SI	Name of the project	Length of the project	Implementation period
01.	Protection of Dhaka-Mawa-Bhanga national highway adjacent to Haji Shariatullah Bridge	R/B 1.440 km L/B 1.080 km	2004-2006 and 2017-2020
02.	Madaripur town protection project along the R/B of the Arial Khan River	2.109 km	1987 and 2004
03.	Khasherhat Bondor protection project along the L/B of the Arial Khan River	0.250 km	1997-1999

3.3 General Hydrology of the River

The GBM basin is the region with one of the highest rainfall intensities in the world. Around 70%-80% of rainfall in this basin occurs within the monsoon period of June to October. In the pre-monsoon (April-May) 16.6 % of rainfall occurs. The rainfall in post-monsoon (October-November) and dry season (December-March) are 4.8% and 2.8% respectively. This rainfall pattern of the river basins along with the snow melted water from the Himalayas is the main source of discharge and responsible for the monthly flow variation in the main rivers and its distributaries like the Arial Khan. Another flow

variation is observed on a daily basis in this river due to the tidal impact from the semidiurnal tidal cycle. Especially during the dry season, this impact remains significant, but during the wet season, the fluvial flow dominates over tidal flow. The tidal range of the Arial Khan River during pre-monsoon is 0.68 m (Begum, 2018) and during monsoon is less than 0.1 m (Roy, 2021). Heavy flow during the monsoon delivers 75% of the total sediment load through the Ganges, Brahmaputra, and Padma River systems (Goodbred and Kuehl, 1999). On the other hand, during the months of low flow, sedimentation occurs in a different location within the river where the low velocity of flow makes a stagnant like water. Around 2%-6% of the flow of the parent river Padma is diverted to the Arial Khan River, year-to-year significant variation of this percentage has been observed from long-term data of previous years. During the study period, the highest maximum water level (WL) and discharge (Q) in the river were found in 1991 and the lowest discharge was found in 2011. Figure 3.1 shows daily WL at the Arial Khan offtake station for the years 1991 and 2011.

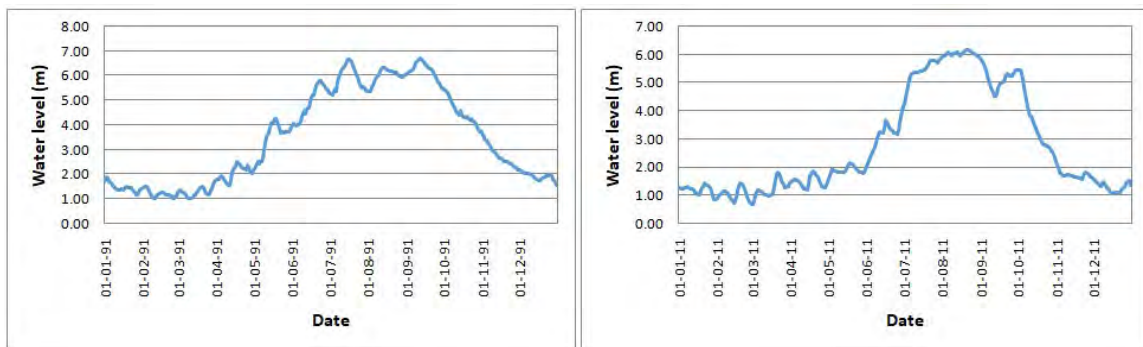


Figure 3.1: Daily water level of the Arial Khan of years (a) 1991 and (b) 2011.

The yearly discharge and sediment of this river are about 30 billion m³ and 25 million tons respectively (Sarker et al., 2013). The yearly average maximum discharge (Q_{max}), minimum discharge (Q_{min}), and average discharge (Q_{avg}) of the river are 3067 m³/s, 56 m³/s, and 795 m³/s respectively. So far, the highest discharge was observed as 5810 m³/s during the 1991 flood. On the other hand, one of the lowest discharge occurrence years was 2011 when the Q_{max} of the river was 1167 m³/s. The daily discharge at the Arial Khan offtake station for the years 1991 and 2011 are presented in Figure 3.2. The recorded old data says during the sixties of the last century the river had the lowest discharge. After that period the discharge had increased successively for the next three decades and during the nineties of the last century, the highest discharge was observed.

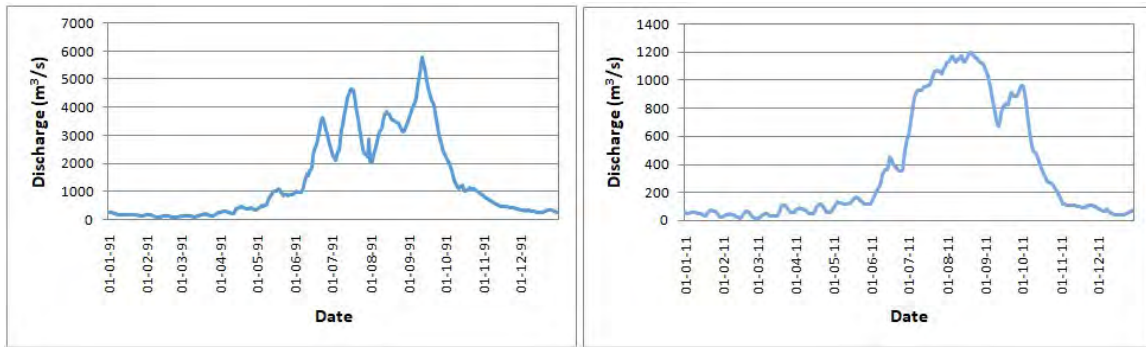


Figure 3.2: Daily discharge of the Arial Khan of years (a) 1991 and (b) 2011.

The last six years have shown an increasing trend of discharge again after 9 years (2005-2013) of the recession period of discharge. According to Coleman (1969), the region is susceptible to floods of different intensities; moderate flood hits every 4 years, severe flood every 7 years, and disastrous flood every 30-40 years interval. The mean annual rainfall of the surrounding region of the Arial Khan is 2105 mm, the wettest month is July, and the driest month is March. The Arial Khan is considered a perennial river, but during the dry season, it carries low flow in some years to properly meet the in-stream demand.

3.4 General Morphology of the River

The entire south-west and south-central regions of Bangladesh consist of separately by the Ganges delta and the Meghna delta. The Ganges floodplain is at an elevation of 5 m PWD (Public Works Department), whereas the Meghna floodplain is at 3 m PWD (Sarker et al., 2013). But a narrow strip of floodplain along the right side of the Meghna River is termed an active delta; the main river, tributaries, and distributaries of the GBM river system carry a huge sediment load, thus the delta building process is still going on. The sediment from the two basins of Ganges-Brahmaputra and Meghna come from completely different geological settings. Thus, the texture of the active delta floodplain is heterogeneous. The Arial Khan River, one of the distributaries, passes through this active delta. Figure 3.3 shows the Arial Khan River System and its tributaries and distributaries. Geologically the floodplain of this river varies both horizontally and vertically, as various types of sediment had deposited in a long-term history of the development of a 5-15 km depth floodplain (Allison, 1998).

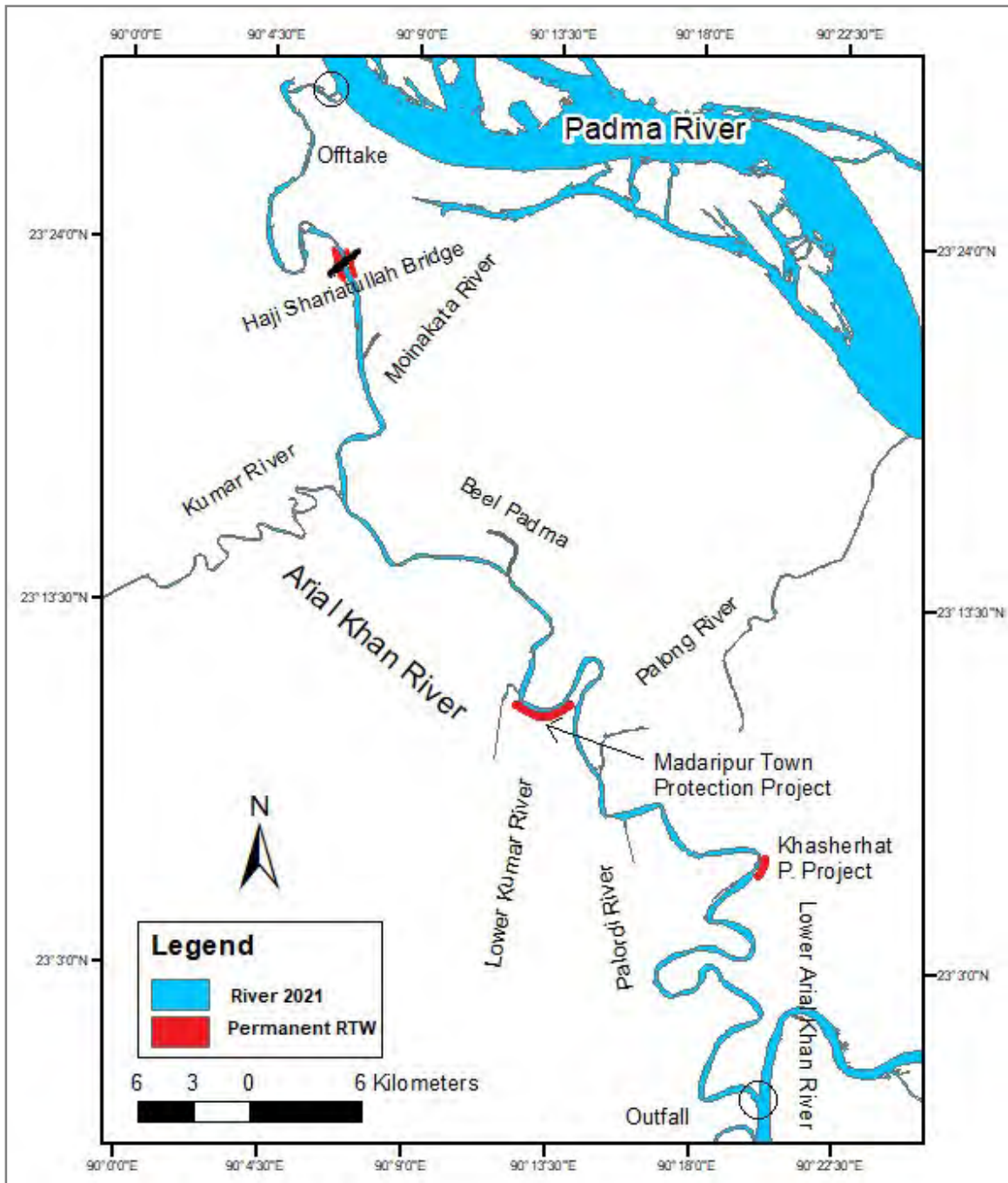


Figure 3.3: The Arial Khan River system

During monsoon, high flow velocity washes away loose sediment from the bank and bed and causes permanent local erosion along the river. But during the dry season, sedimentation forms narrow and shallower channel due to very low/ negligible flow velocity. As a result, yearly as well as monthly morphological variation is very common within the Arial Khan River, which causes permanent and temporary changes in cross-section, slope, thalweg, etc. All these phenomena render floodplain geology and geomorphological characteristics of the Arial Khan River. The Arial Khan River has

morphologically differences in upstream and downstream and its adjacent floodplains; the upstream is comparatively more dynamic than the downstream. Several meander scars and clay plug existence and oxbow lakes formation through meander neck-cutoff are very common in the floodplain of the upstream, some oxbow lakes and meander scars of the Arial Khan River are seen in Figure 3.4. Besides this, the morphology of this reach is the fluvial type and whereas the downstream has some tidal influences. The river has a section in the middle, which is dominated by channel avulsion; two times avulsion had been observed within less than 30 years in the same location. The second-time avulsion followed the older channel. The downstream is morphologically homogeneous. Here, the erosions of the bends are continuous and unidirectional, and the bend cutoff form is generally chute cutoff.



Figure 3.4: Oxbow Lake and meander scars of the Arial Khan River floodplain [Google Earth].

3.5 Arial Khan Offtake

The river course change of the Padma River changes the direction flow field into this river (Nippon Koei Co., 2005) and consequently influences the accretion and erosion process along the bank of the river. The year-to-year changes in offtake morphology of the Arial Khan River have been found (Mamun, 2008), which have been playing a vital role in the

change of the fluvial processes of the river. Figure 3.5 shows the shifting of the offtake of the Arial Khan River in different time intervals due to the change of the Padma River course, starting from 1972.

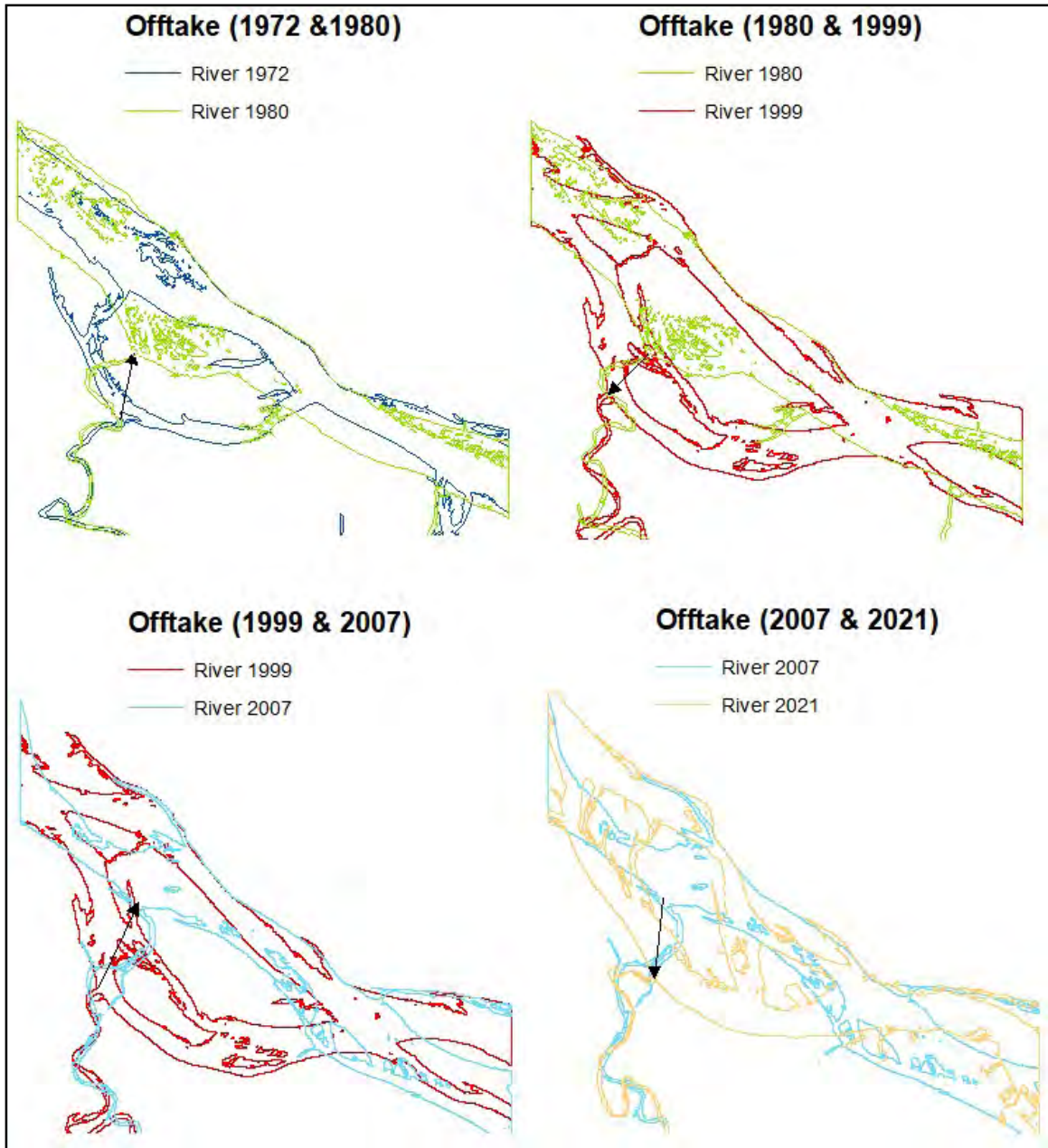


Figure 3.5: Offtake shifting of the Arial Khan River in different time intervals, (→) indicates direction of previous to next location of offtake.

Different literatures (Dewan et al., 2017; Sarker, 2008) have suggested that new mid-channel bars appear, and several existing small bars get expanded through accretion and migrate along the Padma River course with time. Concave shape bend formation starts

through erosion in several locations of the Padma River banks, which occur repeatedly in a specific year of interval along the right bank. These erosions at the bend further become faster, which could be due to the combined effects of concave bend shape and bar push. After reaching an ultimate point, instead of erosion, deposition of sediment starts at the same location. This phenomenon renders the change of direction of the flow regime and the planform of the Padma River from straight to meandering and again from meandering to straight. Long-term historical data shows that meander bend formation and disappearance have been occurring at the location of the Arial Khan Offtake maintaining a time span of 8 years and 19 years, thus the offtake point oscillates across the bank of the Padma River.

CHAPTER FOUR

METHODOLOGY AND DATA COLLECTION

4.1 Introduction

Nowadays, the time- and bend-scale analysis of meander rivers are accomplished by utilizing different tools, techniques, and methodologies. Among them, the empirical and theoretical studies based on remote sensing imageries have great appeal to the researchers due to the least effort and cost. The improvement of the resolution of satellite images and availability of different image possessing software, increase the popularity of the spatio-temporal hydro-morphological analysis by using remote sensing imageries. But the multiple bend-scale analysis in an effective way is the challenge. Especially the bends of a very active meander river like the Arial Khan are neither smooth with a perfectly round shape, nor its migrations are homogeneous in terms of magnitude and direction. In this study, different methods and techniques have been used step by step to achieve a satisfactory outcome. The first step was the delineation of bank lines of the river from time-series satellite images using GIS software. In the second step, the bend geometry was precisely identified and quantified by CAD software. The hydrological and bathymetric data collection and processing was another important part of this study. All necessary data from the river including offtake position with respect to the parent river; channel planform, cross-sections, depth; bend geometry, and floodplain characteristics were acquired and carefully incorporated for this research.

4.2 Time-series Remotely-sensed Data

Remotely-sensed satellite imagery is frequently used for the study of river migration and lateral migration as well (Jarriel et al., 2021; Morais et al., 2016; Constantine et al., 2014; Hickin and Nanson, 1984). In the case of meandering rivers, the increasing availability of satellite images ensures the possibility to build up an extensive and reliable data set from which river planform configurations and channel width distributions can be extracted. In this study, Landsat images provided by the U.S. Geological Survey (USGS) Earth Explorer portal have been used, which have the advantages of being open source, georeferenced, and available since 1972. River migration is a reach-scale and more

specifically bend-scale response; the appropriate observation, measurement, and future prediction of this migration are a laborious task for the management of the river system. Many researchers quantify the measurement of migration in two different approaches. The first approach is the linear movement of the channel during specific periods of time where some characteristic river reaches and bends are selected and studied (Guo et al., 2021; Mason and Mohrig, 2019; Mirzaee et al., 2018; Hickin and Nansin, 1975; Leopold, 1972). In the second approach, the time-series analysis of the progressive movement of the channel positions is conducted using the GIS technique (Hooke and Yorke, 2010).

In this study, spatial planform variations in the time series of the river were preliminarily analyzed by Google Earth Pro. The time period for the study was from 1972 to 2021. The years of time series were considered as the years when the Padma River had reached its final stage of meandering/ straight channel formation alternately, after that stage the channel had started to reverse back, the years were: 1972, 1980, 1999, 2007 and 2021. The years 1988, and 2017 were also included as interim years.

The satellite images of Multispectral Scanner (MSS), Thematic Mapper (TM), and Operational Land Imager (OLI) of different nos. of bands were collected from a tool of the USGS named USGS Earth Explorer from the website: <https://earthexplorer.usgs.gov>. The information on the images is given in Table 4.1.

Table 4.1: Landsat images used for the analysis

Satellite Sensor - Bands	Path/ Row	Date (D/M/Y)	Collection-Level	Resolution(m)
LM1 - B4567	147/44	28/12/1972	C2-L1	60
LM3 - B4567	147/44	02/02/1980	C2-L1	60
LT5-B1234567	137/44	02/01/1988	C2-L1	30
LT5-B1234567	137/44	01/02/1999	C2-L1	30
LT5-B1234567	137/44	23/02/2007	C2-L1	30
LC8- B123456791011	137/44	17/01/2017	C2-L1	30
LC8- B123456791011	137/44	13/02/2021	C2-L1	30
LM1: Landsat 1 MSS; LM3: Landsat 3 MSS; LT5: Landsat 5 TM; LC8: Landsat 8 OLI				

The images for different years of the winter season: December, January, and February were chosen as during this time images remain cloud-free, and the river maintains a consistent hydraulic condition for most of the years. After performing radiometric correction of each year of the image, the river banklines were delineated. As a part of water body extraction during bankline delineation, the water was classified by a specified positive lower value based on BWDB water width data of the river for the year 2019. This lower value for water classification was used for the images all through the years.

4.3 Ground-Truthing

Ground-truthing is an important tool to identify the accuracy of satellite images. Among various techniques, using GPS to identify the actual location in the field is the simplest technique in ground-truthing. Figure 4.1 presents the GPS points in the field and the delineated right bank of the river at bend B3.

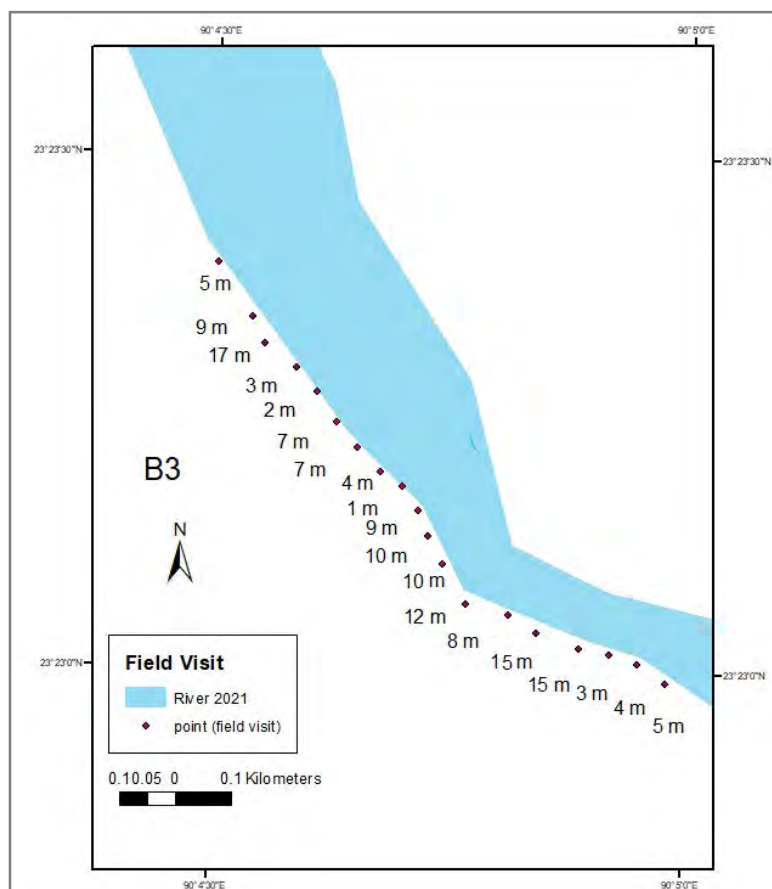


Figure 4.1: Ground-truthing of image from the identified locations of bend B3.

The deviations between the delineated bankline from the image of 2021 and the actual bankline based on GPS locations were linearly measured, from which the error was calculated (ASPRS, 1990). In this bend B3 site total of 19 GPS points were taken along 1.05 km length of the right bank at 50-60 m intervals. The lowest and highest deviations were found as 2 m and 17 m respectively. The root mean square error is 8.9 m, which is 0.3 pixel of the image.

The main part of the analysis has two component – one for offtake hydro-morphology and another for the rest of the river.

4.4 Data for Offtake Hydro-morphology

The gauge station no. near the offtake is SW4A. The available data of this station were discharge and water level. The bathymetric measurements were accomplished at different sections of the river, such as AKU1, AKU2, etc. These sections along the river at a certain interval were fixed by BWDB. All of the secondary data were collected from BWDB. The morphology study of the offtake was completely based on image analysis and secondary data; no data from the field survey were introduced.

4.4.1 Development of rating curve for the offtake station

To establish a relationship between discharge Q and water level (WL) of a specific gauge station of the Arial Khan Offtake, the rating curve was developed for the data of the monsoon season (June-October) from 2008 to 2019. Both Q and WL data were available during this time period, except for the years 2015 and 2018. The general equation relating to Q and WL is as follows:

$$Q = C_r(G - a)^\beta \quad (4.1)$$

The above equation is called the rating curve equation, where Q is the estimated discharge (m^3/s) for the gauge reading G (m) and “ a ” is the value of G (m) corresponding to $Q = 0$. C_r and β are two constants derived from the two established equations, where C_r and β are rating curve constants:

$$\beta = (N\sum(XY) - \sum X\sum Y) / (N\sum X^2 - (\sum X)^2) \quad (4.2)$$

$$\log C_r = \left(\frac{\sum Y - \beta \sum X}{N} \right) \quad (4.3)$$

where, $X = \log(G - a)$, and $Y = \log Q$. As the “a” differs from year-to-year for the river with dynamic bed level, the values were determined for each year from measured G and corresponding Q using the following equation:

$$a = \frac{G_1 G_3 - G_2^2}{(G_1 + G_3) - 2G_2} \quad (4.4)$$

The gauge values of G and Q are plotted in Figure 4.2 to calculate “a” by using G1, G2, and G3 values corresponding to Q1, Q2 and Q3 from the graph.

Appendix B presents detailed calculations of the rating curve and yearly Qmax, Qavg, and Qmin values estimated by using river stage data and the rating curve.

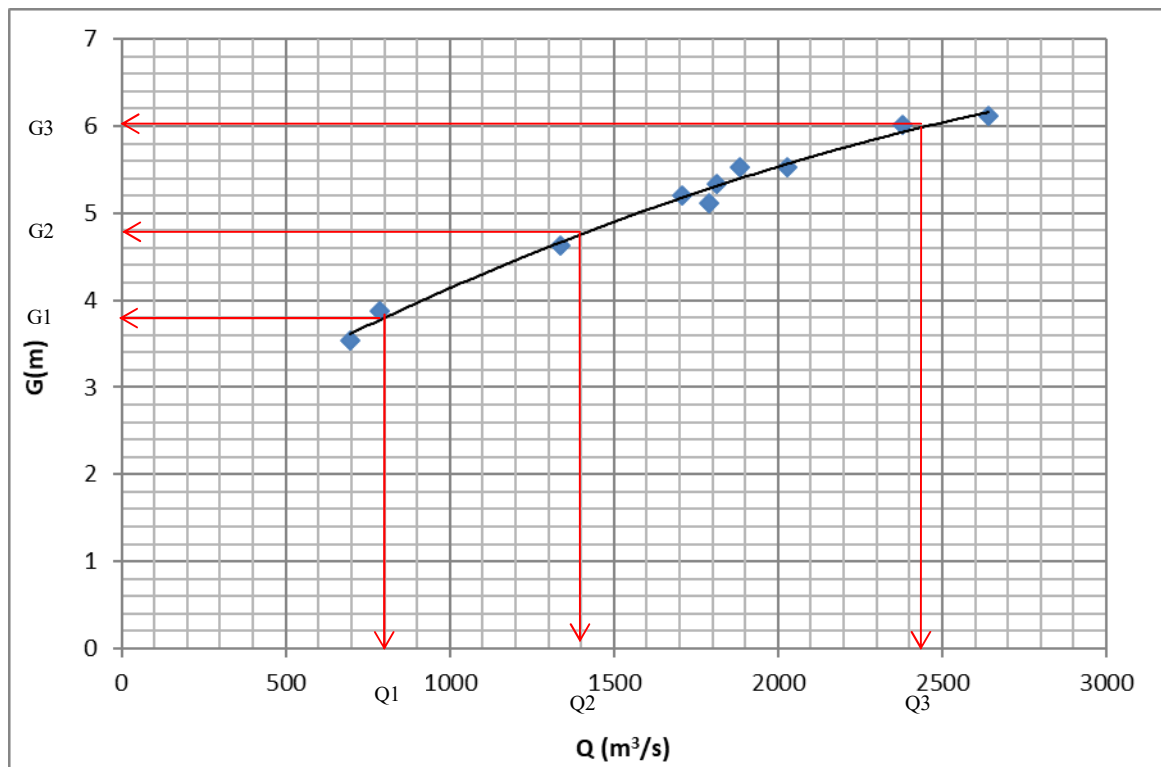


Figure 4.2: Stage (G) vs. discharge (Q) plot for the gauge reading at offtake of the Arial Khan River.

4.4.2 Determination of bed level change at the offtake

Bathymetry data for AKU1 were available from 1978 to 2019. Year-to-year change of bed level in terms of thalweg elevation was found out and the pattern of these changes was estimated from these data.

4.4.3 Evaluation of the offtake shifting

The shifting of the offtake location was identified for the selected years, starting from 1972; and then successively for 1980, 1999, 2007, and 2021. These years were indicating the time period when offtake had been situated to extreme lower/upper position successively due to the change of channel form of the Padma, i.e., meandering and straight. The shifting of the offtake between two consecutive years was measured as linear distance. The year 1988 and 2017 were also included as interim years when the offtake was situated at a certain mid-point of directional shifting.

4.5 Assessment of River Planform

4.5.1 Bankline delineation

The bankline of the river course is delineated after the extraction of the river course from the land and vegetation. In this study, the river course is extracted by the formula of normalized difference water index (NDWI): $NDWI = (Green - NIR) / (Green + NIR)$; where the Green and NIR bands of the images were utilized (Mcfeeters, 1996).

Though modified normalized difference water index (MNDWI) performs well for the extraction of the water body as it can extract the maximum number of water bodies than any other indices (Gautam et al., 2015), it is not applicable for the images of Landsat 1-5 MSS. Moreover, for the non-urban river course extraction, NDWI gives a good result (Mukherjee and Samuel, 2016). The Green and Near Infrared bands are designated in different band nos. for different nos. of Landsat. For example: for LM 1-3, the Green band no. is B4 and Near-Infrared band no. is B7; for LM 4-5, the Green band no. is B1 and Near-Infrared band no. is B4; for LT5, the Green band no. is B2 and Near-Infrared band

no. is B4; for LC8, the Green band no. is B3 and Near-Infrared band no. is B5. During formulation, the band nos. were carefully entered into the equation.

4.5.2 Selection of river reach

The length of the Arial Khan River along the channel centerline from the upstream offtake to the downstream confluence point with the Tetulia River is an average of 108 km, considering the distinct hydro-morphological characteristics found from the preliminary river planform study, the river was divided into three reaches as presented in Figure 4.3.

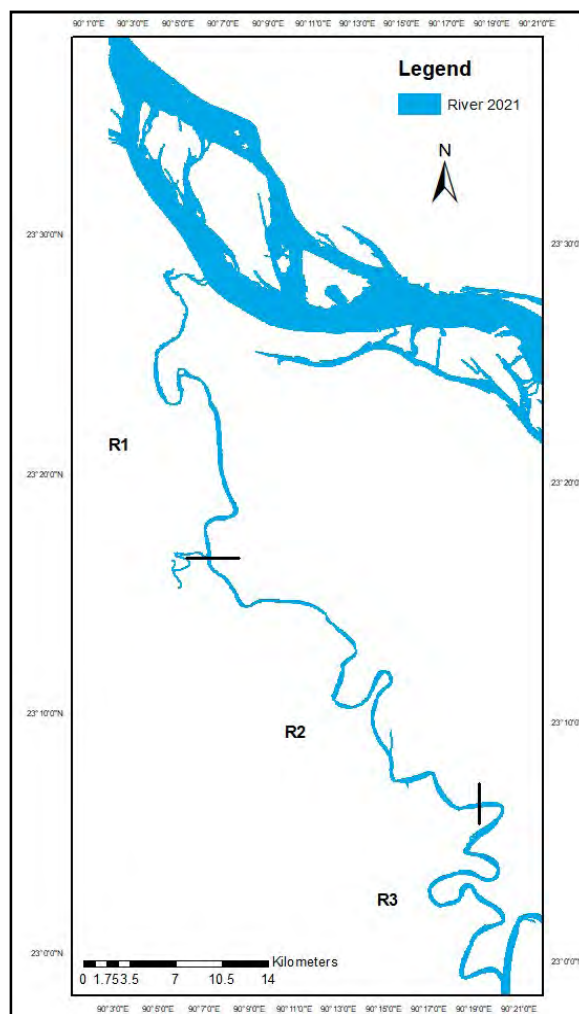


Figure 4.3: The Arial Khan River divided into three reaches: R1, R2 and R3.

The upper reach (R1) is extended up to the offtake of the Kumar River, though this offtake location changes over time. The R2 reach starts at the endpoint of R1 and ends up some km downstream of the Palordi River confluence. The rest of the river is specified as R3

reach. The average lengths of the three reaches are about 38 km, 40km, and 30 km respectively. The morphometric parameters of all the three reaches and for the entire river have been analyzed for different years.

4.5.3 Existing river sections

The BWDB had divided rivers into different sections with specific section names/ Ids for most of the major rivers of Bangladesh. The total no. of sections for the study river is 17 and denoted by AKU for the upper two reaches and AK for the lowermost reaches which have seen in Figure 4.4. Thus, the sections of AKU1- AKU7 are in R1 reach; AKU8- AKU12 is in R2 reach and AK7-AK11 is in R3 reach.

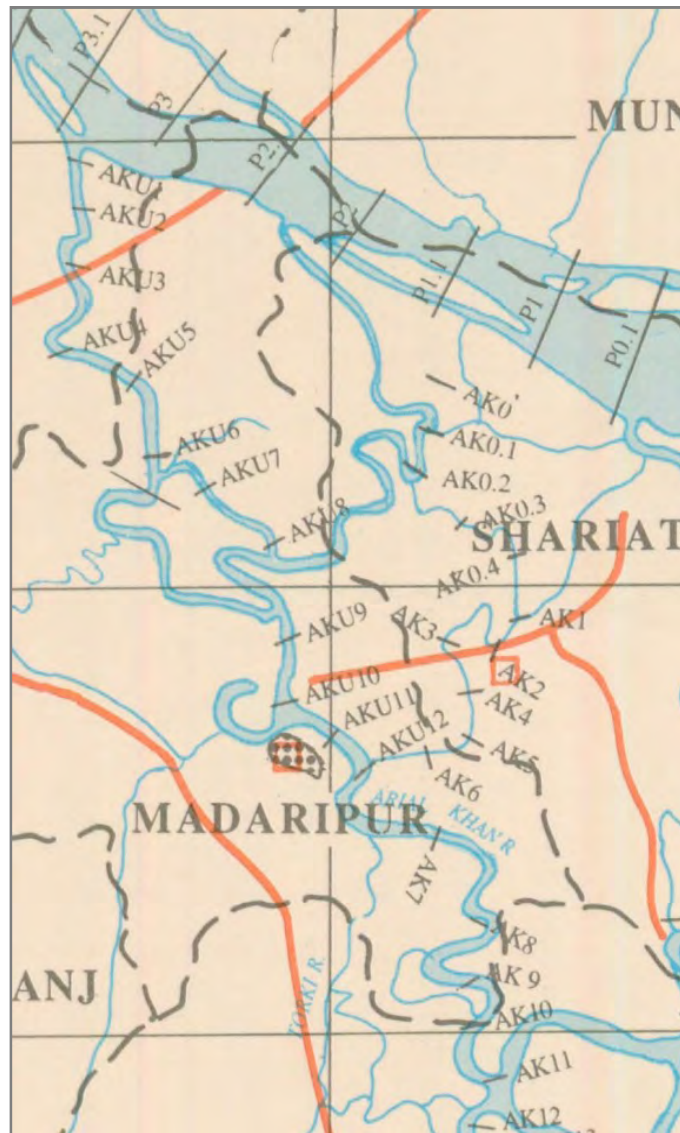


Figure 4.4: BWDB sections of the Arial Khan River.

4.5.4 Measurement of river width

River width (W) was measured in two ways from satellite imageries: at the selected bends and at the outside of bends. At an individual bend, W was measured at two crossings/inflection points and the apex of each bend for each time period. But at the outside bends, W was measured on an average every 1.5 km interval for each time period. The values were averaged for the proposed sections of AKU1-AKU12 and AK7 –AK11. For example, W for AKU1 represents the average width of the river length between sections AKU1 and AKU2. Averaging the values gave the river width for the entire river and for the specific bend during that specific time period. In bathymetry data, there is another width called the water width at 17 sections along the river during the study period (1972-2019), which were also retrieved and used in the estimation of aspect ratio at a different sections of the river.

4.5.5 Measurement of river depth and slope

Detail bathymetry data of all the sections of all three reaches are available only for the year 2019. But the R1 and R2 reaches have bathymetry data from 1972. Along a cross-section at a specific section, water depths (D) for a certain meter interval were measured, from which the average D was calculated. The dry channel was excluded during this calculation. Thus, the average water depths for all the gauge stations were found. The slope of the riverbed was determined for the year 2019 from the average depth of the river.

4.5.6 Estimation of river thalweg

From bathymetric data, the thalweg elevation of the river was estimated by plotting year-to-year maximum depth along the river at different gauge station points.

4.6 Determination of meander geometry

The meander watercourse is termed as meander geometry and consists of individual bends and parameters of bend geometry. The identification and quantification of different bend parameters were crucial. CAD software was used because it was the best option for drawing elements and taking the measurement of several geometric parameters precisely.

As user-friendly software, the straightforward quantification of migration is possible by both linear and angular measurement. The characteristic bend selection was the initial task and then the other parameters of bend geometries, i.e., the radius of curvature, meander length/wavelength (M_L), meander width (M_w), migration, and migration rate (M_r) were considered to be quantified. The bend apex and two crossing points are very important for the study of bend analysis.

4.6.1 Selection of meander bend

Active meander river pronounces its meander behavior by continuously evolving numerous bends of different shapes and lifetime throughout its length. The Arial Khan is a so dynamic river that no single bend stays at the same position, as the location of erosion changes within 2-5 years (Akter et al., 2013). Thus, the characteristic bend selection is a challenging task for a meander bend study of this river, particularly from the upper and middle reaches. In this study, most of the meander bends were selected for the bend with an arc angle of around 60° along the channel centerline (Brice, 1974). Some bends of lower arc angle were also selected when their life spans had exceeded a minimum of two time periods, which were approximately 14 years. A total of 37 bends were selected during the study period and given an individual bend ID for each bend, as in Figure 4.5. Some bends had regenerated in the same location after bend cutoff, which were identified by a suffix (a, b....) with bend ID. The coordinate of each bend with radius of curvature (R_C) of bends, W , and migration of the bend are listed in Appendix A.

4.6.2 Identification of crossings/ inflection point and bend apex

Another challenging task was pointing out the upstream and downstream crossings/ inflection point and apex for each bend as natural rivers generally form the complex bend, which carries more complex bend components. The crossing is identified as either the location of lowest width or the location where the river bankline changes its direction of alignment, near the comparatively straight portion of two consecutive bends.

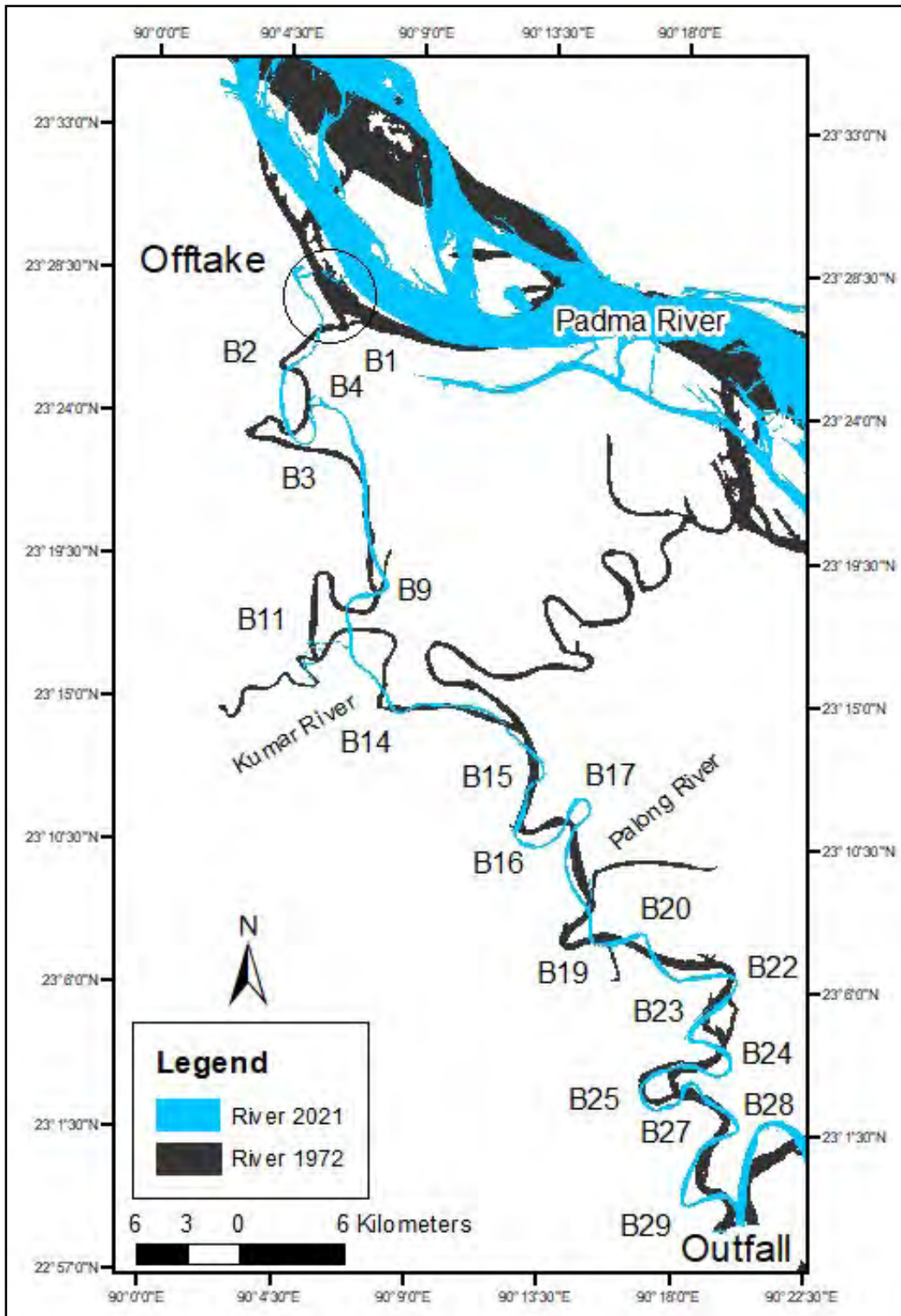


Figure 4.5: Some bends of the Arial Khan River from the years of 1972 and 2021.

The selection of inflection points/ crossings and the bend apex of the bend B28 are presented in Figure 4.6. The apex point was selected as the maximum deflection point of the outer bank of a bend, which was nearly the midpoint for most of the bends.

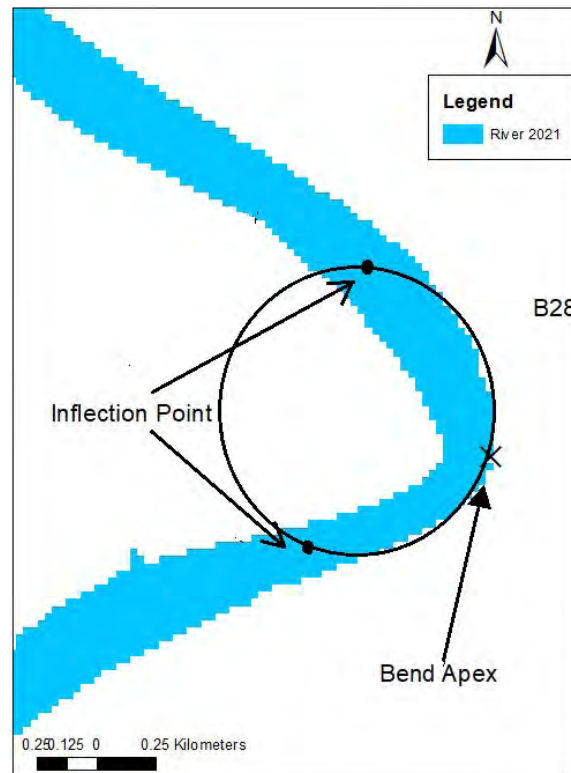


Figure 4.6: Inflection points and apex of a selected bend of the Arial Khan River.

4.6.3 Estimation of radius of curvature

In a typical bend, the bend curvature is generally an arc of a circle, drawn along the outer bank which passes through the bend apex and the two crossings on the upstream and downstream sides of the bend; is the radius of that curvature (R_C). But in reality, most of the bend shapes differ from the typical shape and thus the best-fitted arc never touches the three points at a time. In this study, curvature was drawn in such a way that it touched the apex or apex-like point and passed through at least one crossing or nearest points of two crossings.

4.6.4 Selection of meander belt

In general, meander parameters: meander length or wavelength (M_L) and meander width (M_w) are derived from an ideal meander belt which is an “S” shaped sinuous curve. But complex bend formation is very common in a natural meander river system, where a typical complete meander belt with explicit sinuous shape neither develops nor precisely exists for a long time. Thus, in most of the studies, the meander belt parameters (meander

wavelength, amplitude and meander width) have been calculated as half of the parameters measured from a single bend, and then simply doubled it. Through this process, sometimes the meander nature of a river derived from meander belt may not be properly interpreted. In this study, at least one meander belt, which was clearly visible and existed for more than two time-scales, was identified from each of the three reaches. Thus, in this study the meander belt parameters were collected from (a) meander belts which were nearly “S” shaped, (b) elongated loop and (c) matured single bend which was representing half meander belt. All together 10 representative meander belts were selected; among which from the upper reach these nos. were 1-4, middle reach 1-2, and lower reach 3-4, varying in different time periods. A schematic diagram of a typical meander bend with some common meander geometries is presented in Figure 4.7.

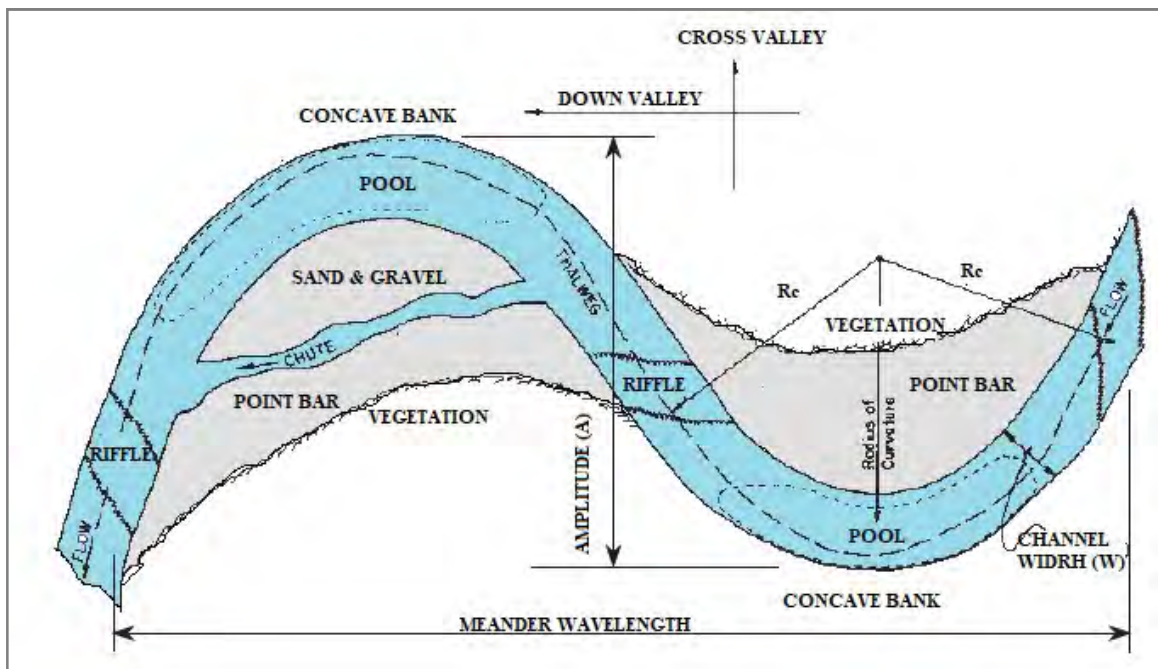


Figure 4.7: Typical meander belt with meander geometry (Lagasse et al., 2004).

4.6.5 Measurement of meander length and meander width

M_L was measured as the distance between two corresponding points, i.e., two apex points on the same side of the valley for an elongated loop, or two crossing points of the same phase. M_w was measured as the linear distance between channel center lines at two apex points on opposite sides of the valley. Thus, M_w is slightly smaller than amplitude. When

M_L and M_w were taken from a single bend, they were considered as half and doubled it to get the full value.

4.6.6 Assessment of mode of bend migration

Unstable bends migrate in different patterns or modes, among them four modes are very commonly used in different literatures, i.e., (1) expansion, (2) extension, (3) translation, and (4) rotation. The mode of migration was found out in three steps: (1) identify the shape of the bend in the initial year of 1972/shape of newly generated bends in different years. (2) Then, spot out which mode of migration was followed by the individual bend during each time span. (3) Finally, the ultimate fate was recognized for all the bends considering the migration mode in the latest years and defined by (a) Cutoff, (b) Lateral Migration, (c) Downstream Migration, (d) Upstream Migration, (e) Straight, (f) Stable and (g) Avulsion. The shape of the bend was defined by the (a) Simple symmetrical bend, (b) Simple asymmetrical bend, (c) Elongated symmetrical loops, (d) Asymmetrical elongated loop, (e) Symmetrical compound loop, and (f) Asymmetrical compound loop (Rosgen, 1994).

4.6.7 Calculation of rate of bend migration

The migration of bend is measured with respect to the outer bank. The best-fitting circle (BFC) method is used to determine the migration rate of bends between two consecutive years (Finotello et al., 2018; Lagasse et al., 2004). The linear migration of a bend from the initial year (Y1) to the final year (Y2) can be expressed by means of calculation of translation (Mt) and expansion (Md) of the bend and the migration rate is obtained as divided the outcome by the number of years.

$$\text{Migration rate (m/y), } Mr = \frac{\sqrt{Mt^2 + M_x^2}}{\text{Duration in year (Y2-Y1)}} \quad (4.5)$$

where,

$$Mt = \sqrt{(x_2 - x_1)^2 + (y_2 - y_1)^2} \quad (4.6)$$

M_t is the quantity of migration (m) for bend translation, which is the linear migration of the centroid of the best-fitted circles from the initial year (Y1) to the final year (Y2). $(x_2 - x_1)$ = migration of centroid in lateral direction and $(y_2 - y_1)$ = migration of centroid in downward direction.

$$M_x = R_{C2} - R_{C1} \quad (4.7)$$

M_x is the quantity of migration (m) due to expansion (contraction) of bend, which is the change of radius of the circle between Y1 and Y2 years. The schematic diagram in Figure 4.8 presents the parameters of the migration rate calculation. The detailed calculation is given in Appendix C.

In this study, the values of equations (4.6) and (4.7) were obtained by linear distance measurement using CAD.

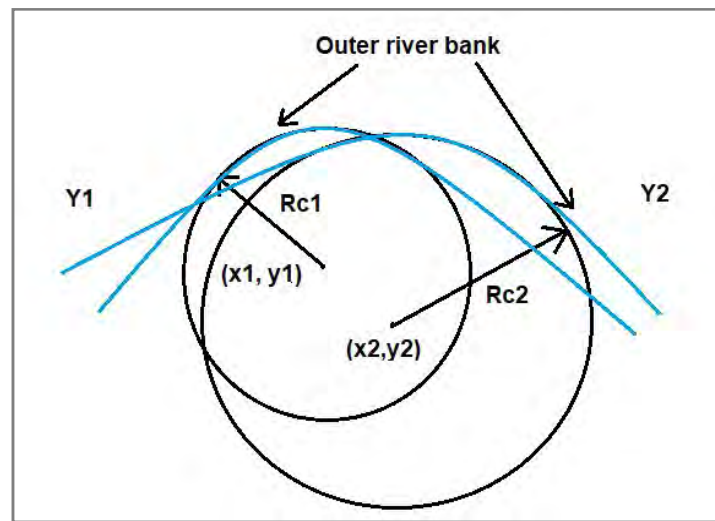


Figure 4.8: Migration of bend from initial year (Y1) to final year (Y2)

4.7 Bend Migration Prediction

Generally, three approaches are used in meander migration prediction: empirical equations, fundamental modeling, and time sequence extrapolation (Briaud et al., 2001). In this study, time sequence extrapolation methods are used for bend migration prediction for three bends B3, B17, and B27.

4.7.1 Time-sequence maps and extrapolation method

In this approach, a database of observed meander migrations and associated parameters is assembled. The drawbacks are that the equation may not include all the essential parameters influencing the process and that the applicability of the equation is limited by the extent of the database both in terms of quantity of data and geographical area. With the time-sequence maps and extrapolation approach, meander migration is predicted by accumulating the delineated riverbanks from the satellite images of previous consecutive years, estimating the migration rate from the images, and extrapolating into the future. The advantages of this approach are that it is relatively simple. The drawback is in the assumption that future flow and soil conditions will be the same as in the past.

The prediction of the bend migration was calculated by means of the change of (1) the bend radius, (2) the magnitude of meander movement, and (3) the migration direction in the future year for which the migration was calculated. The migration direction of the individual bend was derived by the angle between the line joining the center of the circles of the bend and an arbitrary vertical line.

Bend migration prediction for any future year was determined in terms of the prediction of:

- a. Radius of curvature, R_C
- b. Angle of migration, θ_c
- c. Magnitude of centroid of the arc migration, D_c

Total three bends: B3, B17, and B27 of important regions of three reaches have been selected to detect the future migration pattern for the year 2030. All the required equations were adopted from Lagasse et al. (2004).

4.7.2 Radius of curvature

The prediction of the radius of R_C for the outer bank of the meander bend is based on the assumption of the occurrence of continuous expansion (or contraction) with the same rate as that of the previous period.

$$R_{C(3)} = R_{C(2)} + \left(\frac{R_{C(2)} - R_{C(1)}}{Y2 - Y1} \right) * (Y3 - Y2) \quad (4.8)$$

where, suffixes 1, 2 and 3 indicate the consecutive values of R_C for the year 1 (Y1), year 2 (Y2) and year 3 (Y3).

4.7.3 Angle of migration

All angles (θ_c) were measured with respect to a fixed reference line.

$$\theta_{C(3)} = \theta_{C(2)} + \left(\frac{\theta_{C(2)} - \theta_{C(1)}}{Y2 - Y1} \right) * (Y3 - Y2) \quad (4.9)$$

where, suffixes 1, 2 and 3 indicate the consecutive values of θ_c for the year 1 (Y1), year 2 (Y2) and year 3 (Y3).

4.7.4 Magnitude of centroid of the arc migration

The amount of migration of the bend centroid (D_c) can be estimated as:

$$D_{C(3)} = \frac{D_{C(2)}}{(Y2 - Y1)} * (Y3 - Y2) \quad (4.10)$$

where, suffixes 1, 2 and 3 indicate the consecutive values of D_c for the year 1 (Y1), year 2 (Y2) and year 3 (Y3).

4.8 Field Assessment

A field visit was made in the month of January so as to coincide with the time period of satellite image collection for this study. The purpose of the visit was to gather some idea on bend morphology and the adjacent floodplain by means of the observation of (a) the location of erosion and thus the migration type of the specific bend. For example, if massive erosion occurs at the bend apex the lateral migration will be dominating. But downstream migration of a bend happens for the erosion at some points downstream of the apex. (b) The form of erosion, the historical evidence, and the view of the local people

about the erosion and the nature of bank material. (c) The floodplain characteristics of the selected reaches. (d) The land use: residence/ cropland/ infrastructure etc. and the land cover type: existence and type of vegetation. (e) The existence of permanent river training work, its performance, and impact to its downstream. (f) The temporary measures of erosion protection and its performance. (g) The actual bank line in the field was detected through GPS at points of 50-60 m intervals along the bends. Local people's views were collected which have given present and historical information about the river training work and the bend evolution. Appendix D contains necessary data and information, collected from the field visit.

The bends were selected based on the dynamic behavior, easy access to the location, and the importance of the location. A total of three bends were selected to visit from three reaches, which have been going through significant erosion. The bends are- B3 from reach R1, B17 from reach R2 and B22 from reach R3. The selected bends are shown in Figure 4.8. Location identification was made by GPS, which was calibrated as ± 3 m.

4.8.1 B3 bend from R1 reach

Bend B3 is situated in Sadarpur Upazila of Faridpur district. The reason behind the selection of B3 was its rapid rate of migration; especially after 2007. This bend is at the upstream of Haji Shariatullah Bridge. The continuous progressive migration is a real threat to the bridge, Dhaka-Mawa-Khulna national highway, and the surrounding localities.

4.8.2 B17 bend from R2 reach

The bend B17 is at Bahirchar Katla under Madaripur Sadar, situated just the downstream of Madaripur Town protection project. The outer bank of this bend is subjected to high erosion, especially near the Jafrabad Notun Bazaar area.

4.8.3 B22 bend from R3 reach

The B22 is the first bend of the R3 reach. The continuous erosion at the outer bank of the bend is destroying important infrastructure and properties of the nearby village. The Khasherhat Bondor Protection Project is situated just downstream of this bend.

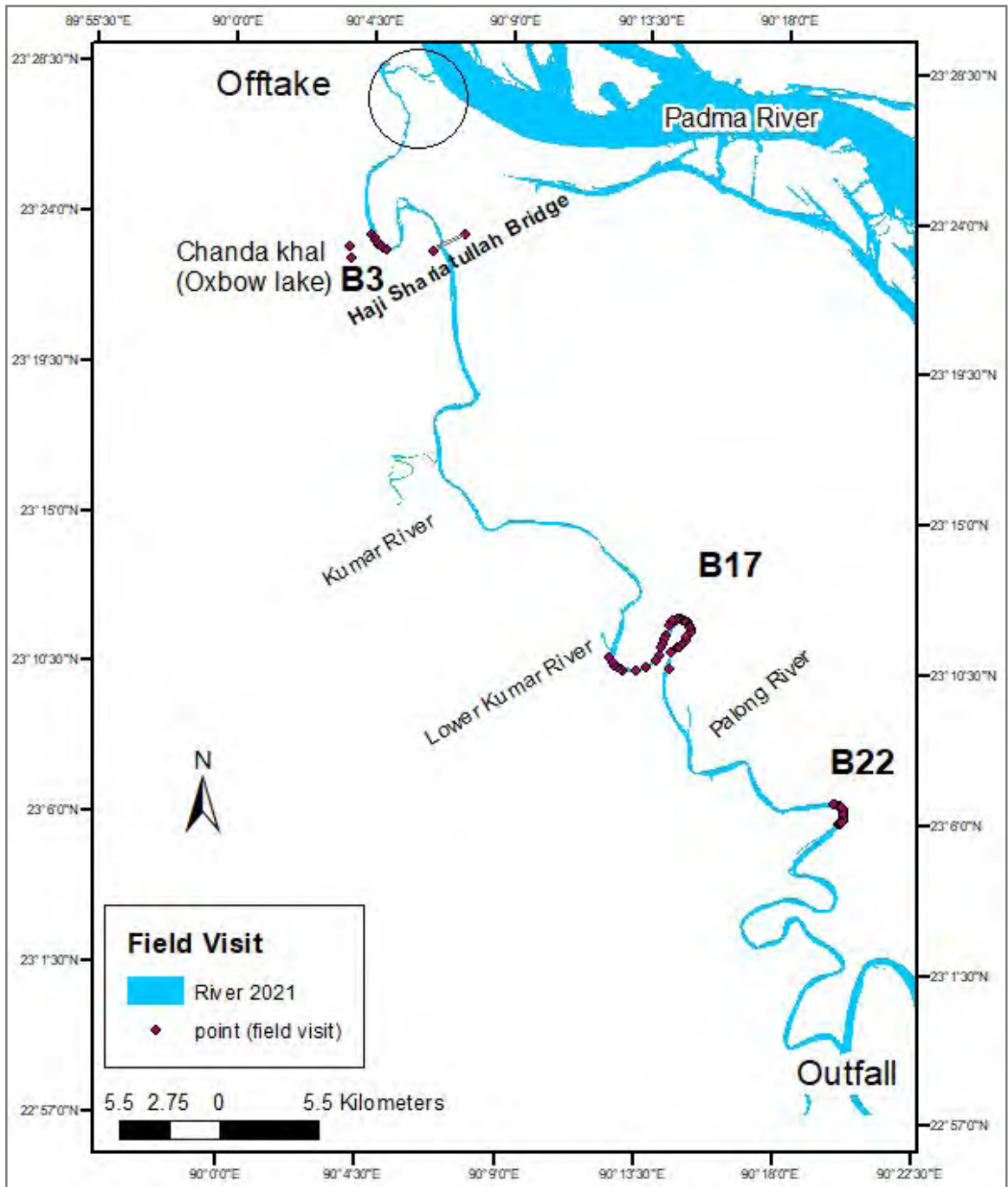


Figure 4.8: Field visit in three bends: B3, B17 and B22 of the three reaches.

CHAPTER FIVE

RESULTS AND DISCUSSION

5.1 Padma River near the Offtake of Arial Khan River

The Padma River planform near the Arial Khan confluence exhibits a periodic change in channel formation; alternate straight- single thread channel and meandering/ braided-anabranches/ double threads with single or multiple mid-channel bars. During the transformation of the channel from meandering/braided to straight/ single-threaded, the accretion process along the right bank dominates over the erosion process, but mid-channel bars are departed and water flows in the comparatively narrower channel. The flow regime is diverted along the left bank. Alternately, when the erosion process dominates along the right bank, the river changes its course from straight to meander/ braided with the multithread channel (Sarker, 2008) and bars accumulate in mid-channel and along the left bank. A significant width variation of the Padma River at the Arial Khan River offtake shown in Table 5.1 proves that the accretion and erosion process has occurred in every alternate period along the right bank during the years of the study period from 1972 to 2021. The bar push phenomenon accelerates the erosion to take place at the outer bank of the meander (right bank), resulting in expansion of the bend and the river width as well. Figure 5.1 represents the different phases of the channel and mid-channel bar formation of the Padma and the shifting of the Arial Khan Offtake consequently, where the red dot is the reference point.

Table 5.1: The Padma River near the Arial Khan River offtake during the study period.

Year	Width of the Padma River Section Near the Offtake (km)	Pattern of the Section
1972	11.25	Meander-double threads, separated by large bar
1980	7.3	Straight- single thread, small mid channel bar
1999	11.00	Meander- double threads, separated by large bar
2007	5.45	Straight
2021	8.25	Meander- double threads, separated by large bar

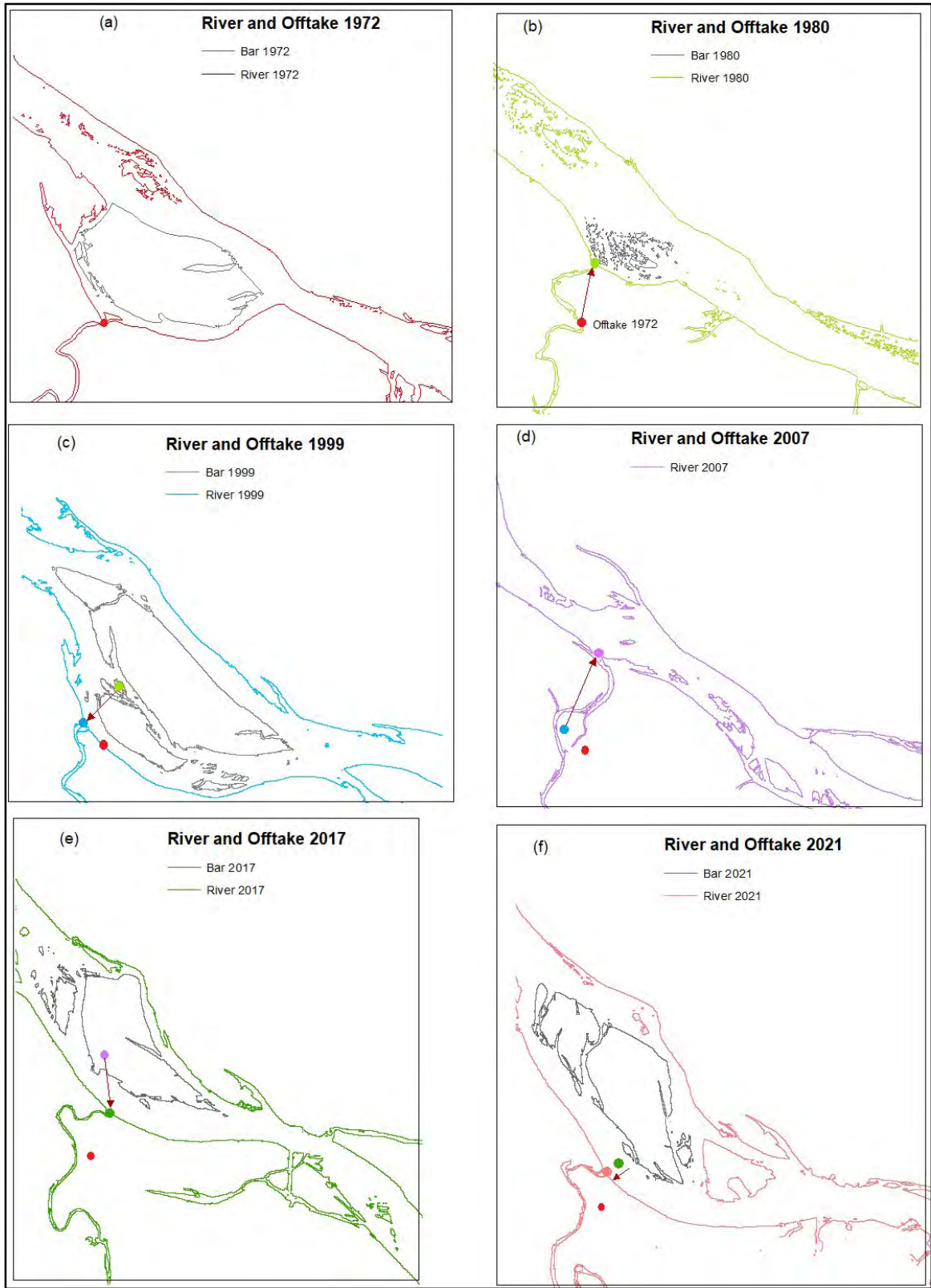


Figure 5.1: The meandering channel and mid-channel bar formation of the Padma and the downward shifting of the off-take in (a), (c), (e), and (f); straight channel and upward shifting of the off-take in (b) and (d).

Historically, the Padma River left bank of this section remains almost in position (Nippon Koei Co., 2005), though temporarily some sand bars have been accumulated during the period of accretion process and washed away along with the mid-channel bars during the erosion process. The erosion process sustains on an average for consecutive 19 years. But accretion/ deposition process takes place in a relatively shorter period of 8 years.

5.2 Diversion of Discharge into the Arial Khan River

The diversion of flow into the Arial Khan from the Padma is not constant but varies from time to time. During 1987 -1990 the diversion was found too higher. During the study period, the analysis reveals that a minimum of 2% and a maximum of 6% flow of the Padma River had passed through the Arial Khan, with an average value of 3%. The Padma River does not follow any particular trend of discharge (Zheng et al., 2021).

The authors have also studied suspended sediment flux and suspended sediment concentration of the Padma River. From the study, Figure 5.2 represents the total suspended matter (TSM) concentration from the period 1991 to 2019.

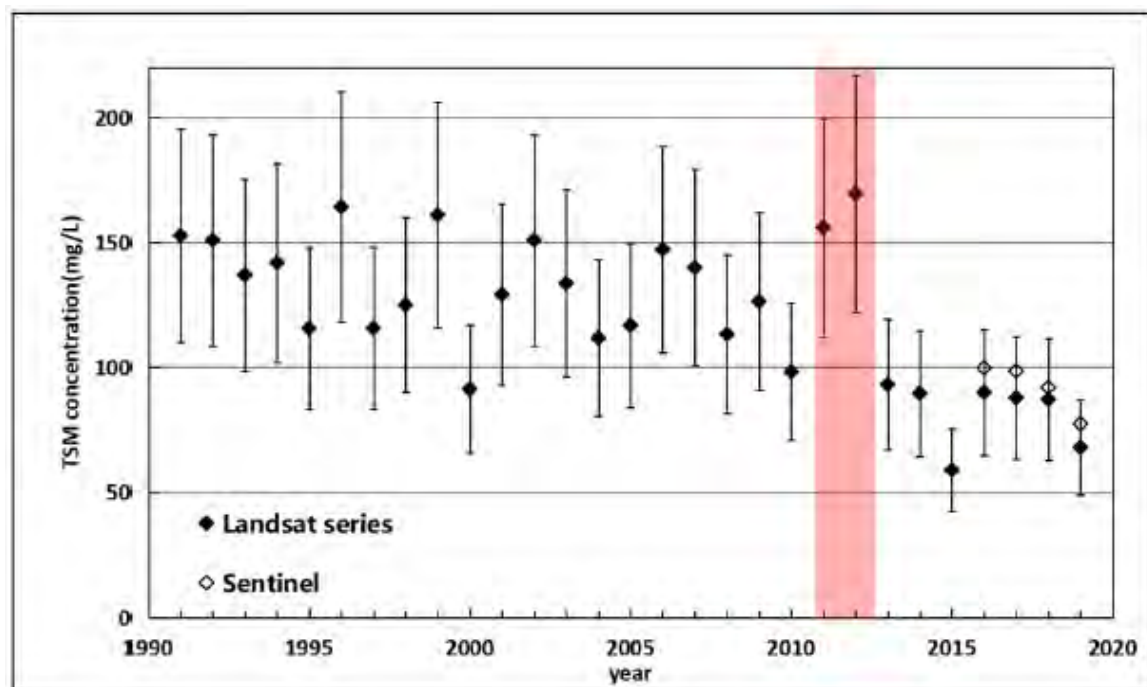


Figure 5.2: The concentration of total suspended matters in the Padma River in the period 1991–2019, and the red area represents the duration of La Niña (Zheng et al., 2021).

It has been found that TSM concentration is in a continuous decreasing trend since 2007 except for the period of La Niña, having heavy rainfall.

5.3 Temporal Change of the Offtake Hydro-morphology

5.3.1 Offtake shifting

The offtake hydro-morphology comprises three interdependent elements: the existence of mid-channel bars in front of the offtake, the channel form of the Padma near the offtake, i.e., straight/meandering, and the direction of the flow regime of the Padma near offtake. Table 5.2 provides some data on the offtake morphological changes of the Arial Khan River; these changes play an important role in flow diversion into the Arial Khan from the parent river Padma.

Table 5.2: Offtake morphology. The (-) sign indicates downward shifting of the offtake.

Year	Offtake Shifting (km)	Bar Size (km ²)	Remarks
1972	-	83	Single mid-channel bar
1980	5.07	> 1	Numerous small bars
1999	-4.31	140	Accumulated bar
2007	6.72	-	Almost no bar
2021	-5.68	79	Accumulated bar

During meandering channel formation, the offtake had shifted along the right bank and was situated nearly at the apex point of the bend. The right bank erosion and the mid-channel bar accumulation had occurred simultaneously and guided the direction of the flow regime. The continuous growth of the several small bars sometimes had formed a single extended bar, which had diverted the flow into two threads along the left and right banks. But when the channel section of the Padma had in straight form, the offtake also had shifted and the directional flow moved towards the left bank (Nippon Koei Co., 2005).

5.3.2 Thalweg position of the offtake

The bathymetry analysis has revealed that the bed level/ thalweg of the offtake at section no. AKU1 is related to the offtake shifting as well as the channel form of the Padma River. From Figure 5.3 it is clear that the increasing pattern of thalweg had found during 1984-1994 and 2005-2015, these periods were within the periods of meander channel formation in 1981-1999 and 2008-2019. The opposite scenario persisted during straight channel formation, i.e., thalwegs were in decreasing pattern. Though the tipping points for both cases were reached some years before/ after the years of the ultimate limit of meander/ straight channel formation, which may be due to lag time in terms of the response of planform change. Thus, the diversion of the flow into the Arial Khan River not only depends on the Padma River flow but also on the morphology of the offtake.

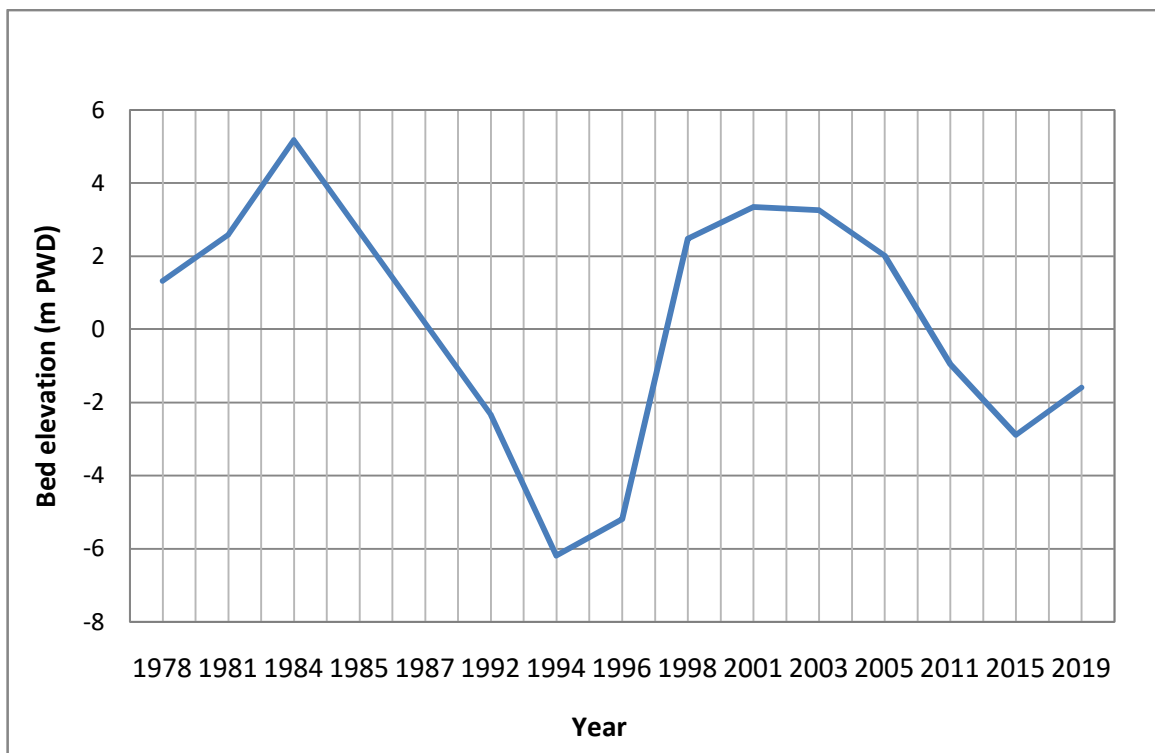


Figure 5.3: Temporal change of thalweg at Offtake-AKU1.

5.3.3 Discharge at the offtake station

The rating curve and graphical representation of the stage-discharge relationship of the Arial River for the years 2008 - 2019 were established by the available five months (June –October) gauge station data. The daily discharges of the offtake station for that period

were estimated by using the rating curve and the available daily stage data. The calculations for coefficients are given in Appendix C. The rating curve equations and the R² values between the relationships of estimated and observed Q are presented in Table 5.3, which indicates the existence of very good correlations in the relationships.

Table 5.3: Rating curve equation (2008-2019)

Year	$Q=Cr(G-a)^{\beta}$	R ²
2008	19.40(G-0.15) ^{2.85}	0.99
2009	40.74(G-0.10) ^{2.35}	0.93
2010	39.72(G-0.19) ^{2.34}	0.99
2011	54.46(G-0.22) ^{1.74}	0.83
2012	76.38(G-0.36) ^{1.93}	0.98
2013	25.35(G-0.67) ^{2.81}	0.97
2014	23.12(G-0.36) ^{2.84}	0.87
2015	52.17(G-0.55) ^{1.94}	0.98
2016	26.31(G-0.60) ^{2.63}	0.92
2017	12.14(G-0.27) ^{2.85}	0.98
2018	22.61(G-0.22) ^{2.68}	-
2019	293.04(G-0.43) ^{0.47}	0.82

The daily discharge data besides the years of estimated data were collected from BWDB. Figure 5.4 represents the Q_{max}, Q_{avg}, and Q_{min} at the offtake station. During 1971-1972, the Q_{max}, Q_{avg} were low, after that the Q_{avg} had been rising periodically and Q_{max} randomly for a long 28 years till 2000. Then plunged in successive years till 2011 except the years of moderate to high flood. But the study of Zheng et al. (2021) has mentioned that the Padma River does not follow any specific trend in discharge variation. Schumm (1968) found that the increase of dominant discharge sometimes increases bankful width and depth and decreases bed slope. On the other hand, an increase in dominant sediment discharge may cause increases in slope and width/depth ratio significantly.

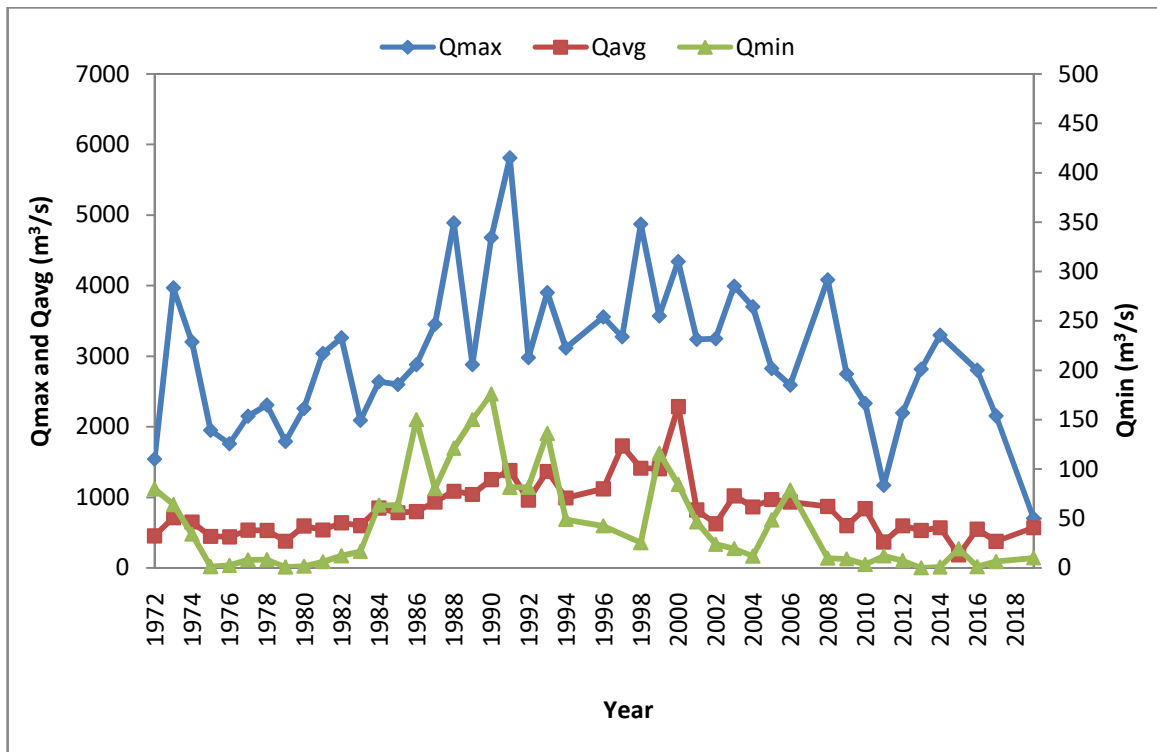


Figure 5.4: Maximum discharges (Qmax), average discharges (Qavg) and minimum discharges (Qmin) of the Arial Khan River at Offtake.

5.3.4 Tidal influence on river width near offtake station

In the Arial Khan River, the tidal water range in the dry season remains higher. In 2019, the highest tidal range of 0.32 m was observed on 20 April at the offtake station SW4A. The bathymetric survey for the same year was conducted on 6 March for the section AKU1, close to the offtake station. The water width of $W = 123$ m was observed from the bathymetric survey on 6 March 2019. The change of river width by the tide of a specific day is presented in Figure 5.5. The observed width would be increased with a value of $W' = 126$ m with the highest tidal range of 0.32 m in the same year. Thus, $(W' - W) = 3$ m, represents the possible highest increase of the water width due to the highest tidal range of the year 2019. Though on the 6 of March, the measured tidal range was 0.25 m. The 3 m increase of width due to tidal influence will create a 1.5 m deviation of width in each bank of image data. According to Begum et al. (2018), the highest tidal range of the Arial Khan River was observed as 0.68 m. The river width would increase by 6 m in 2019 due to this tidal range. Thus, in the extreme case the maximum possible deviation between image data from actual data in each bank will be 3 m due to tidal influence if the image is

collected during low tide. As the tidal influence is less than 0.1 m during monsoon (Roy et al., 2021), the data of widths in monsoon have no variation due to tide.

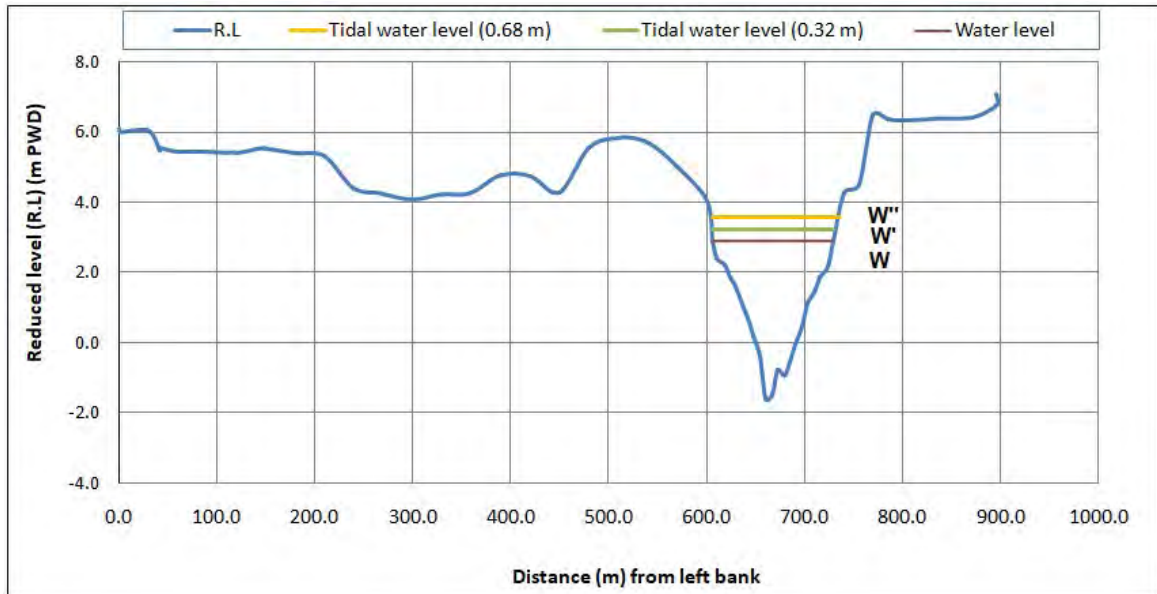


Figure 5.5: River water width for measured water level (W) and tidal water level (W' and W'')

5.4 Arial Khan Channel Geometry

5.5.1 General stability of river reach

The satellite image analysis of the planform has revealed that the upper reach R1 is very dynamic in terms of channel shifting and the bend migration as well, where bend cutoff occurred several times. The middle reach R2 can be described as avulsion prone region; two times channel avulsion had taken places where the latest channel has been following the path of the oldest channel. The lower reach R3 is relatively stable in terms of bend creation/ dissipation and the direction of the migration, as all the bends have existed from the beginning of the study period from 1972 to 2021 and have been migrating in the same direction. Though small-scale chute cutoff had occurred in some bend apexes; no significant change in the shape of the bend, location of the bend, and direction of the bend migration happened due to those chute cutoffs. According to the modified Brice classification scheme of the channel, presented in Figure 2.1, the R1 and the upper part of R2 reaches are class C type, which is described as channels of single-phase, the existence

of point bars and wider at bends. The rest of the lower part and R3 reaches are classified as type D, the channels described as single-phase, wider at bends with point bars and chutes common.

5.5.2 Length of river

There is a certain relationship between offtake shifting and the change in length of the Arial Khan River. This change is mostly resonated in the R1 reach. From Figure 5.6, it is found that the total length and the length of R1 reach have increased during the meandering of the Padma River or downward shifting of the offtake. Contrarily, the length has decreased during straight channel formation of the Padma or upward shifting of the offtake. But the opposite phenomenon should be occurred, as downward shifting makes reduction and upward shifting makes extra addition of the river flow path to some extent. On the other hand, the lengths of R2 and R3 reaches have increased successively during most of the time period, indicating offtake shifting has no impact on the change of the lengths of R2 and R3, but has a control on the change of the length of R1 and thus the entire River.

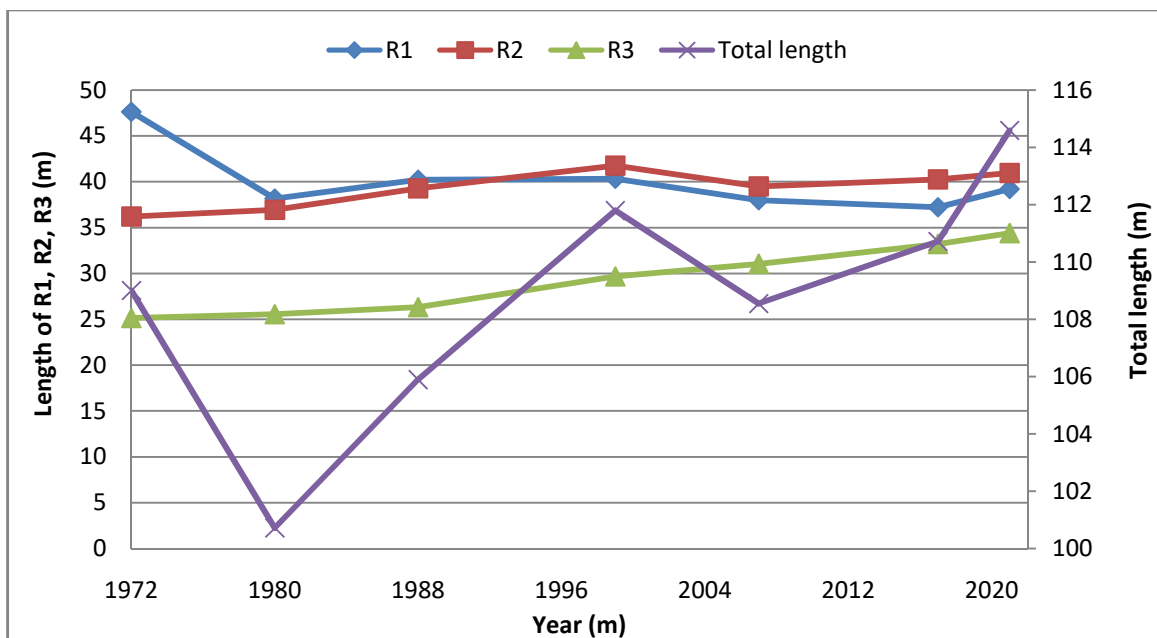


Figure 5.6: The changes of lengths of three reaches - R1, R2 and R3, and the entire river during different periods.

The change of length of the Arial Khan River and its correlation with the offtake shifting is shown in Figure 5.7. Generally, during upward shifting offtake follows northeast direction and during downward shifting southwest direction. There exists a moderate positive correlation between these two parameters.

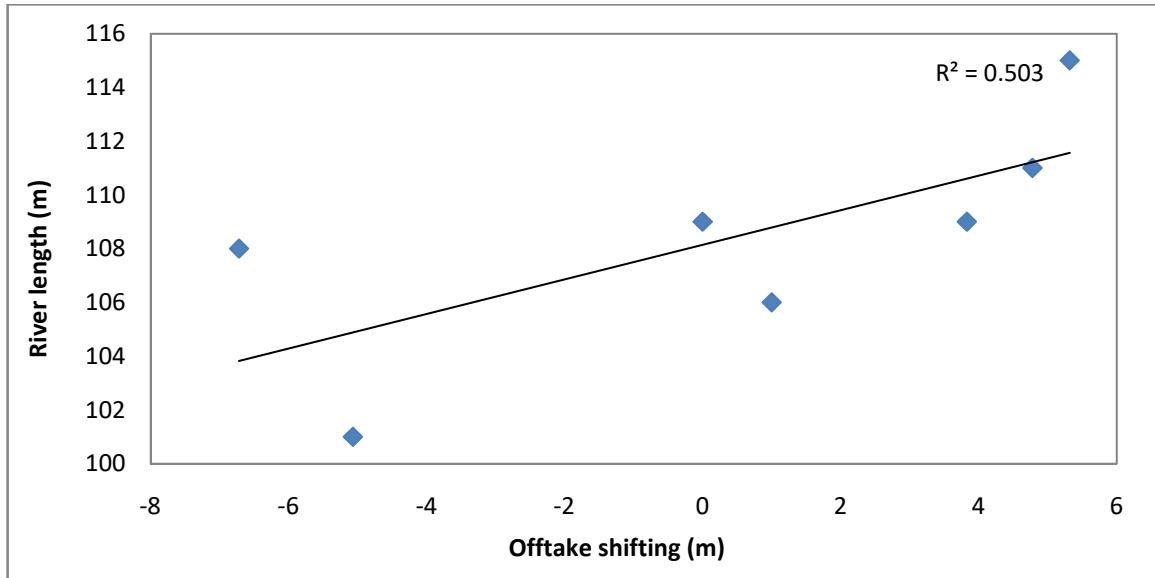


Figure 5.7: The relationship of offtake shifting and change of river length.

5.5.3 Width of river

The flow width of a river is an important parameter. Because the river cross-section increases by the increase of flow width than mean depth when discharge increases to a large extent (Rhoads, 2020). The average width of the river and reach-wise width variations with time are given in Figure 5.8. The pattern of these variations is almost similar for all the reaches and the entire river as well.

After 1972, the maximum width was generated in 1988 and then the width of all the reaches had been decreased till 2017. The reach-wise average width is found in the study as 237 m, 277 m and 320 m for the reaches R1, R2 and R3 respectively. The entire river has an average width of 281 m during the study period. In very recent years from 2017, an increasing spatial trend of width is seen in all the three reaches. The width variation is more likely interlinked with the variations of river discharge and the variation of sediment concentration, as presented in Figures 5.2 and 5.4. Notably, the impact of extreme floods in 1988 was captured in the width, as this data was the pre-monsoon (January/ February)

for the year 1988. On the other hand, the data of 1999 carried to some scale the impact of extreme flood occurred in 1998. Thus, extreme flood has an insignificant impact on river width variation, whereas higher discharge of consecutive years has a significant influence in changing the width of the Arial Khan River. Leopold and Maddock (1953) proposed a relationship between river flow width to discharge as $W \propto Q^{0.5}$.

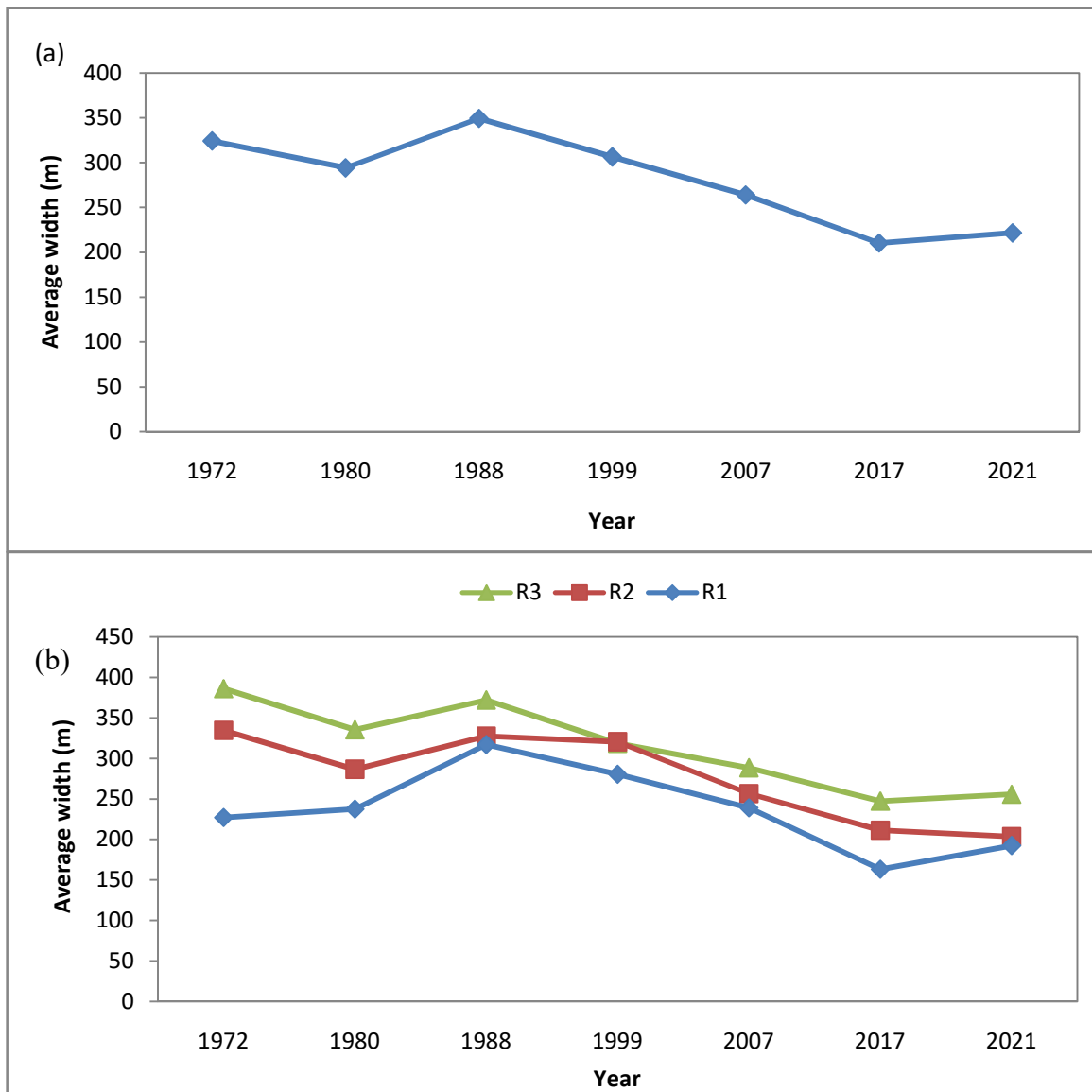


Figure 5.8: Temporal change of river width of (a) entire river and (b) different reaches - R1, R2 and R3.

It was estimated that the migration rates are generally 10% of the channel width but sometimes the rate is as high as 20%, though large alluvial rivers exhibit even more annual migration (Hooke, 1997). Generally, in large rivers, the dimensionless migration rates are

converted into considerable absolute rates. An example is given by Lagasse et al. (2004) as meanders had been observed to move at 750 m/year in large alluvial rivers. Again, the width measured in a 5 km interval along the entire river and in each bend (crossings and apex) is presented in Figure 5.9.

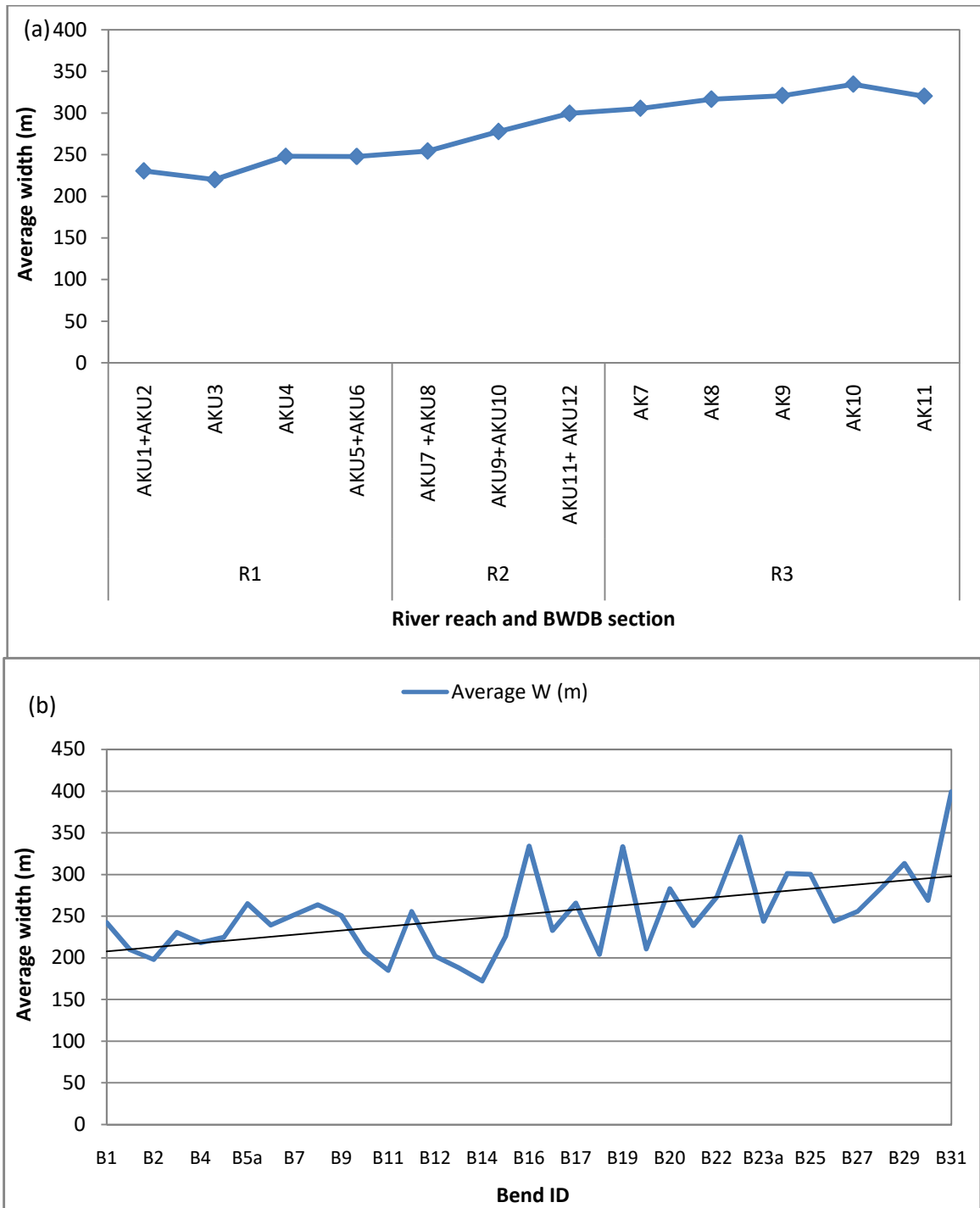


Figure 5.9: River width measured along (a) the entire length and (b) at 37 bend crossings and apex points from upstream to downstream.

There is a certain trend of width variation in sections and reaches, as width has successively increased from upstream to downstream. But the variation of the width of bends changes randomly along the river. The maximum average width of 335 m has been generated in section AK10, which is situated before the last section near the river outfall. On the other hand, the narrowest section of the river is AKU3 with an average width of 220 m. In the bend-scale, the bends B16, B19, B23, and B31 have higher values of width of 334 m, 333 m, 345 m, and 399 m respectively. The widths of the consecutive bends have huge variations. Overall, an increasing trend of width variation has been observed towards the downstream bends.

5.5.4 Depth and slope of river in a recent year

Available dry season data were used for the calculation of the depth and slope of the river. Figure 5.10 represents the average water depth along the river of each x-section in 2019. The water depth has successively increased from upstream to downstream. The highest depth was formed immediately before the downstream river mouth at section AK11. The average bed slope of the river was found as 0.037 m/km during this period.

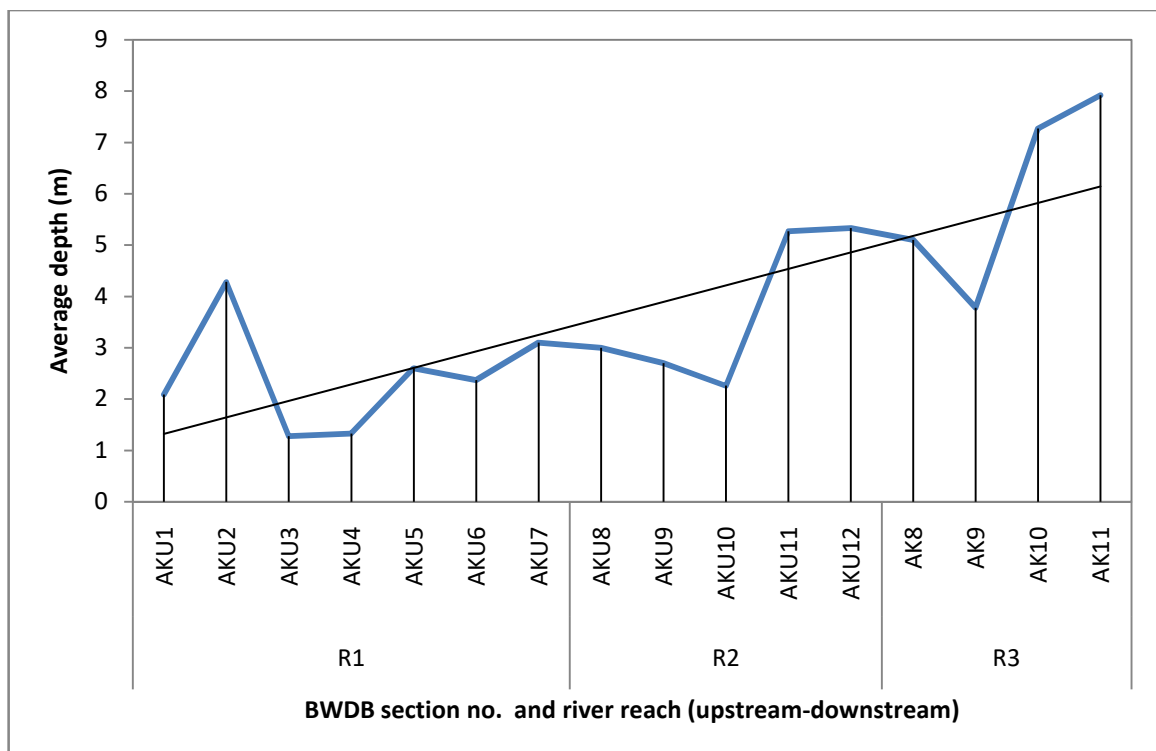


Figure 5.10: The average water depth at the sections corresponding to the three river reaches: R1, R2 and R3 in 2019.

5.5.5 River thalweg

The maximum depth/ thalweg of the river at different stations of the river reaches R1, R2 and R3 have changed with time, which are demonstrated in Figures 5.11 and 5.12. The river reaches of R1 and R2 attained its deeper bed level/ thalweg in three distinct periods, which were 1981-1985, 1994-1996, and 2003-2005. On the other hand, the deeper thalweg positions in R3 were attained in 1995 and 2003, which are marked by black circles on both the figures. The significant flood events were absent, but the value of Q_{max} and Q_{avg} were moderate during that period. The shallower thalwegs were formed during 1978-1981 and 2015 -2019 in R1 and R2, and during 1992-1994 and 2015 in R3; which are marked as red circles. The year 2003 exhibited the deepest bed level/ thalweg formation, whereas 2015 can be assigned as the year to form the shallowest bed level/ thalweg in most of the sections along the Arial Khan River.

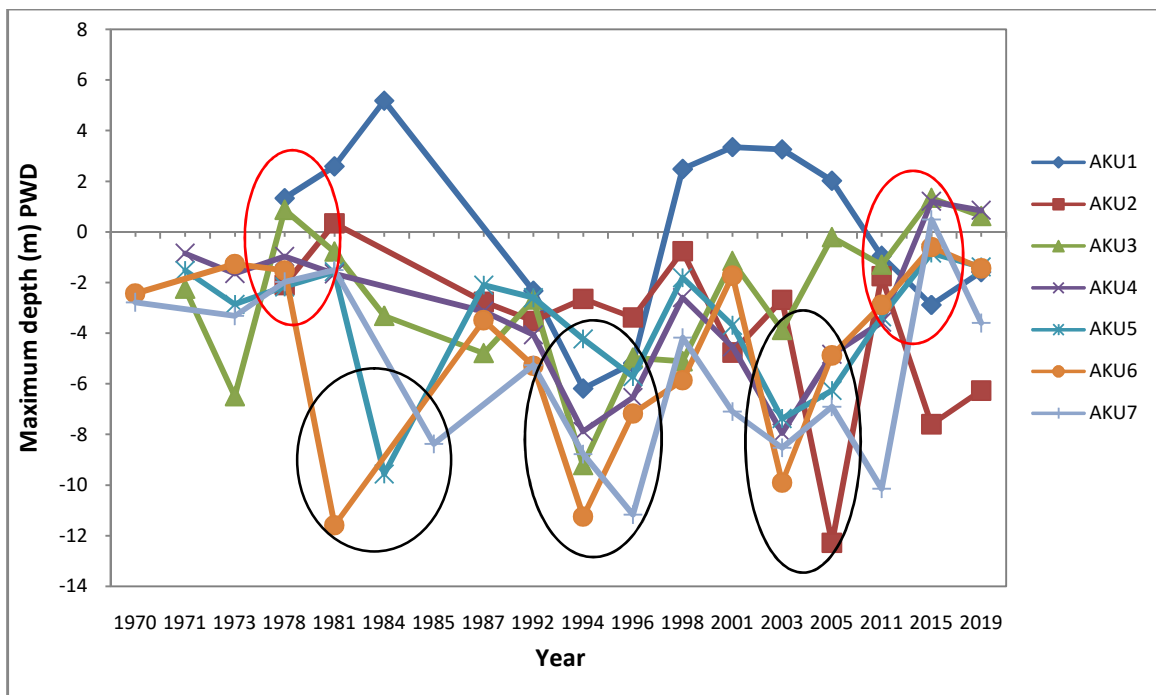


Figure 5.11: Change of maximum depth/ thalweg at different sections of the R1 reach.

Based on the time-scale variation of the thalweg of the river, the average thalweg of different sections is presented in Figure 5.13. The thalweg is the shallowest in the section - AKU1 near the offtake and the deepest in the section - AK10, in the river mouth before the downstream confluence. Because the section of the channel facing highly variable discharge regimes is comparatively narrower and shallower than the section with less

variable regimes (Rosgen, 1994). The average thalweg of R2 is quite constant. Along the entire river, a climbing up pattern of average thalweg downstream to upstream has been found.

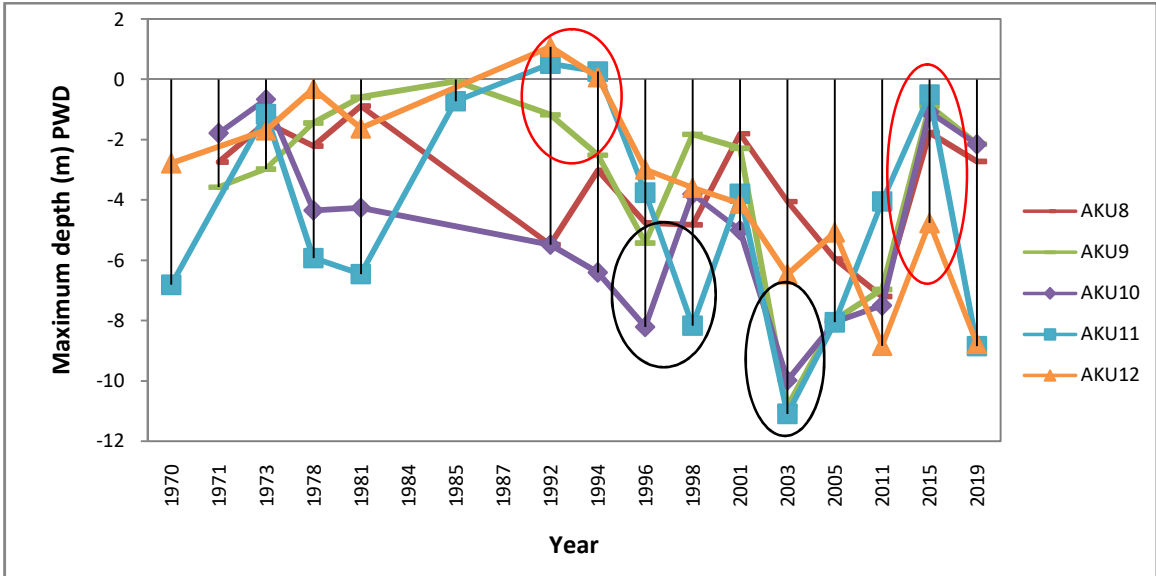


Figure 5.12: Change of maximum depth/ thalweg at different sections of the R2 reach.

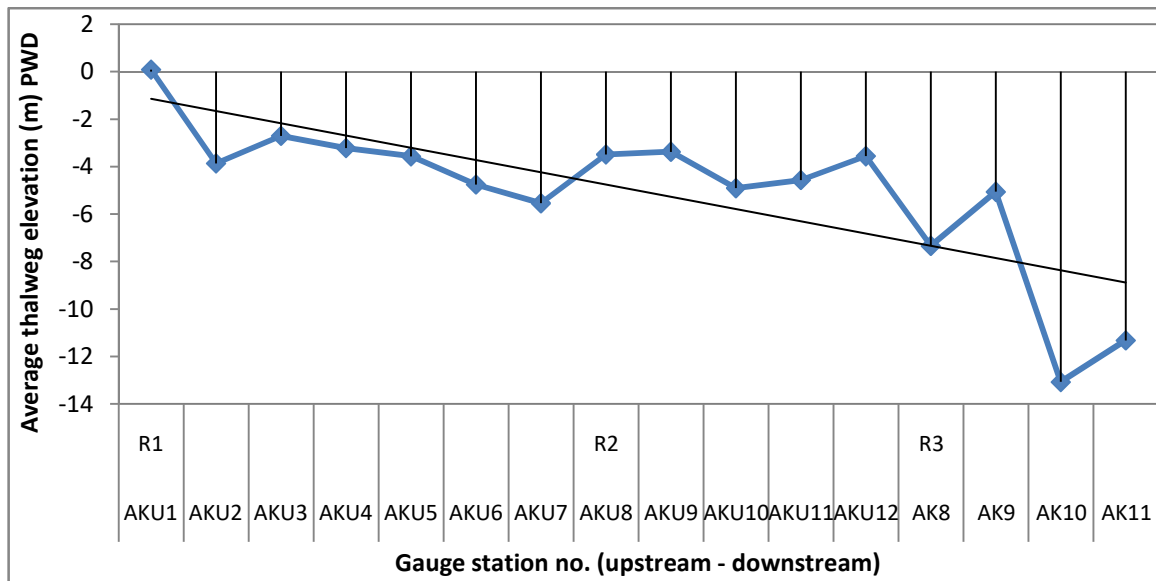


Figure 5.13: Average thalweg elevation at all the stations, estimated from 1972 to 2019.

5.5.6 Sinuosity of the river

The meander/ straight channel formation into the section of the Padma River is translated and responded into the Arial Khan which is initiated by the shifting of the offtake position.

Analysis has revealed that a certain correlation exists between offtake shifting and change of the river SI, especially in the R1reach as demonstrated in Figure 5.14. The R1 reach has exhibited great variation with time in SI value. But in R2 reach, SI has been quite constant with a value around 1.5. There is an increasing trend of SI in R3 reach. Like R1reach, the SI of the entire river has shown fluctuation within a shorter range of 1.5- 2. The SI value of R1, R2, and R3 reach, and the entire river have a range of 1.5-2.5.

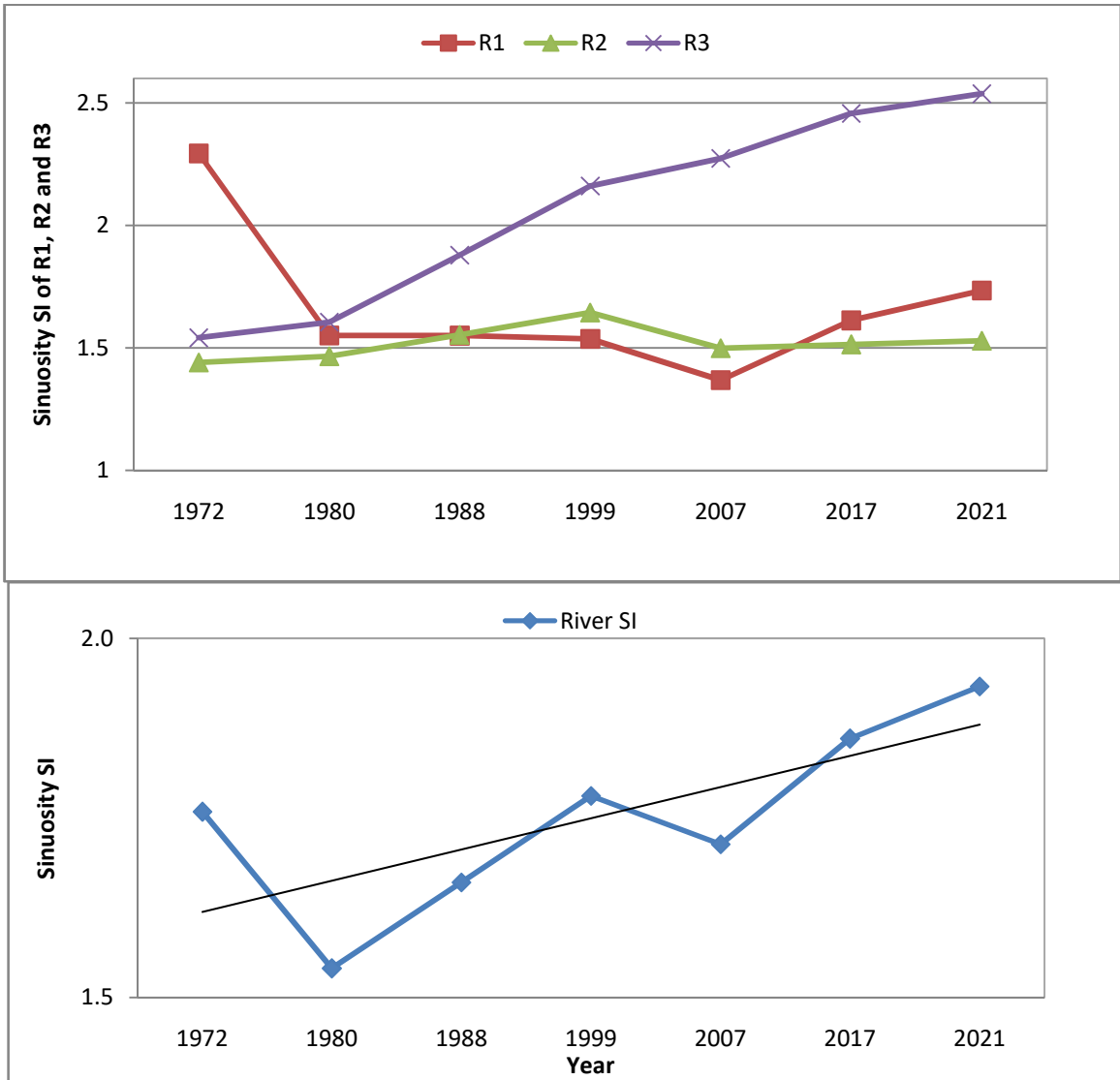


Figure 5.14: The change of SI in different reaches: R1, R2 and R3 and in entire river in different periods.

According to channel classification, the channels are called meander when $1.3 < SI < 2.5$. Thus, the Arial Khan River and each reach of R1, R2, and R3 individually are meandering river/ reach. The meandering in planform had decreased in 1980. After that, the river

meandering has been increasing almost successively till 2021. For the meandering river, the SI is scale-independent, which means it does not vary with the increase of discharge or channel width but depends on sediment load and the channel boundary condition (Rhoads, 2020).

The change of sinuosity and its correlation with the offtake shifting of the Arial Khan River are shown in Figure 5.15. The correlation of determination is 0.66, which means that there exists a moderate positive correlation between the offtake shifting and the change of river sinuosity. Both the values of SI and length were higher during downward shifting of the offtake or meander channel formation in the Padma and the values were lower during upward shifting of the offtake or straight channel formation in the Padma. Though a mounting trend has been observed over the study years in the value of SI and the river length, the SI is related to the length of the river, and thus the change of SI is obvious due to the morphological change of the offtake.

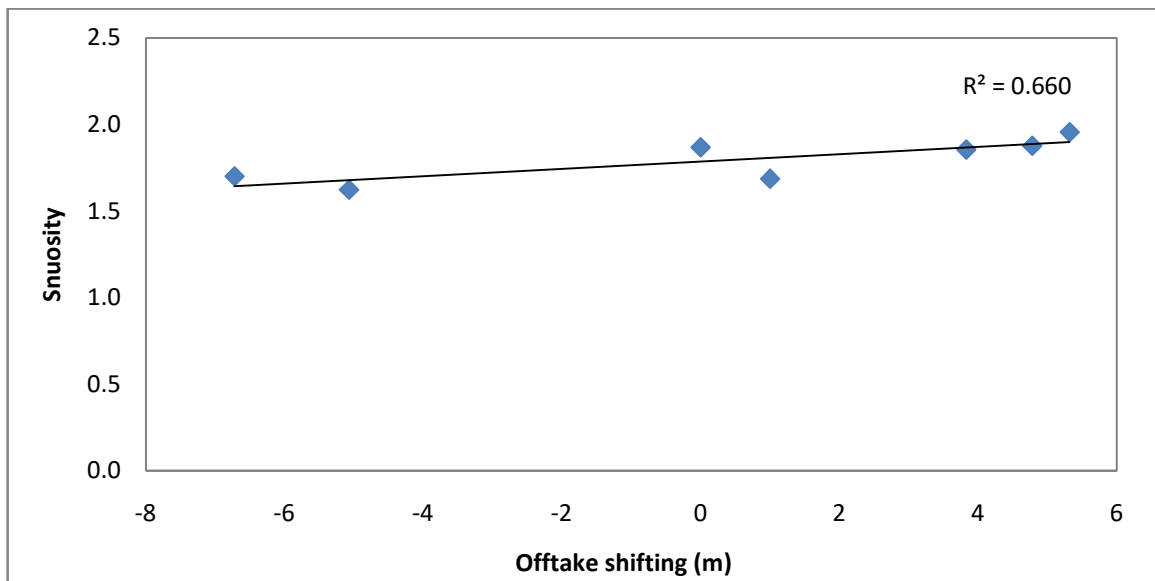


Figure 5.15: The relationship of offtake shifting and change of river sinuosity.

5.5.7 Channel aspect ratio and river migration

As the river morphology of an active alluvial river continuously goes into an adjustment process with the variation of hydrology, time-scale change in river width and depth is very common. An important parameter is the river width to depth ratio and termed as the aspect ratio (W/D), which determines whether the channel will migrate or not and which section

of a long channel will migrate comparatively more in near future. In general, the channel with a larger W/D migrates more than the smaller one. Figure 5.16 presents that during the higher value of W/D the river had migrated more than at the lower value.

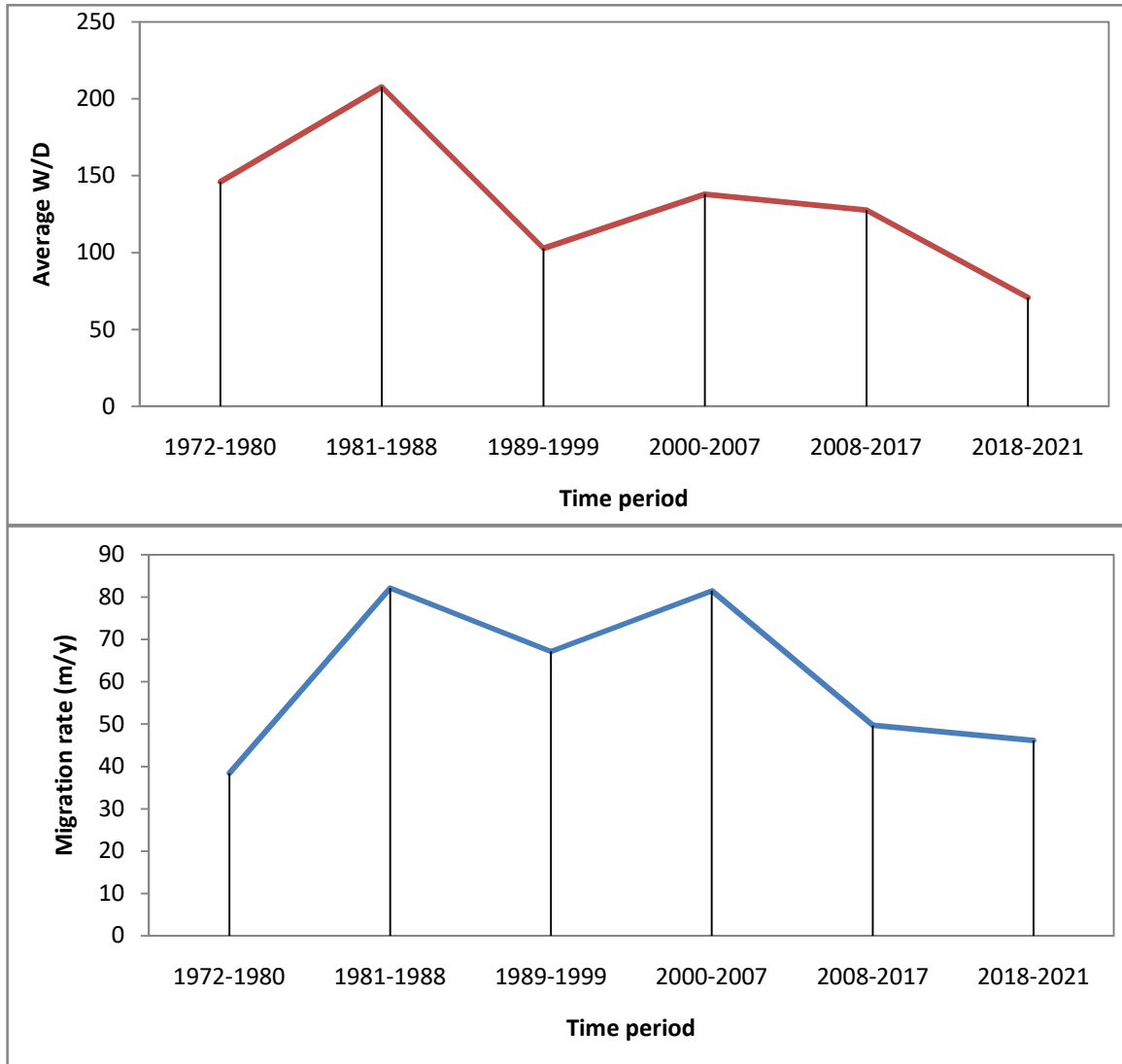


Figure 5.16: Time-scale change of the average aspect ratio and migration rate of the Arial Khan River.

The literature has suggested that in the narrow channel in which the W/D ratio is less than 10–20, bar units do not develop (Seminara and Tubino, 1989). Because in this case thalweg passes through almost the middle of the channel and a mid-channel concentrated flow regime develops. As a result, less chance is arisen to build up bar units and banks stay away from flow attacks. But the W/D of the Arial Khan River is high and greater than 50. Thus, the river is susceptible to a faster river migration and bar unit formation. Figure

5.17 demonstrates the river reach-wise average aspect ratio and average migration rate during the study period from 1972 to 2021. The aspect ratio is higher at R1 reach and successively decreases toward downstream, but the migration rate is the highest in the upper reach R1 and the lowest in the middle reach R2. These two parameters are consistent for R1 and R3 but in that sense not consistent for R2. Perhaps the presence of bank protection measures in R2 has been interrupting the free adjustment of the river course.

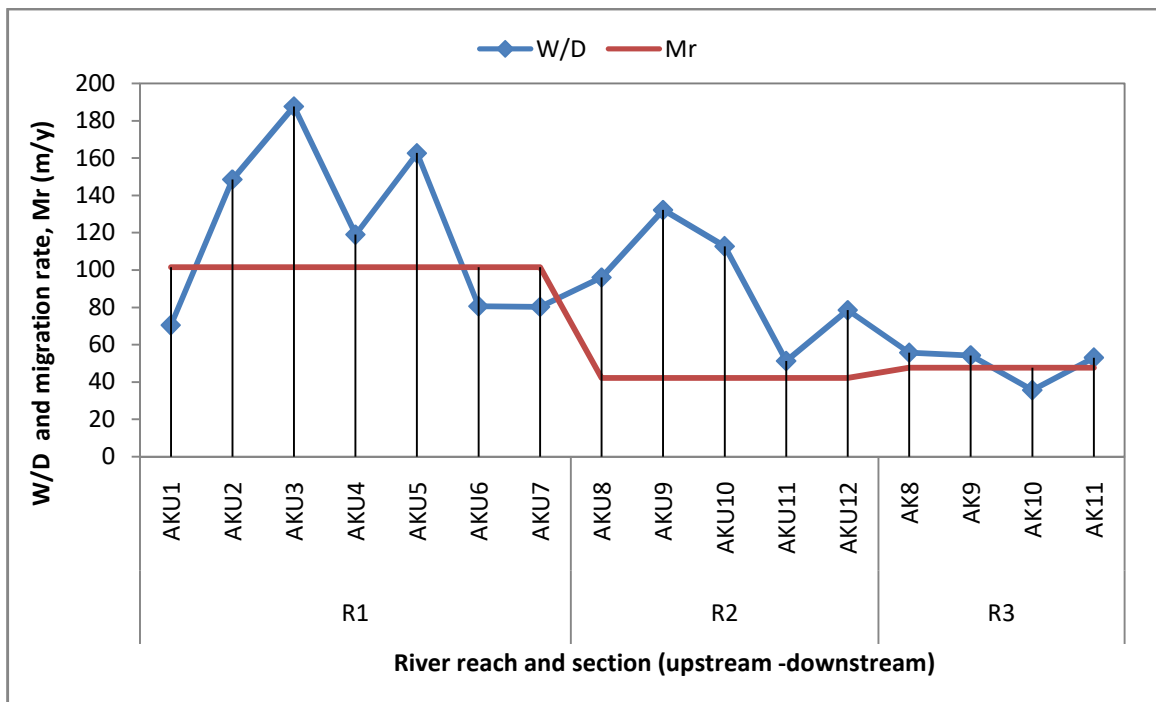


Figure 5.17: The dimensionless aspect ratio (W/D) and average migration rate at different sections and reaches of the Arial Khan River.

5.6 Arial Khan Bend Geometry

The meander bend is represented by a starting point (upstream end), an ending point (downstream end), a location of the center of bend radius (bend centroid), an orientation with respect to a baseline (e.g., down valley direction), and an outside bank curvature (R_C) (Lagasse et al., 2004).

The natural meandering channels have bends with varying curvatures which transports bed material in different degrees. The helical motion and the curvature effect promote the deposition of sediment flux along the inner bank and the erosion along the outer bank,

resulting in bend migration, bend cutoff, new bend generation, and sometimes change of floodplain. During the study period from 1972 to 2021, the existence of the total bends was 37. Some bends had changed its shape in terms of neck cutoff, chute cutoff, or sometimes bends were disappeared by straightening the channel. The modes of change of the bends and the channel are listed given in Figure 5.18.

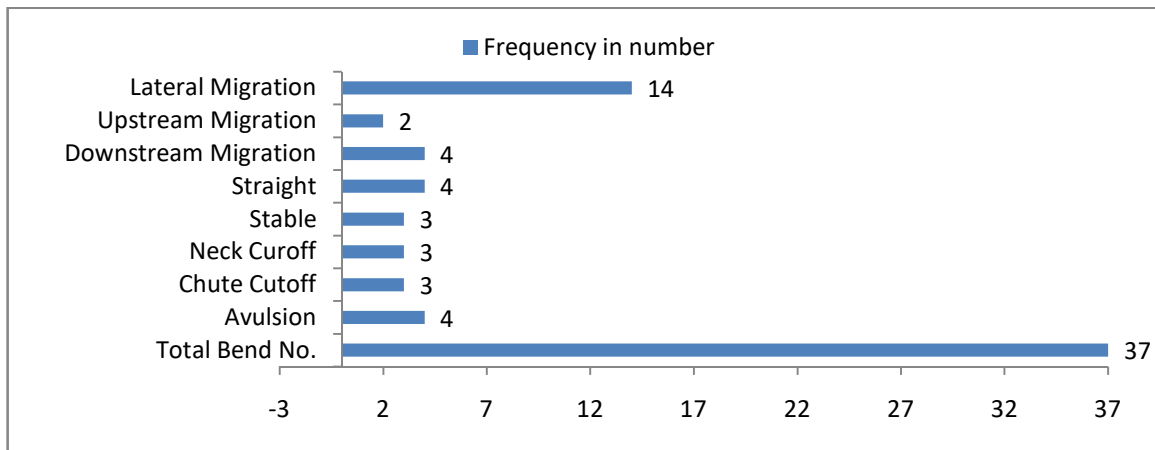


Figure 5.18: Bend geometry of the Arial Khan River.

5.6.1 Bend Generation

The evolution of a natural meander river is associated with new bend generation, matured bend modification, and continuous migration of the river within the river valley. The Arial Khan River is also a natural meander river, except very few kilometers of protected banks exist in some places. A total of 37 characteristic bends are analyzed in this study; the list of the bends is given in Table 5.4. During the long 49 years of the study period, several bends formed and disappeared. In some time periods, the bend formation was high, and in other periods the no. of bend disappearance and migration at a fast pace were noticeable. From 1988/1989 to 1999/2000, no. of bend formation was high. The lowest no. of bends existed in 1972 and 2021. The generation, development, and representative years of existence of these bends are different. Initially, in 1972, the total bend nos. were 17; it increased to 25 during the period of 1989-1999, and again it got decreased. In 2021, the total no. has turned as the initial no. of bends, 17. New bend generation, bend cutoff, and migration; all are very prompted in the R1 reach and slowed down towards downstream.

Table 5.4: Generation of the bends in the Arial Khan River in different time periods.

River Reach	Bend ID	1972	1980	1988	1989	1998	1999	2007	2017	2018	2021	Age (years)	Average Age (years)	
R1	B1	√	√	—	—	—	—	—	—	—	—	15	18	
	B1a	—	—	√	√	√	√	√	√	√	√	33		
	B2	√	√	—	—	—	—	—	—	—	—	8		
	B3	—	√	√	√	√	√	√	√	√	√	41		
	B4	—	—	√	—	√	√	√	√	√	√	33		
	B5	√	—	—	—	—	—	—	—	—	—	6		
	B5a	—	√	√	√	√	√	√	—	—	—	27		
	B6	—	—	√	√	√	√	√	√	—	—	—		19
	B7	—	—	√	√	√	√	√	√	—	—	—		19
	B8	—	—	√	√	√	√	√	√	—	—	—		19
	B9	—	—	—	—	√	√	√	√	√	√	√		23
	B10	—	—	—	—	—	—	—	—	√	√	√		4
	B11	√	—	—	—	—	—	—	—	—	—	—		4
	B11a	—	√	√	√	—	—	—	—	—	—	—		8
R2	B12	√	√	√	√	√	√	—	—	—	—	27	25	
	B13	√	√	—	—	—	—	—	—	—	—	6		
	B14	—	—	—	—	√	√	√	√	√	√	23		
	B15	—	—	—	—	√	√	√	√	√	√	23		
	B16	√	√	√	√	√	√	—	—	—	—	27		
	B16a	—	—	—	—	—	—	√	√	√	√	14		
	B17	√	√	√	√	√	√	√	√	√	√	49		
	B18	—	—	—	—	√	√	√	√	√	√	23		
	B19	√	√	√	√	√	√	—	—	—	—	27		
	B19a	—	—	—	—	—	—	√	√	√	√	14		
	B20	√	√	√	√	√	√	√	√	√	√	49		
R3	B21	—	—	—	—	√	√	√	√	√	√	23	32	
	B22	√	√	√	√	√	√	√	√	√	√	49		
	B23	√	√	√	√	√	√	—	—	—	—	27		
	B23a	—	—	—	—	—	—	√	√	√	√	14		
	B24	√	√	√	√	√	√	√	√	√	√	49		
	B25	√	√	√	√	√	√	√	√	√	√	49		
	B26	—	—	—	—	√	√	√	√	√	√	23		
	B27	—	—	—	—	√	√	√	√	√	√	23		
	B28	√	√	√	√	√	√	√	√	√	√	49		
	B29	√	√	√	√	√	√	√	√	√	√	49		
	B30	—	—	—	—	—	—	√	√	√	√	14		
B31	√	√	—	—	—	—	—	—	—	—	10			
Total No. of Bends		17	18	19	25	25	25	23	23	23	17	Avg =24		

As the flow direction frequently changes in R1 within a very shorter period along with a high rate of erosion and deposition, the valley width is higher, and the sediment remains in an unconsolidated state in this region. Again, in the R1 reach, downstream migration dominates over lateral migration.

The age of each bend with bend ID and river reach position is presented in Figure 5.19. Only seven bends have fulfilled the lifetime of the study period (1972-2021), situated mostly in R3 and R2. The average age of the bends in R1 was low, intermediate in R2, and relatively high in R3.

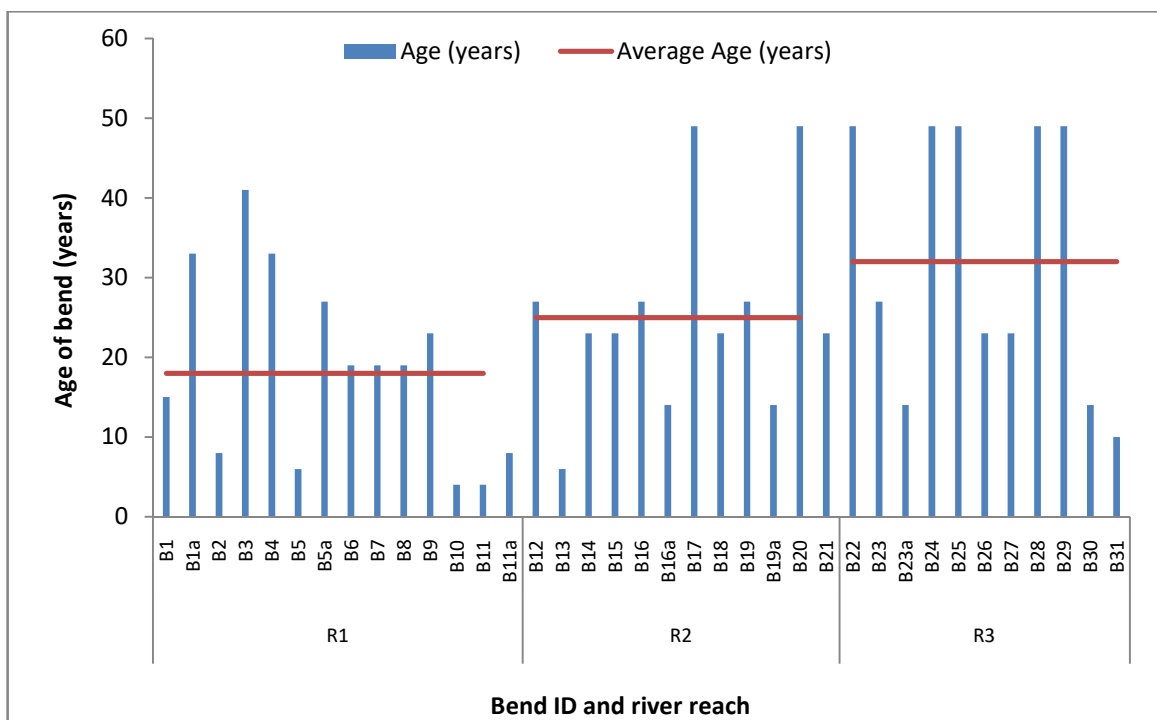


Figure 5.19: Age of each bend and the reach-wise average age of the bends.

5.6.2 Modes of migration of different bends

Some distinct modes of migration are visible in different reaches and are represented in Table 5.5. Among all the three reaches of the river, R1 is very dynamic. All modes of migration existed in R1, where a significant number of bend cutoffs had taken place. Some bends had converted into straight channels, especially downstream of R1; those straightening could be due to the effect of river training work for the Haji Shariatullah Bridge. R2 reach can be characterized as avulsion prone as avulsion had occurred two

times in this reach. But during the second time, the avulsion channel followed almost the same path as that of the initial channel. This part of the river has been occupied by several stable bends and the overall channel stability of this section is higher than the rest of the two reaches R1 and R3. The mid-section of this reach R2 has a long and sustain protected bank for Madaripur town protection; the project was implemented in 1987. The bend migration of the lower reach R3 had been dominated by mostly lateral migration and the erosion was unidirectional.

Table 5.5: Shape of different bends and their modes of migration.

River Reach	Bend ID	1972	1980	1988	1999	2007	2017	2021	Migration Mode
R1	B1	SA	Ep	—	—	—	—	—	CO
	B1a	—	—	SS	Ep	Ep	Ep	Ep	LM
	B2	SS	Ro	—	—	—	—	—	Straight
	B3	—	SS	Ep	Tr	Tr	Tr	Tr	DM
	B4	—	—	SS	Ep	Tr	Ro	Ep	UM
	B5	ACL	—	—	—	—	—	—	CO
	B5a	—	SS	Et & Ro	Et	—	—	—	CO
	B6	—	—	SS	Ep & Ro	Tr	—	—	Straight
	B7	—	—	SS	Et & Tr	Et & Tr	—	—	Straight
	B8	—	—	SS	Et & Tr	Et & Tr	—	—	Straight
	B9	—	—	—	SS	Et & Tr	Et & Tr	Stable	DM
	B10	—	—	—	—	—	New	Ep	LM
	B11	SCL	—	—	—	—	—	—	CO
B11a	—	AEL	Ex & Ro	—	—	—	—	Avulsion	
R2	B12	SS	Et	Tr	Ep	—	—	—	Avulsion
	B13	SA	Ro	—	—	—	—	—	Avulsion
	B14	—	—	—	SS	Et	Et & Tr	Stable	LM
	B15	—	—	—	SS	Tr	Tr	Ep	LM
	B16	SS	Ep	Ep & Ro	Stable	Stable	Stable	Stable	Stable
	B16a	—	—	—	—	SS	Ep	Ep	LM
	B17	SS	Stable	Ep	Ep	Ep	Ep	Ep	LM
	B18	—	—	—	SS	Ep	Stable	Stable	Stable
	B19	SS	Stable	Ep	Tr	—	—	—	CO
	B19a	—	—	—	—	SS	Et & Tr	Et & Tr	DM
	B20	SS	Stable	Ep	Ep	Et & Tr	Ep	Stable	LM
B21	—	—	—	SS	Ep	Ep	Ep	LM	

Table 5.5: (Continued...)

River Reach	Bend ID	1972	1980	1988	1999	2007	2017	2021	Migration Mode
R3	B22	SS	Stable	Ep	Tr	Ep	Stable	Stable	Stable
	B23	SA	Stable	Ep	Ep	—	—	—	CO
	B23a	—	—	—	—	SA	Ep	Ep	LM
	B24	SA	Stable	Et	Ro	Ro	Et	Ep	LM
	B25	SS	Ep	Ep	Ro	Ep	Et	Et	LM
	B26	—	—	—	SS	Tr	Tr	Tr	DM
	B27	—	—	—	SA	Ep	Ep	Ep	LM
	B28	SS	Ep	Ep	Ep	Ro	Ep	Ep	LM
	B29	SS	Et	Ro	Ro	Ep	Ep	Ep	LM
	B30	—	—	—	—	SS	Ep	Ep	UM
	B31	SS	Ep	—	—	—	—	—	Avulsion
Total Bend		17	18	19	25	25	23	23	37

Note: ACL = Asymmetrical Compound Loop, CL = Compound Loop, SS = Simple Symmetrical, SA = Simple Asymmetrical, AEL = Asymmetrical Elongated Loop, Ep = Expansion, Ro = Rotation, Tr = Translation, Et = Extension, CO =Cutoff, LM = Lateral Migration, DM = Downstream Migration, UM = Upstream Migration.

The R3 reach had experienced only small-scale chute type cutoffs in two bends, which did not significantly change the shape of the bends. In R3 reach, the plan-view shape of most of the bends did not change from its initial shape in 1972. The channel shifting in this reach was only bend oriented; other than the bend portion the channel shifting was comparatively low or negligible.

In a total of 37 bends, considering the last two time periods of 2007-2017 and 2017-2021, the no. of stable bends is 3; 14 bends have migrated laterally; downstream migration has occurred in 4 bends; upstream migration in 2, so far total bend cutoff no. is 6, bend avulsion no. 4 and 4 nos. of bends have diverted to the straight channel.

5.6.3 Radius of curvature of bend

The bends of the Arial Khan River are of different sizes and shapes. The river course adjustment and numerous changes in the shape of bends are very common for this river. Thus, the bend curvatures were also formed with varying radii. The average R_C of the Arial Khan River bends was 921 m, though most of the curvatures were below the average radii as shown in Figure 5.20. In the reach scale, the average R_C were 775 m, 1127 m and 883 m in the reach of R1, R2 and R3 respectively. These values were relatively higher in R2 than in R2 and R3.

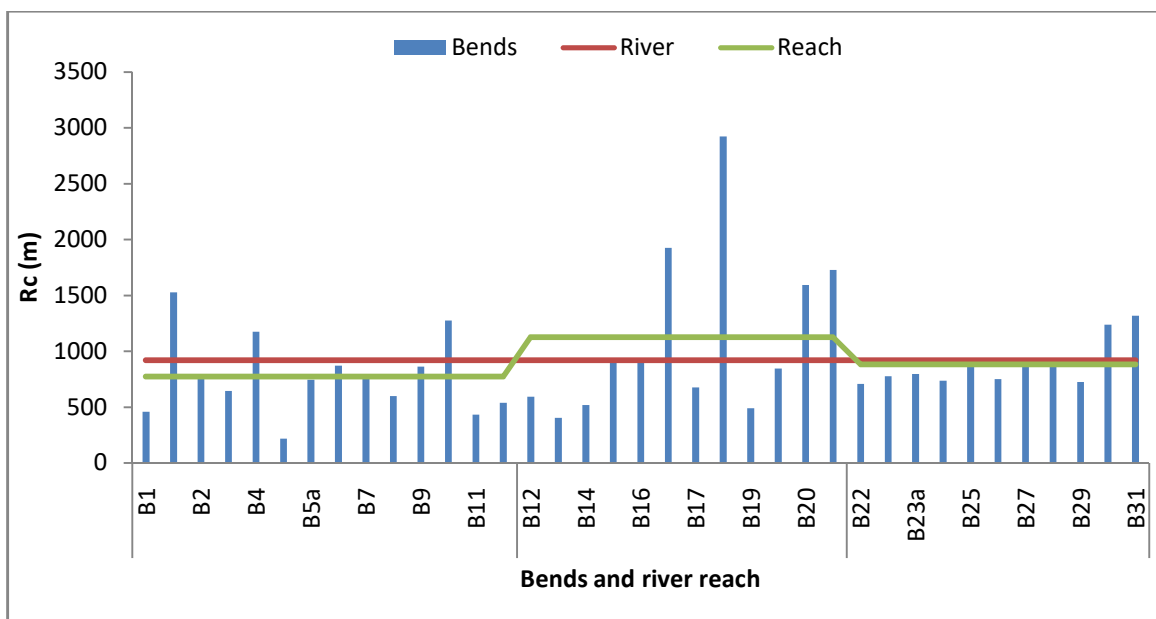


Figure 5.20: R_C values for different bends of the Arial Khan River.

5.6.4 Bend cutoff

Among different types of migrations, cutoffs are a very important phenomenon for the planform dynamics of meander rivers. Cutoffs generally take part in the removal of bends from meandering rivers. It involves sudden lateral changes of the river by decreasing channel length and channel sinuosity, and increasing channel slope, velocity, and sediment transport (Julien, 2018). Generally, a new bend develops soon at the cutoff point and evolves in the same direction as the previous bend. Neck cutoffs are independent of overbank flow, but the occurrence of chute cutoffs generally depend on overbank flow. However, the initiation of cutoff and further propagation may take place in any discharge.

The oxbow lake and meander scars are the resultant of cutoffs. The R_C of the cutoff bends and the year of cutoff are presented in Table 5.6. Among the six significant cutoffs during the study period, three occurred during 1972- 1990 and the rest three occurred during 1991-2004.

Table 5.6:Types of cutoff and radii of curvatures at the cutoff bends

Bend ID	R_C (m)					Cutoff type	Cutoff year
	1972	1980	1988	1999	2007		
B1 (Chute cutoff)	426	494	-	-	-	Chute	1988
B5 (Neck cutoff 1978)	218	-	-	-	-	Neck	1978
B5a (Neck cutoff 2004)	-	407	786	975	817	Neck	2004
B11 (Chute cutoff 1976)	432	-	-	-	-	Chute	1976
B19 (Neck cutoff 1999)	547	491	474	453	-	Neck	1999
B23 (Chute cutoff 2004))	881	848	857	521	-	Chute	2004

Figure 5.21 shows different common modes of migration in the bends, all three types of cutoffs are also existed here.

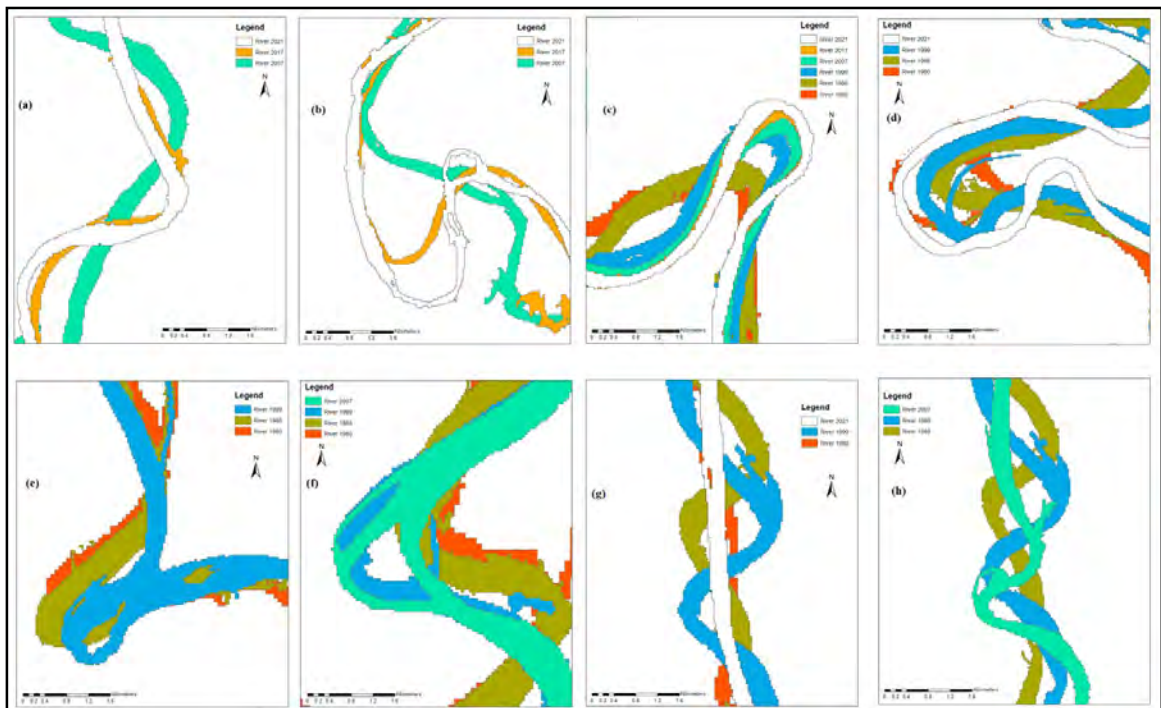


Figure 5.21: Different modes of migration in the Arial Khan River; (a) translation, (b) rotation, (c) extension, (d) expansion, (e) neck cutoff, (f) chute cutoff, (g) straight and (h) downward shifting.

The average period of cutoff is 8 years or 0.055 cutoffs per kilometer of the river, though R1 reach alone occupies 67% cutoff. The average R_C of the cutoff bends for the Arial Khan River is 501 m and the range is from 218-817 m. Harvey (1988) found in his study that 90% of total cutoffs occur for the bends with R_C less than 533 m.

5.6.5 Relative curvature of bend and reach

The helical motion is held responsible for the bend creation and migration (Chang, 1992). The strength of this motion depends on the sharpness of the bend, defined by the Relative Curvature (R_C/W); the sharper the bend, the more strengthened the motion. For the sharper bend at a certain value of R_C/W , M_r becomes saturated, below which the outer bank flow separation occurs. Thus, the outer bank remains protected by the flow with comparatively weaker stress. Again, R_C/W reaches the highest value, above which M_r declines again. Thus, a higher M_r occurs within a certain range of R_C/W , which differs from the river to the river depending on the river system of a region. Hickin and Nanson (1975, 1984) and Nanson and Hickin (1986) studied around 125 bends of 19 different river reaches in Canada and stated that the maximum migration rate occurs when $2 < R_C/W < 3$. The average value R_C/W of each bend and reach of the Arial Khan River is presented in Figure 5.22. The reach R2 carries the highest value of 4.8 and then R1 with a value of 3.5. The lowest value of R_C/W is carried by the river reach R3 with the value of 3.1.

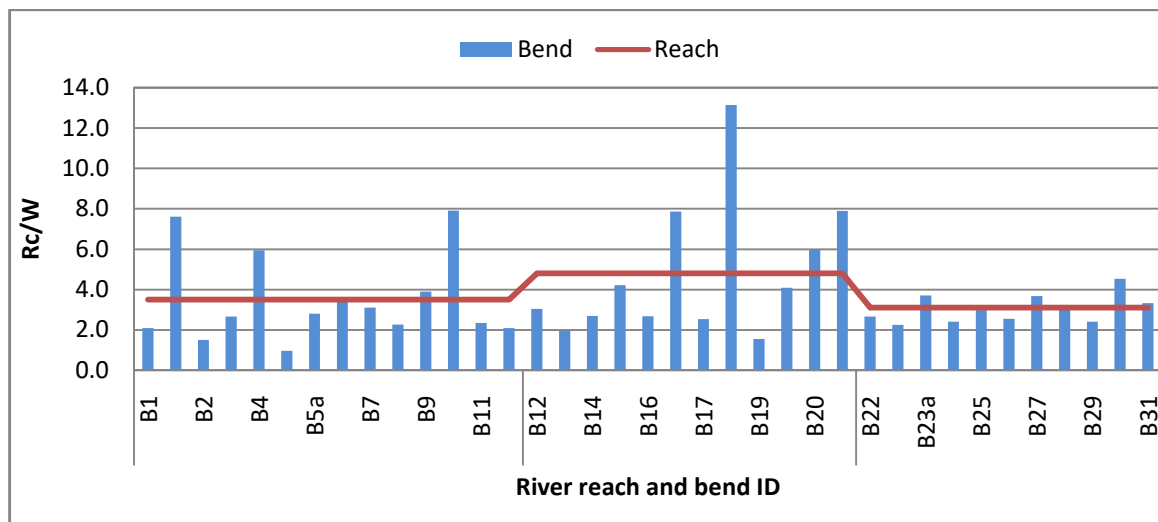


Figure 5.22: The relative curvature of the three reaches and the consecutive bends of the Arial Khan River.

5.6.6 Bend migration and migration rate

In a meander river having an erodible bed and bank material, secondary flow into a bend can easily scour the outer bank at its toe, resulting in a transverse/ lateral migration. During lateral migration, two processes of point-bar sedimentation and outer-bank erosion simultaneously interact with each other. The downstream/ progressive migration reaches to peak during bankfull discharge, though this migration may occur in a different range of discharge. The planform evolution of a meander river is the ultimate outcome of lateral and downstream migration. In an active meander river, bank retreat is responsible for channel migration, which occurs by two mechanisms: (1) fluvial entrainment (detachment of grains or aggregates by the flow) and (2) mass failure (slumping or sliding caused by gravity) (Lagasse et al., 2004).

The average migration of bends in terms of lateral and downstream migration and the linear migration of each time period are presented in Table 5.7. During the time period of 1989-1999 and 2008-2017, downstream migration was higher and in the rest of the time, lateral migration was higher.

Table 5.7: Average migration in different time period.

Year	Average migration (m)		
	Lateral	Downstream	Linear
1972-1980	192	124	307
1981-1988	435	384	657
1989-1999	382	543	739
2000-2007	415	394	652
2008-2017	265	371	497
2018-2021	130	111	184

There is significant spatial variation in the Mr of the Arial Khan River. Figure 5.23 illustrates the Mr of each of the 37 bends and the corresponding river reaches. The bends of the R1 reach have a higher average Mr, which is more than double of the R2 and R3 reaches. Bend B11a has exhibited the highest Mr of 203 (m/y) of the river, which is situated at the end of the R1 reach. A big neck cutoff occurred at bend B11 in 1976, after that a new bend was developed at that position, which is B11a. In R1 reach, some bends

have a higher M_r , whereas some adjacent bends have a lower M_r . Local control, i.e., meander scars and clay plugs, may have influence on the bends of R1 reach. Several meander scars and oxbow lakes were found in the Arial Khan, and most of them are in R1 reach.

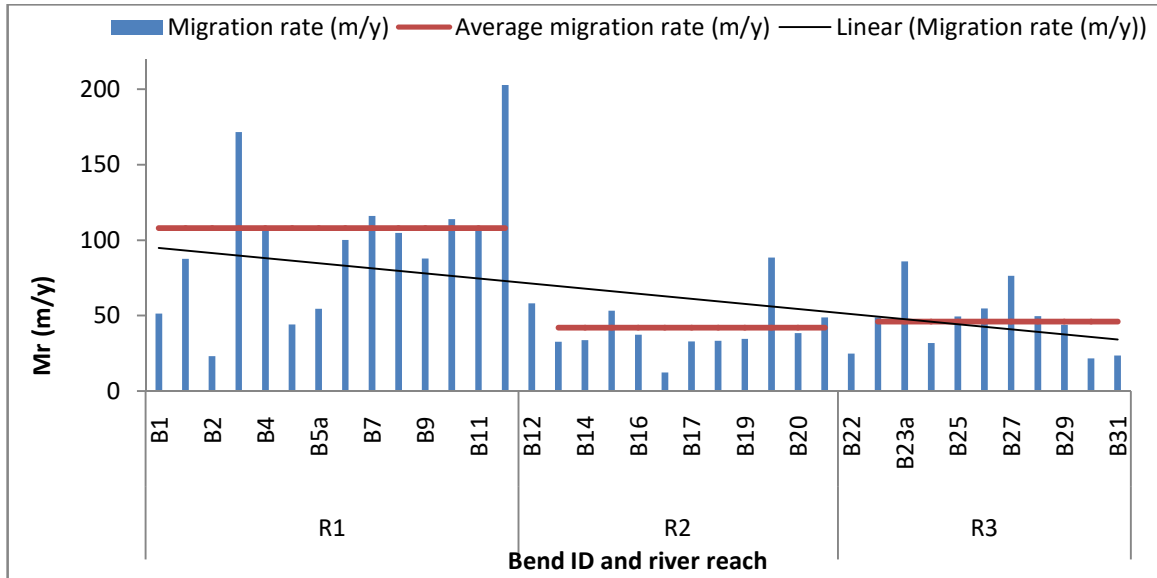


Figure 5.23: Migration rates (M_r) at different bends of different reaches of the Arial Khan River (1972-2021).

The bends from B6-B11 are located near the Haji Shariatullah Bridge and some downstream portions of the bridge; the region is very erosion-prone among the entire river, having a migration rate of 108 m/y.

Though R2 is characterized as avulsion prone, on the bend-scale the M_r is the lowest with an average value of 42 m/y. But in an actual sense, most of the bends in R2 have a M_r below 40 m/y. The lower reach of the river R3 is started from 10 km downstream of the confluence of the Palong River, a tributary of the Arial Khan River. Here the average M_r of 46 m/y is slightly higher than R2. Among all the natural, matured and longer life bends, B22 is one of them having the lowest migration rate of 25 m/y and has been existing all through the study period. This bend is situated in R3 reach. In this reach, the discharge is contributed by three means: upstream fluvial flow, fluvial flow from the Palong River which is also a diverted flow of the Padma, and tidal backwater flow from the downstream confluence. Figure 5.24 presents the temporal change of M_r in different reaches and the entire river.

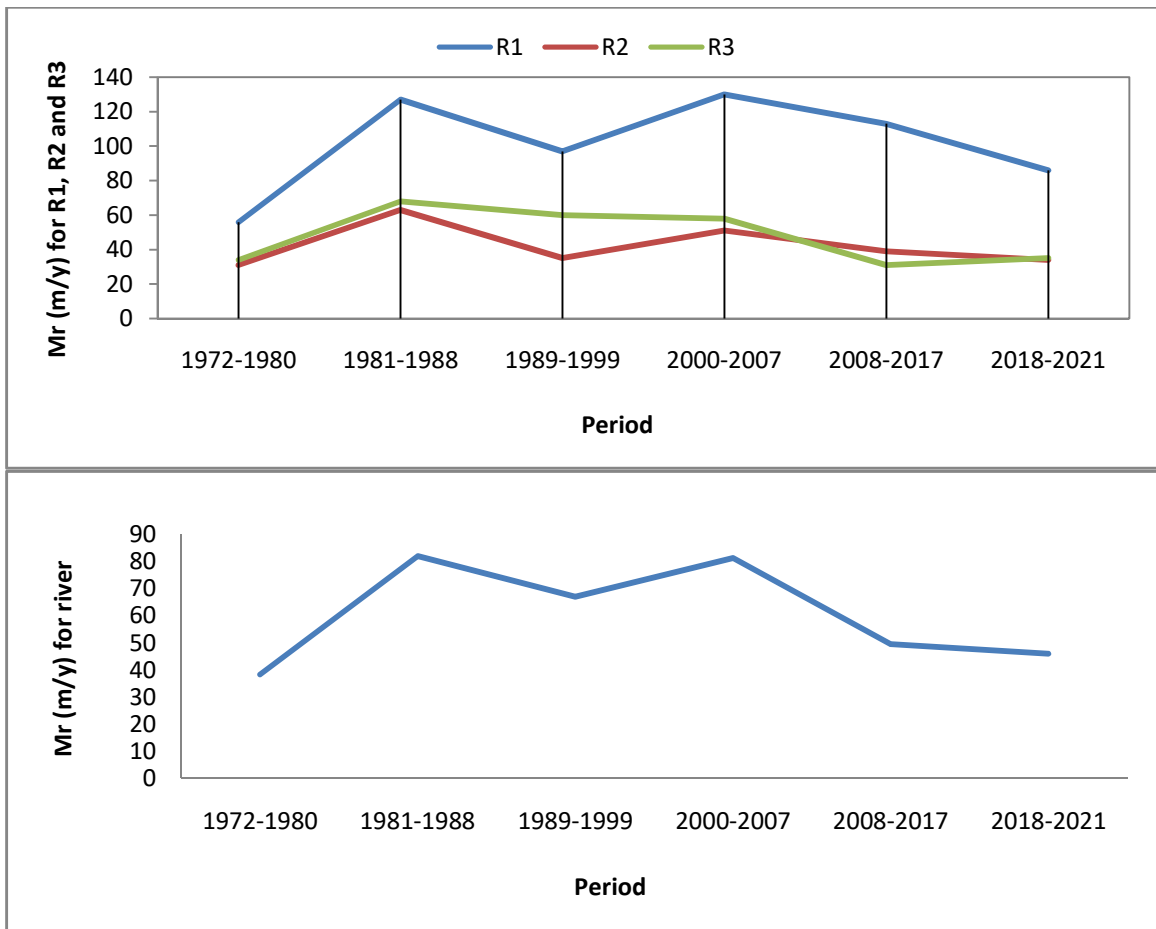


Figure 5.24: Migration rates (Mr) of the Arial Khan River and its three reaches: R1, R2 and R3 in different time periods.

The Mr in R2 and R3 reaches are very close, which indicates similar floodplain characteristics. All the cutoff bends, i.e., B5, B11, B19, and B23, exhibited a comparatively higher Mr and cutoff occurred two times in the same position of the B11 bend. The Mr of the three reaches and thus of the entire river change periodically and maintain a certain pattern. The pattern of the temporal change of Mr is similar for R1, R2, and the entire river. During the 1972-1980 time period, the Mr showed a minimum value, after that, it climbed up to 1981-1988. The next alternate plunging and mounting points have formed during the time period of 1989-1999, 2000-2007, and 2008-2021. The temporal change of Mr for R3 is quite different, though the higher Mr is alike to R1 and R2, which had happened during the time period of 1981-1988 and 2000-2007, then successively plunged till 2019. Duan and Julien (2010) stated that the meander river sinuosity when turned sufficiently large, the migration rate reduces, and the planform

geometry changes become small or unchanged for some time. The Arial Khan River has been following this characteristic, especially for the last 14 years.

In short, from 1981 to 2007 was a time period when the Mr of the Arial Khan River was higher, which coincided with the time periods of relatively higher discharge, i.e., higher Qmax and Qavg. The average Mr of the Arial Khan is around 60 m/y.

Chronologically the time periods according to the bend Mr can be arranged as:

1981-1988 (82.1 m/y) > 2000-2007 (81.5 m/y) > 1989-1999 (67.2 m/y) > 2008-2017 (49.7 m/y) > 2018-2021(46.5 m/y) > 1972-1980 (45.6 m/y).

5.7 Some Developed Relationships

5.7.1 Width, depth, and flow velocity vs. discharge

The discharge of a river is the most influential independent parameter for river morphology. At an increasing discharge when stream power is higher, bed scouring, and transportation of bed material occur and resulting in the increase of the average cross-section of a river. The width (W), depth (D), and velocity (U) of rivers increase as power functions of discharge (Leopold and Maddock, 1953), which are expressed as:

$$W = aQ^b \quad (5.1)$$

$$D = cQ^f \quad (5.2)$$

$$U = kQ^m \quad (5.3)$$

where, a, c, k, b, f, and m are numerical constants. To satisfy the continuity equation of $Q = WDU$, the sum of exponents should give unity, i.e., $b+f+m = 1.0$ and the product of coefficients should also give unity, i.e., $a*c*k = 1.0$. According to Leopold and Maddock (1953), the average values for exponents b, f, and m are: 0.26, 0.40, and 0.34 respectively, these values globally vary depending on regional climate and physiography (Park 1977). The variation also occurs between the values for the gauge station and at points downstream of the gauge station. Figure 5.25 demonstrates the relationship of W, D, and U with Q of the Arial Khan River for the gauge station near the offtake. The D, U, and Q

are the available measured secondary data of monsoon (Jun-Oct) from 2008 through 2019, and W is collected from satellite images of the corresponding years. For the Arial Khan River $b+f+m = 0.24 + 0.36 + 0.47 \sim 1.0$ and $a*c*k = 57.2*0.37*0.05 \sim 1.0$, which indicate that in this river, the morphologic variables are highly interrelated.

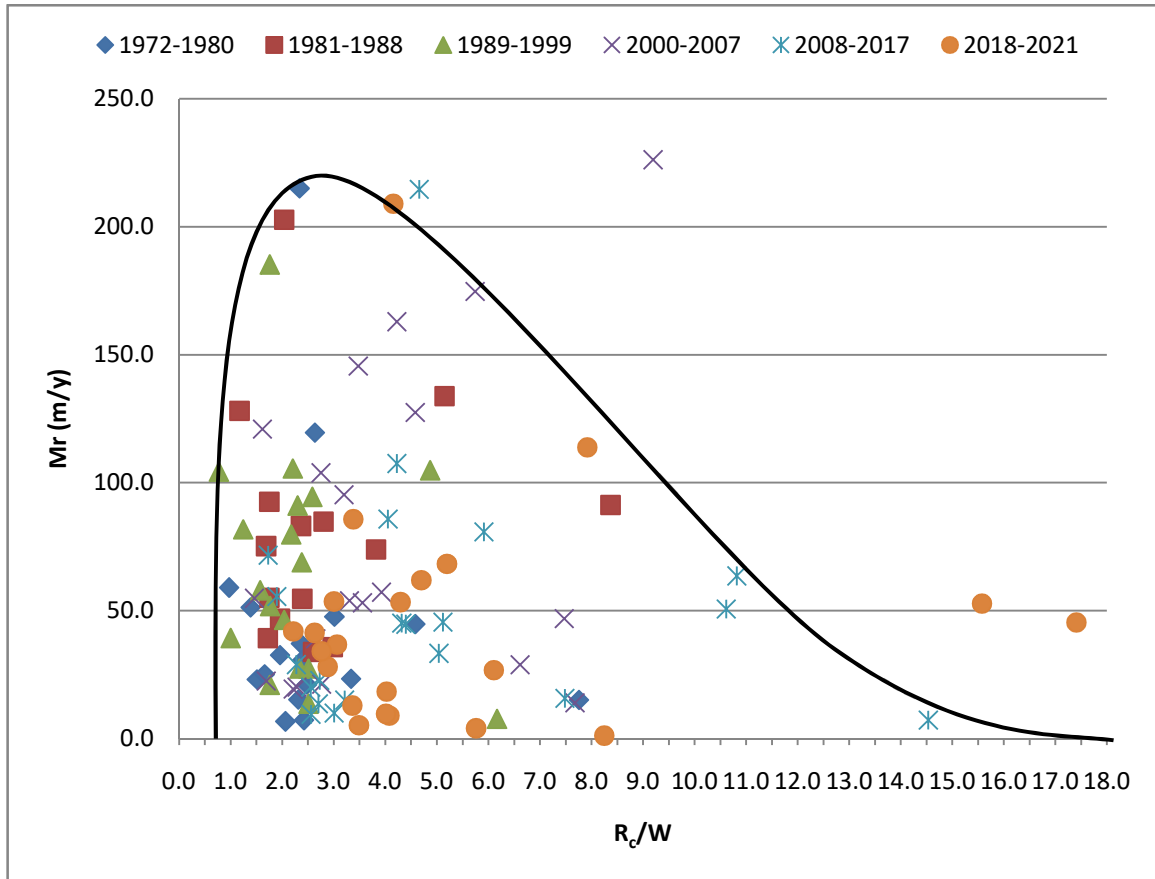


Figure 5.25: The relationship of W , D and U to changing Q at the station of the Arial Khan River offtake.

5.7.2 Migration rate vs. relative curvature

A well-established relationship for the study of the meander river is the Mr vs. R_c/W , from which an envelope curve is generally developed. The curve in fact defines a range of R_c/W values for which maximum bend migration occurs at a specific river. Figure 5.26 presents the relationship between Mr and R_c/W along the entire length of the Arial Khan River in different bends for different time periods. It shows that for the R_c/W value within the range from 1.5 to 3.5, most of the bends had migrated and the Mr was also high for this range with a peak value of ~ 3.0 . Beyond this range (>3.5 and <1.5), the Mr was low for most of the bends.

From Figure 5.22, it is seen that the bends from R1 and R3 reaches have average R_C/W values within the range of 1.5-3.5. But the bends from R2 reach the average R_C/W value is 4.8, which is beyond the range.



5.26: Migration rate (Mr) and relative curvature (R_C/W) along the Arial Khan River of heterogeneous floodplains. Maximum Mr occurs at $R_C/W = 1.5$ to 3.5 with the peak at ~ 3.0 .

Again, Figure 5.23 shows that the Mr for the bends of R1 and R3 reaches are higher than R2 reach, which proves the authentication of the empirical relationship developed in Figure 5.26. Thus, the moderate curvature bends for the Arial Khan River are highly susceptible to erosion, and the large, as well as the sharp bends, are less erosion prone. In the time-scale, the average R_C/W of the Arial Khan River is presented in Figure 5.27. Here, it is seen that the bends which had developed within a time period of 1972-1999 were more likely to maintain the R_C/W value within a range of 1.5 – 3.5 than the bends which had developed after the 1999. From Figure 5.25 and Figure 5.26, it has also observed that the bends of recent years exhibit very much scattered R_C/W value, and the

average value is far beyond the range of maximum migration. The evaluated R_C/W value of this study differs from the ideal range of 2.0-3.0, which has been described in different literature, though there is a similarity in the shape of the curve. This difference may be due to the heterogeneous floodplains of the Arial Khan River. The valley width at upper and middle reaches is comparatively extended and covered with loose sand of river sediment than that of the lower reach.

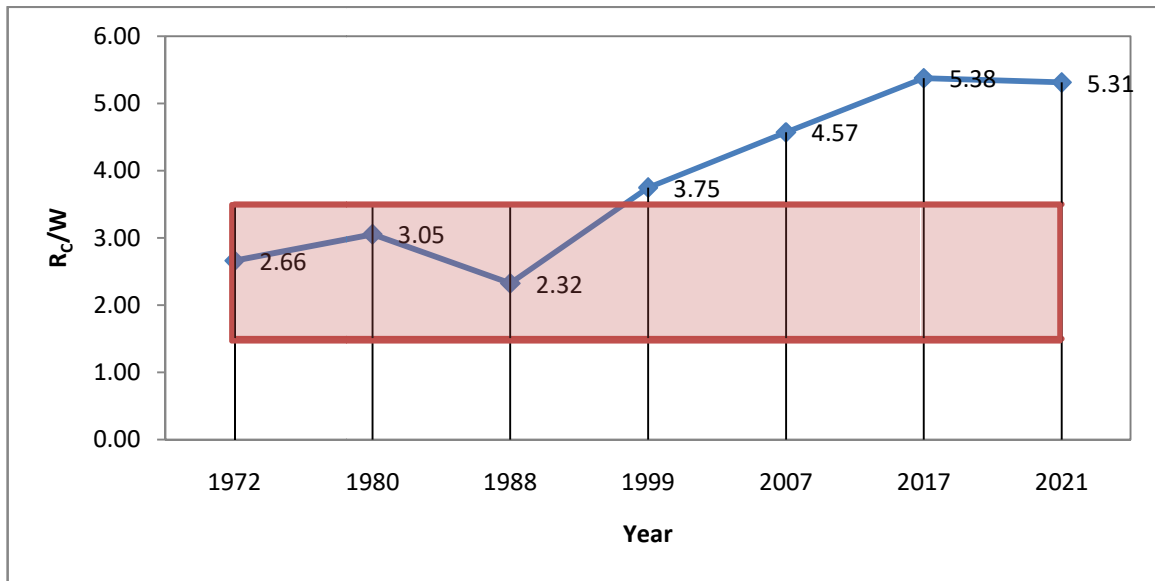


Figure 5.27: Average R_C/W of the Arial Khan River in selected years. The R_C/W values within the range 1.5-3.5 indicates higher migration rate.

The geological features of meander scars and clay plugs are very common at the upstream floodplain, which may interact with the river adjustment through bend migration. On the other hand, the human interventions for bank protection may have constrained the free movement of the riverbanks across the river valley. Several tributaries and distributaries of the Arial Khan could have put a significant influence on bend migration as they contribute or intake large quantities of discharge and sediment. For R_C/W values of 2 to 3, Bagnold (1960) showed that energy losses caused by the curving of flow in the bend were minimized.

5.7.3 Relationship between meander length and river width

In different literatures, the active meander river with the high complexity of river bend shifting and shape formation has been observed, and found the variation of the discharge

with the variation of the river width (W) and meander wavelength (M_L). A certain relationship between M_L and W of the Arial Khan River exist which differs with time periods. Figure 5.28 presents their relationship; the data of the two parameters were acquired from the image analysis of the selected years.

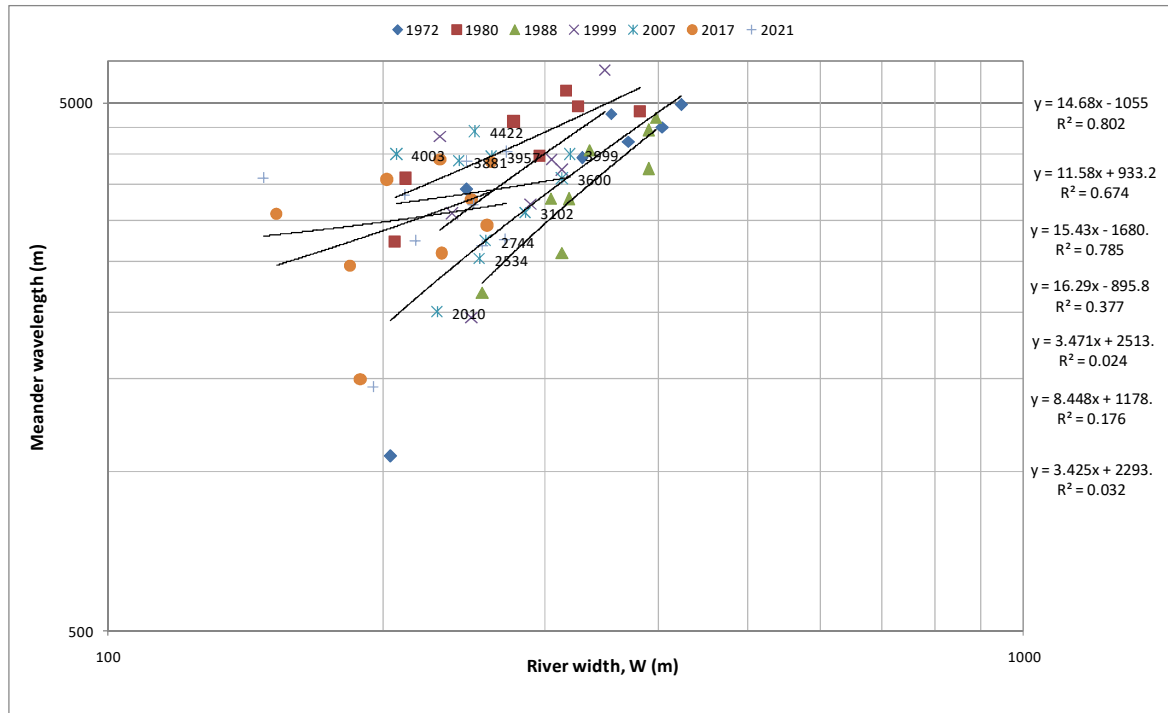


Figure 5.28: Relationship between M_L and W of the Arial Khan River.

In the graph, two distinct types of relationships are generated. One type for the years 1972-1999, where the coefficients of “x” are more than 10, and the other type where the coefficients are less than 10. Thus, the river migration in the past was more responsive to width change than in the present. The ratio of M_L to W for the Arial Khan River is around 11-16 for the time period 1972-1999. After 1999, this ratio is within 3-8. But the study of Leopold and Wolman (1957) has established that M_L is generally 10 to 14 times W . It is mentionable that after 2000, the discharge of the Arial Khan had decreased continuously except for the years of moderate floods in 2007 and 2018.

5.7.4 Relationship between meander length and discharge

M_L of an alluvial meander river depends on both Q and sediment characteristics. Due to the lack of sediment data, only the data of Q have been used in the establishment of the

relationship. Here, average M_L values for selected seven years and corresponding average Q of monsoon have been taken for the analysis. According to Leopold and Wolman (1957), $M_L = 65.2 Q^{0.5}$. The relationship between M_L and Q for the Arial Khan River is found as: $M_L = 92.4 Q^{0.49}$ with a correlation of determination value of 0.92. The relationship between M_L and Q is presented in Figure 5.29.

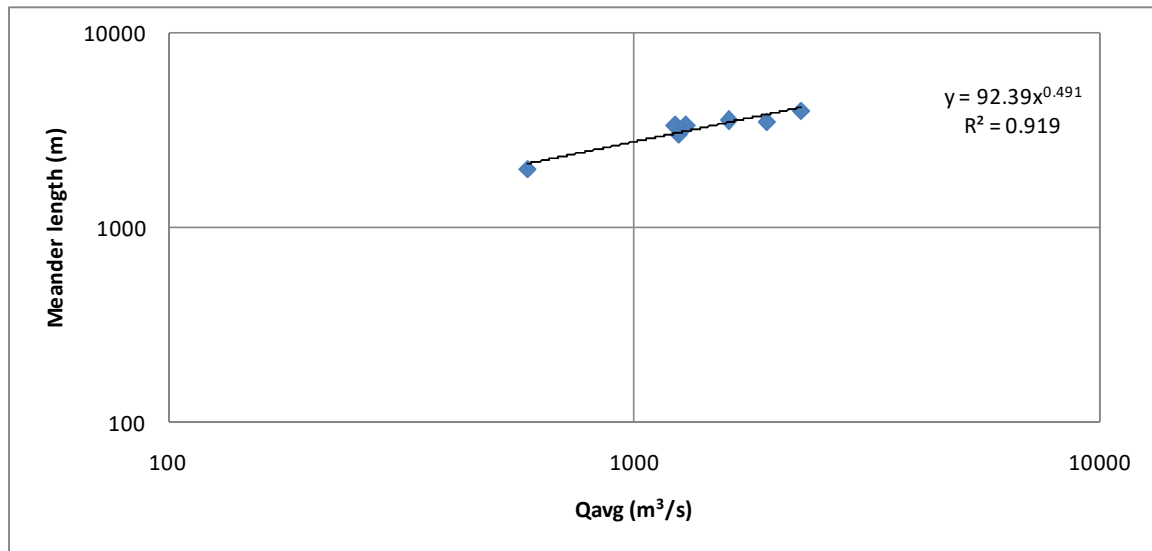


Figure 5.29: Relationship between M_L and Q of the Arial Khan River.

5.7.5 Relationship between meander width and river width

The common parameters which are used to predict M_w are M_L , R_C , and bankfull channel width, stream power and discharge. In this study two parameters, W and average monsoon discharge are considered to establish relationships with M_w . Large discrepancies are found in the coefficient of equations of M_w and W , which are described as due to spatial variabilities of channels. Considering the varying coefficients from different studies, Howett (2017) proposed that M_w is ranges from 4.3 to 17.6 times the W . From 5.30, it is evident that for the Arial Khan River the range is 2- 25, year-to-year variations are existed in the relationship between M_L and W .

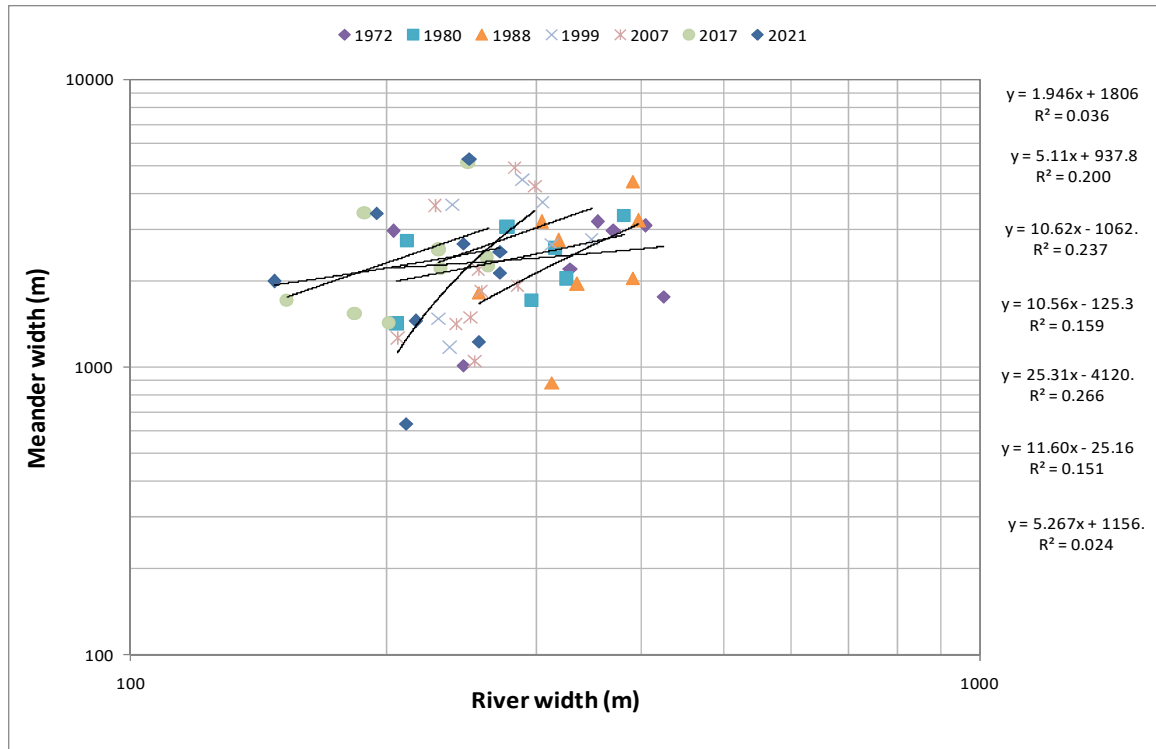


Figure 5.30: Relationship between Mw and W of the Arial Khan River.

5.7.6 Relationship between meander width and discharge

Leopold et al. (1964) established a relationship between Mw and mean annual Q based on 31 samples as $Mw = 65.8 Q^{0.47}$. Authors stated that the correlation is very poor with bankfull discharge. The meander belt width shows a positive correlation with mean monsoon daily discharge of the Arial Khan River, which is presented in Figure 5.31, with a R^2 value of 0.76.

Thus, from Figure 5.28, Figure 5.29, Figure 5.30 and Figure 5.31, an understanding is developed for the Arial Khan River as how hydraulic characteristic in terms of discharge can make changes in river width and hence the changes in the meander belt.

5.8 Prediction of Bend Migration

The bend B3 at R1 reach is one of the highest erosion-prone bends and very important as it is located near the Haji Shariatulla Bridge on Dhaka-Mawa-Bhanga national highway and has migrated in such a way that a channel avulsion may occur in the near future, which may result in the abandonment of the old channel of guided riverbanks.

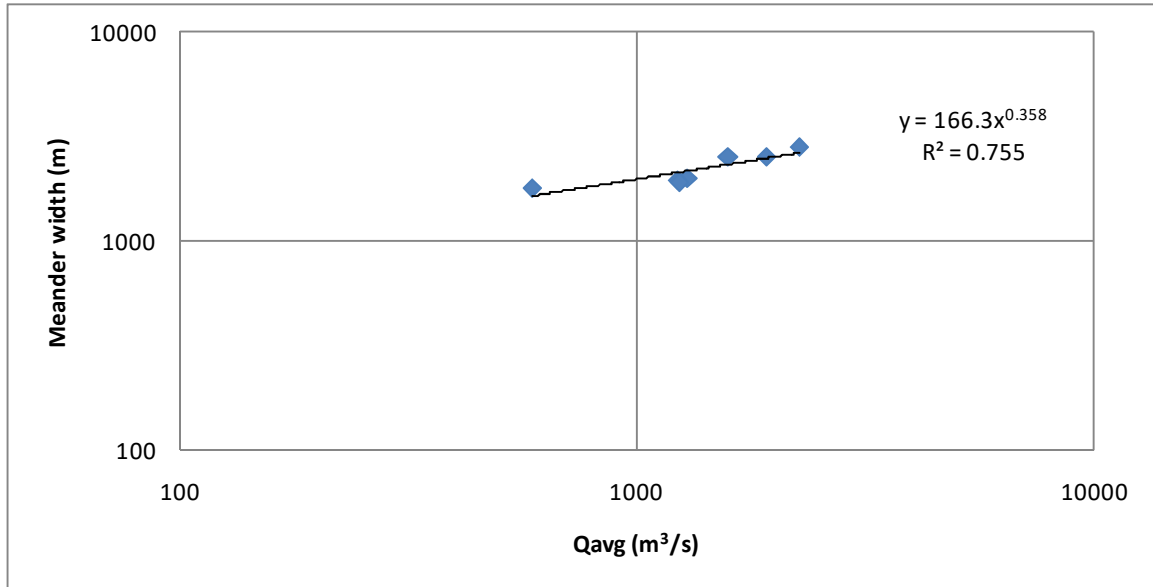


Figure 5.31: Relationship between Mw and Q of the Arial Khan River.

Another bend B17 of R2 reach is located at Madaripur Sadar; the inner bank of this bend has protection work to save Madaripur town since 1987. According to local people, the severe erosion of this bend is due to mainly inner bank protection. On the other hand, the anchored small cargoes and trawlers increase the erosion of this site. The bend B27 is in R3 reach. In recent years the erosion at the outer bank has significantly increased. If the present rate of erosion will sustain for several years, a huge channel avulsion may occur in near future. A vertical line is considered as a reference line during the prediction of all three bends. During the analysis period, the migration rate and direction maintained an almost similar pattern.

5.8.1 Bend B3 of reach R1

The bend B3 is located near the Haji Shariatullah Bridge. During the new development phase of this bend in 1988/1989, it was situated around 5 km upstream from the current position (2021). This bend is very dynamic and has been treating unlikely with all other bends of this reach and with the bends located in the same position before. Because this bend poses almost double the lifetime of the average lifetime of bends of this reach. The bend was generated in 1988. Since then, the bend traveled downward without any pattern in shape direction and migration rate. But after 2013, bend has been following a specific

pattern. The migrations of this bend were predicted for different years starting from 2016 and compared with actual migrations, which are presented in Table: 5.8.

Table 5.8: Actual and predicted R_C , θ_c and Dc for bend B3

Year	R_C (m)			θ_c (Degree)			Dc (m)		
	Actual	Predicted	Difference	Actual	Predicted	Difference	Actual	Predicted	Difference
2011	371	-	-	-	-	-	-	-	-
2013	511	-	-	24	-	-	261	-	-
2016	618	604	14	31	-	-	376	391	-15
2017	640	654	-14	31	35	-4	135	125	10
2021	697	728	-31	34	31	3	620	540	80
2024	-	740	-	-	43	-	-	376	-

Since 2007-2008, excessive erosion downstream of the apex has been occurring which causes downstream migration of the bend rapidly through continuous bend translation. But the erosion at the upstream location of the bend apex is insignificant, thus lateral migration is absent for several years. It has been seen that from 2013 the year-to-year changes of R_C , θ_c , and Dc have followed an increasing pattern. The bend has been migrating in the southeast direction with respect to the vertical reference line. As the reach R1 is very dynamic, prediction for the long term is not suitable for the bends of this reach. Thus, the bend was predicted for the year 2024.

The prediction of migration has revealed that the bend will make an avulsion and thus there will have some chance of abandonment of the bridge in near future. The predicted values of R_C , θ_c , and Dc are 740 m, 43° , and 376 m respectively for the year 2024. The long journey of the bend and migration prediction is presented in Figure 5.32.

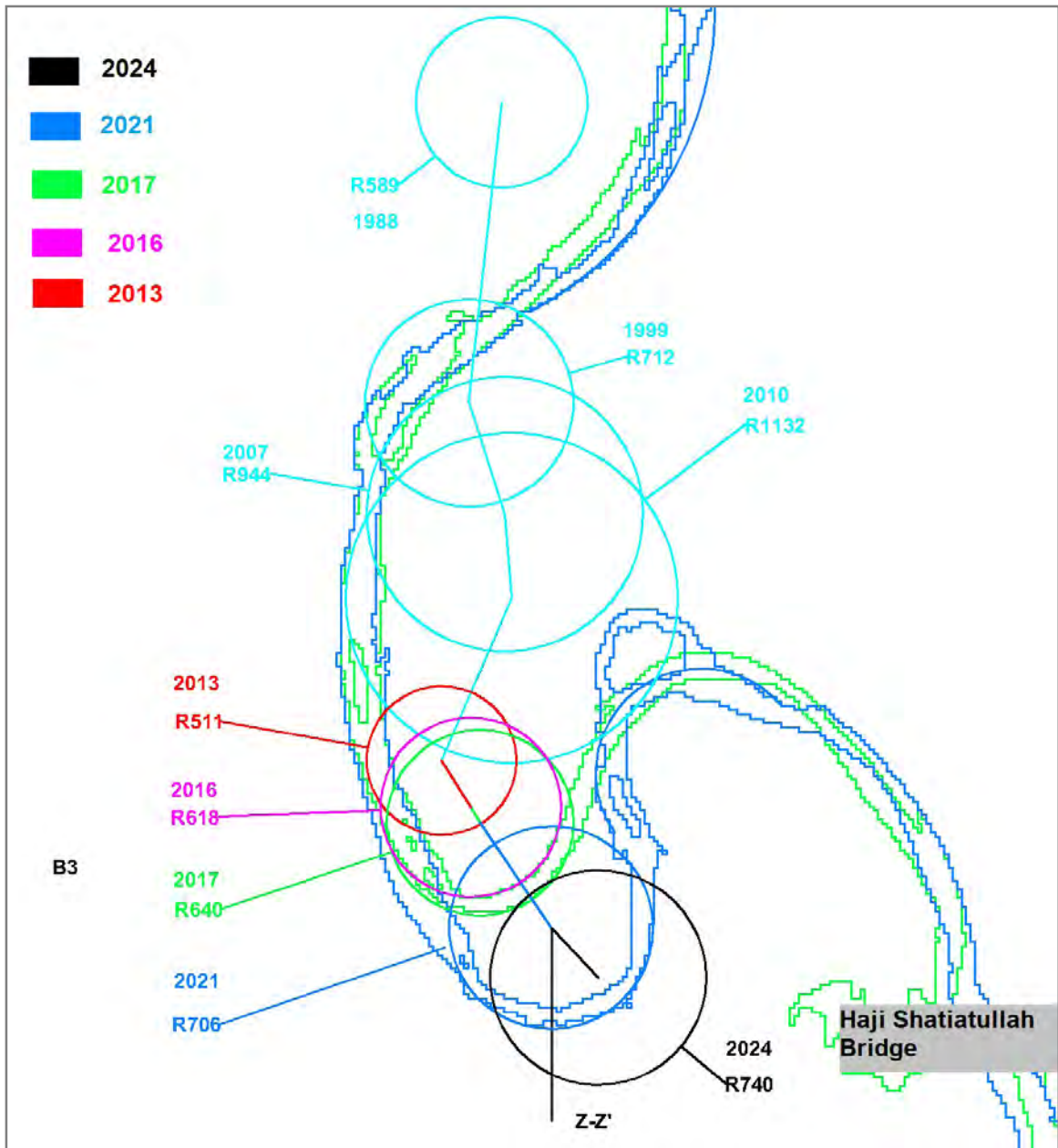


Figure 5.32: Actual and predicted migration of bend B3.

5.8.2 Bend B17 of reach R2

The morphology of bend B17 has been greatly influenced by human intervention to its upstream riverbank made in 1987. The migrations at bend B17 were predicted for different years starting from 2013 which are presented in Table: 5.9. The migration of this bend is occurring in the northeast direction with respect to the vertical reference line. As the migrations have been following a similar pattern since 2003, long term prediction is possible for this bend.

Table 5.9: Actual and predicted R_c , θ_c and D_c for bend B17

Year	R_c (m)			θ_c (Degree)			D_c (m)		
	Actual	Predicted	Difference	Actual	Predicted	Difference	Actual	Predicted	Difference
2003	605	-	-	47	-	-	-	-	-
2007	621	-	-	35	-	-	98	-	-
2011	627	637	-10	31	23	8	75	98	-23
2017	654	636	18	29	25	4	115	113	2
2021	679	672	7	10	28	-18	88	76	12
2025	-	704	-	-	-9	-	-	88	-

The future prediction is made for the year of 2025. The erosion at the upstream of the apex is high in the northwest direction with respect to vertical reference line and with time the bank curvature of this bend will expand more, which is presented in Figure 5.33.

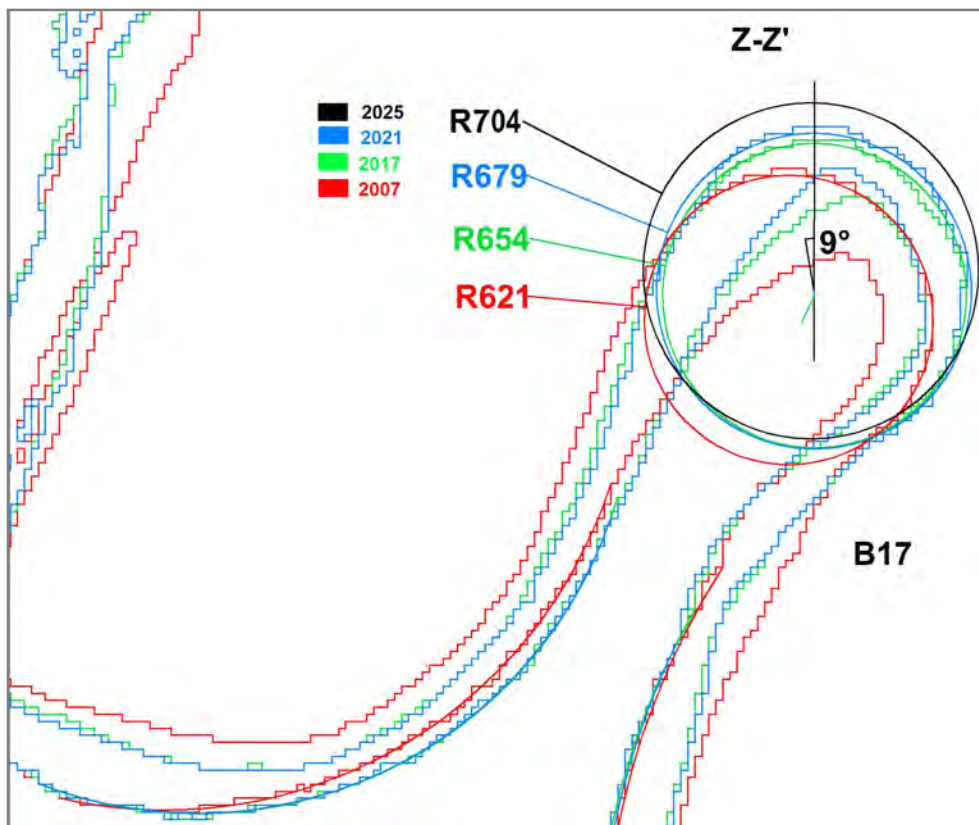


Figure 5.33: Migration prediction for bend B17

There is no possibility of bend cutoff in near future, though the elongated loop shape may sustain for a long time. The predicted values of R_C , θ_c , and D_c are 704 m, 9° counterclockwise with reference line, and 88 m respectively for the year 2025.

5.8.3 Bend B27 of reach R3

This bend is situated in the middle of the lower reach R3. Initially, in 1972, the river section at the bend location was straight. After the development of the bend B27, lateral migration of the bend has continuously taken place at a significant rate and in the same direction. As a result, a great possibility of avulsion has arisen, through which the bend B27 would be abandoned in near future. The bend had reached in maturity stage during 2002/2003 when the R_C turned into an average value of 883 m of this reach. As the migrations of this bend have been following a regular decreasing pattern in R_C value and nearly in the same direction, long term prediction is possible for this bend. The actual and predicted values of migration of this bend are presented in Table 5.10.

Table 5.10: Actual and predicted R_C , θ_c and D_c for bend B27

Year	R_C (m)			θ_c (Degree)			D_c (m)		
	Actual	Predicted	Difference	Actual	Predicted	Difference	Actual	Predicted	Difference
2003	732	-	-	-	-	-	-	-	-
2007	660	-	-	37	-	-	170	-	-
2011	630	617	13	35	-	-	232	213	19
2017	614	570	44	38	32	1	180	232	-52
2021	558	603	-45	31	40	-9	150	180	-30
2025	-	502	-	24	24	-	-	150	-

During 2003/2004, the R_C of the bend reached a value near the average value of this reach through a continuous decrease of curvature from previous years. The erosion occurs slightly downstream location at the bend apex. Thus, the lateral migration persists in this bend. As the bend has been following a specific pattern of change in migration direction and migration rate for a long time, future predictions are made for the year 2025, which are presented in Figure 5.34. The predicted values of R_C , θ_c , and D_c are 502 m, 24° clockwise with reference line, and 150 m respectively for the year 2025.

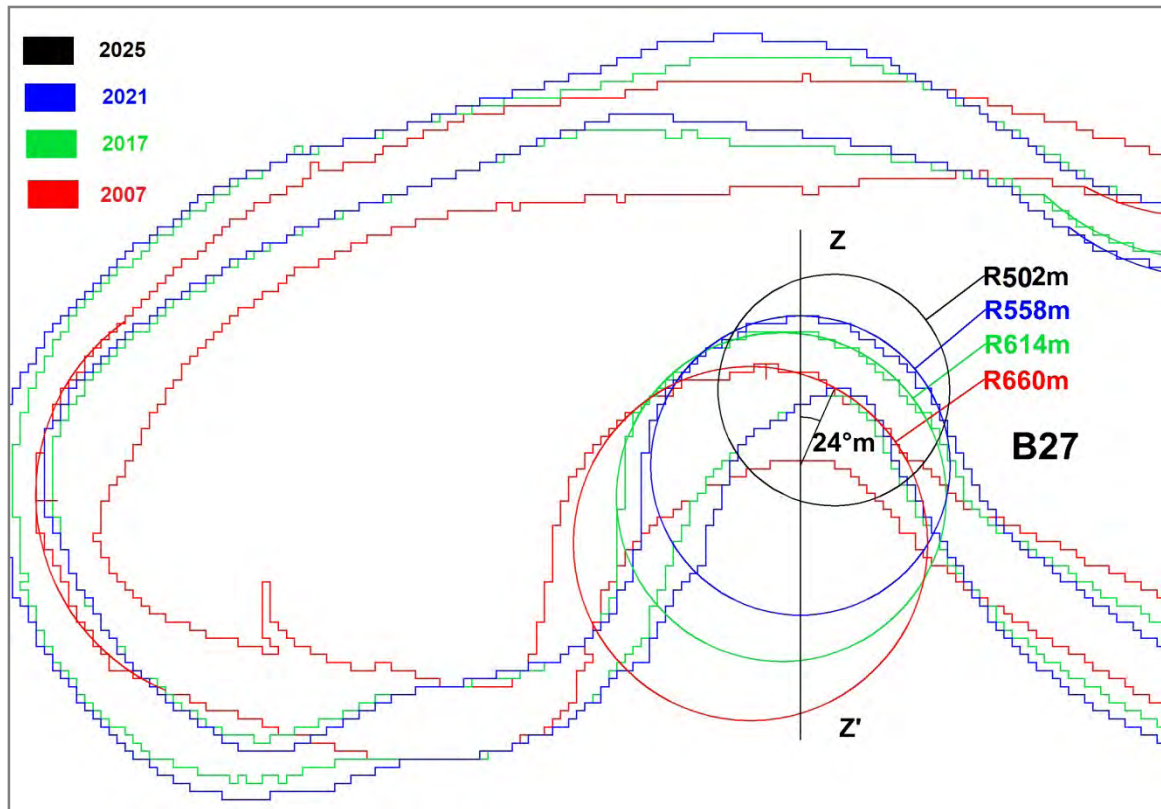


Figure 5.34: Migration prediction for bend B27.

5.9 Observations on Existing Conditions of Bends Based on Field Visit

A field visit was made on the last week of January 2022 to observe the existing condition of three bends- B3, B17, and B22. From the field visit, the data and information have been collected by observing the physical condition of the outer bank of the bend from approximately crossing to the apex point along the bank and the existing permanent and temporary protection measures. The views of the local people from the three locations and the BWDB officials were also collected and carefully considered.

5.9.1 Bend B3 of reach R1

The GPS data was collected from a 1 km length along the outer bank of the river bend at Molla Kandi, SadarpurUpazila, Faridpur. Among the three observed bends, B3 is the most dynamic bend. Several exposed and submerged mid-channel bar formation in recent years has made the river so narrower and shallower that a dredging scheme has been taken near the upstream of the bend. Local people informed that due to uncertainty and lack of proper knowledge of river migration, an entire village near the bank has relocated elsewhere,

even from the non-eroded region too. They also mentioned that small-scale bank protections are not suitable there. An elderly villager of Mollakandi said that his family was relocated three times within around 40 years. Initially, they lived near the left bank of the present oxbow lake. Due to the river shifting, moved far away from the bank. They moved again three to four years ago to the newly developed charland of the inner bank.

Upper reach is characterized by several oxbow lakes in the floodplain and extended point and mid-channel bars. Some collected sample data and picture clips are presented in Appendix D.

5.9.2 Bend B17 of reach R2

Data were collected from 2 km length along the outer bank of the river bend B17 at Bahir Char Katla, Madaripur Sadar, Madaripur. The bend is on the opposite side of the Madaripur town protection project, the project was undertaken in 1987. After completion of the project, the shape of the bend completely changed from simple asymmetry to an elongated loop through a very rapid erosion at the apex of the bend, which is clearly visible in Figure 5.35.

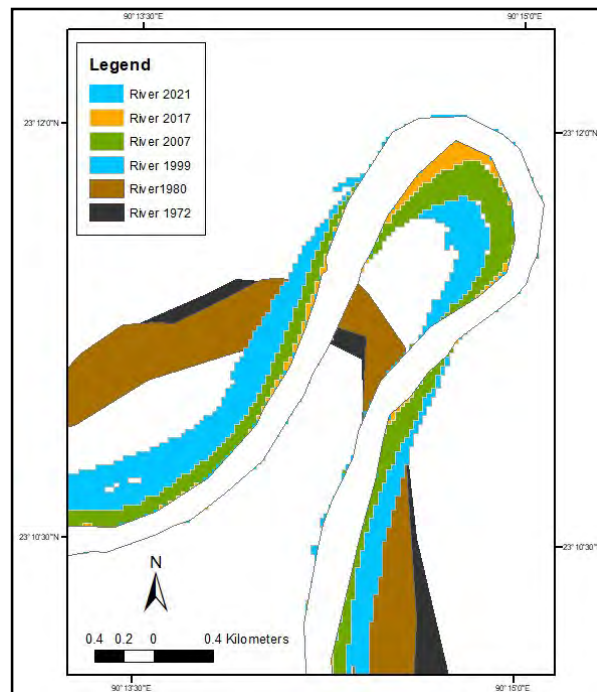


Figure 5.35: Shape of the bend before and after the Madaripur town protection project in 1987.

The bend location and the Madaripur town are at two opposite banks of the river. Thus, the area is valuable, having two developed launch ghats for river crossing and transportation. Local people are very concerned about erosion. They think that the unloading of trawlers near the bank enhances erosion. The average height of the bank mass failure is 2.7 m at the excessive erosive location. During the wet season, when erosion becomes severe, the local authorities just dump geobag as an immediate measure; the majority of which do not sustain even for a single year. From the ground survey, it has been observed that erosion is mainly at the bend apex and to its downstream. But at the upstream location of the apex, erosion is negligible which is represented in the picture in Appendix D.

5.9.3 Bend B22 of reach R3

The bend is located at the upstream of Khasherhat Bondor protection project and the Khasherhat Bridge. Local people said that the erosion of this bend has suddenly increased especially from the monsoon in 2017. Erosion of the bend occurs by means of mass bank failure with an average value of 4.6 m. The village near the bend is well established, having some concrete houses, a two-storied primary school named Kanurgau Government Primary School, soling road, etc., all are under threat. Some villagers gave the opinion that temporary protection measures by means of scattered dumping of geobag are undertaken during every monsoon when the river remains in harsh mode. These types of measures are completely useless; not even lasting for a single season. Some collected sample data and picture clips are presented in Appendix D.

5.10 Discussion

The Arial Khan River has acted as a bridge between the Padma River and the long way of the south-central region. This river receives the discharge from the Padma River through tributaries, such as - the Palong River, Beel Padma, and Moinakata River, and then the combined discharge shares and diverts into the distributary rivers and khals of different sizes and locations, such as - the Kumar River, Lower Kumar River, Torki River/ Palordi and River. The entire region has vast inter-connected water channel networks, and the Arial Khan River plays an important role to maintain harmony in the natural environment

in the water of this region. But on the other side, this river brings misfortune to the locality when hundreds of acres of arable land and properties along the riverbank extinct into the river. In some years and locations, these extinctions rise to a higher degree but in other years it remains into a tolerance limit, which depends on the migration characteristics of the river. If the dynamic behavior of a river morphology can be properly understood, it may be possible to keep human – river negative interruption in an endurable stage.

The migration of an alluvial meander river is mainly bend-oriented, which is influenced by some common factors such as hydro-morphology of the river, the geometry of bends, and the characteristics of the floodplain and river valley. Besides these, the offtake morphology of the Arial Khan River plays a vital role in the migration phenomena. Hence, the study of the river morphology in terms of river migration largely depends on the appropriate incorporation of all controlling factors, use of long-term river data in a suitable analysis technique, accurate measurement and observation, and future prediction of the migration.

In this study time-and bend-scale responses of the Arial Khan River morphology are analyzed for 49 years from 1972 to 2021 using historical data, remotely sensed satellite images, image analysis GIS software, CAD software and some well-established theories and empirical relationships. The river is divided into three reaches: upper, middle, and lower, based on the spatial variability of floodplain, morphology, and bend migration pattern and direction. The upper reach has comparatively wide active floodplain and valley width, having loosely compacted soil. The middle reach is avulsion prone, having two distributary rivers and a continuous 2.11 km long protected bank. The lower reach has consistent and unidirectional erosion in almost all the bends. The average water depth and thalweg elevation of the river increase towards downstream, currently the bed slope of the river is 0.037 m/km. The specific findings of the study are discussed below:

5.10.1 Offtake shifting and change of river planform

The discharge variability of the Padma does not follow any pattern. As a distributary, the Arial Khan River receives the lowest 2% and highest 6% of the Padma discharge. The Padma River planform near the Arial Khan Offtake influences the flow regime of the Padma and the Arial Khan Offtake morphology influences the amount of diversion of the

flow into the Arial Khan. The change of offtake morphology comprises the change of bed elevation and in-front bar size which correlate with the location of the offtake. A certain type of offtake morphology persists during upward (north/northeast) shifting and other types during downward (south/southwest) shifting of the offtake, which takes around successive 8 and 19 years respectively. These changes of the offtake morphology keep reflections on the hydro-morphological variability of the Arial Khan through river planform and bend-scale changes of the river. It has been found that the river acquires a 5-7 km extra linear river path during every period of upward shifting of the offtake, but the overall length shrinks significantly. During these periods the average length of the river remains 104 km. On the other hand, during the periods of downward shifting of the offtake, 4-6 km linear path deducts from the uppermost portion of the river, though the length of the river gets stretched to several kilometers. During these periods the average length of the river becomes 109 km. So far, the Arial Khan River exhibits the highest length of 114km in 2021 and the lowest length of 100 km in 1980.

The sinuosity, as linked with the length of the river, changes to a certain extent due to alternate river length shrinkage and stretching. The river had exhibited the highest SI of 1.96 in 2021 and the lowest of 1.62 in 1980. The average SI is found as 1.78 for the study period of the river. The bend-scale analysis reveals that the river had experienced four bend cutoffs among six during the upward shifting.

The bend migration and thus migration rate are also linked with this offtake shifting. During the upward shifting of the offtake, a higher migration rate 60-70 m/y occurs compared to the rate during downward shifting. Thus, the river responses become quick and slow alternately in the morphological changes during upward and downward shifting of the offtake respectively.

Zheng et al. (2021) have shown that there is a large periodic variability in the concentration of total suspended sediment of the Padma River. Thus, it can be concluded that the periodic offtake shifting, and the river shape and sinuosity changes have a definite link with the sediment concentration of the Padma River and the Arial Khan itself. Different literatures have suggested that the discharge, i.e., the absolute quantity of water and sediment, is less important to give channel shape and sinuosity than the type and percent of sediment load (Rhoads, 2020; Shen et al., 1979). On the other hand, the Arial

Khan has reached in higher SI and relatively lower and constant migration rate in recent years, which indicates that the river attains a morphological adjustment, especially in the middle and lower reaches, and will sustain unless a discharge variable in great extent is faced by the river in near future. Because, when the SI turns into sufficiently large, the migration rate reduces, and the planform geometry changes become small or remain unchanged (Duan and Julien, 2010).

5.10.2 Spatial variability of planform and morphology

The understanding of bend-scale dynamic behavior is important for proper planning and designing against river reworking in the floodplain. The study of bend migration characteristics helps develop the perception on spatial and time-scale variability of river response in terms of migration and adjustment against hydraulic parameters, which in turn will allow the prediction of meander behavior. The bend geometry and the migration largely depend on floodplain characteristics. The Arial Khan River has significant spatial variability in floodplain and river morphology. In this study the river is divided into three reaches: R1, R2 and R3 by considering this variability. The floodplain is relatively wider, and soil is loosely compacted in R1 reach where frequent channel shifting within a very shorter period is a very common phenomenon. Here the existence of big point bars at bends and scattered mid-channel bars make the active channel width narrower which are represented in the photograph of Appendix D. The R1 represents the river reach of the most dynamic behavior. Here the changes of morphological parameters occur exclusively during all the periods. New bend generation and bend evolution occur at a fast pace. The matured bends either migrate in the form of downstream migration or go through bend cutoff. Bend disappearance by channel straightening also happens in this reach. For these reasons, the average age of the bends of this reach is the lowest, which is 18 years and none of the bends could survive the entire study period of 49 years. Here, the average curvature radius is 775 m, which is the lowest compared to the other two reaches. But the migration is 108 m/y, more than double of other two reaches. The strong flow immediately after the offtake of the river and the floodplain characteristics make the upper reach more sensitive in fluvial response than the lower two reaches. During the wet season excess flow submerges the bars and thus a wider channel has formed compared to the other two reaches.

Apart from the channel avulsion, the reach R2 has bends of relatively less migration prone. This local stability could be achieved by the existence of the maximum number of permanent interventions and the influence of interventions of the R1 reach as well. Thus, the morphological response of this reach is not fully natural. The artificially enforced banks cope with the anticipated flow stress. However, the non-enforced banks like that at Jafrabad Notun Bazaar (Bahir Char Katla0), experience excessive erosion. Moreover, flow diversion from this reach into the Kumar and Lower Kumar River reduces stream power to some degree. The average lifetime of the bends in this reach is moderate, which is 25 years and two bends (16 %) have been surviving all through the study period. The bends have the highest average value of the radius of curvature of 1127 m. The reach has the lowest migration rate of 42 m/y, which is less than half of that of R1 reach. The three reaches of the river have huge bend-to-bend variation in lifetime, the radius of curvature, mode of migration, rate of migration, etc. The spatial variations of the parameters are given in Table 5.11 as a summary. In the Arial Khan River, the characteristics of the R3 reach are quite opposite to that of the R1 reach. No bend gets completely disappeared, though small chute cutoffs near the apex made little changes in the shape of two bends. The average lifetime of the bends is the highest in this reach, which is 32 years. A total of 5 out of 11 bends (45%) have fulfilled the study period of 49 years. Both curvature radius and migration rate are moderate in this reach with the values of 883 m and 46 m/y respectively.

Table 5.11: Values of the parameters from three reaches: upper, middle, and lower reach.

Parameters	Upper reach	Middle reach	Lower reach
Length (km)	38	40	30
Sinuosity	1.60	1.54	2.11
Width (m)	237	277	320
Depth (m)	2.64	3.26	5.46
Aspect ratio	90	86	66
Permanent intervention no.	2	1	1
3 bends of highest migration rate	B3, B7, B11a	-	-
3 bends of lowest migration rate	-	B16a	B22, B24
Lifetime of bend (year)	18	25	32
Bend cutoff no.	4	1	1
Radius of curvature (m)	775	1127	883
Relative curvature	3.5	4.8	3.1
Migration rate (m/y)	108	42	46
Migration mode	downstream	lateral	lateral

The envelop curve from the relationship of migration rate and relative curvature for the Arial Khan River has been developed in this study, from which a definite range of relative curvature value has been identified. The range is from 1.5 to 3.5 with a peak value of ~ 3.0; at which most of the bends had migrated and the rate of migration was also high within this range. On the outside of this range (>3.5 and <1.5), the migration rate is low for most of the bends. Again, the analysis of relative curvature for individual reach reveals that the average relative curvature value for the R1 and R2 reaches are 3.5 and 3.1 respectively, which have fallen within the range. But the average relative curvature for the R3 reach is 4.8, which is far beyond the range. Thus, the outcome of the relationship of migration rate and relative curvature coincides with the individual reach scale migration rate.

Based on migration characteristics, the reach scale river response of the Arial Khan can be expressed as:

$$R1 > R3 > R2.$$

The R1 reach faces a higher range of discharge variability; thus, it is the narrowest and shallowest among all the three reaches. Both the width and depth increase successively in the other two reaches. But the parametric behaviors of R2 and R3 in the bend-scale are nearly similar. Here width, depth, and maturity of the bends are higher, and the migration rate is lower. In general, the width and depth of the downstream reach increase, which indicates the adjustment of the river against increased discharge and sediment supply of these reaches (Rhoads, 2020).

5.10.3 Temporal variation in the planform and morphology

The temporal variabilities of the length and sinuosity of the river mostly correlate, with the time-to-time evolution of the offtake morphology. But some morphological parameters, i.e., width, depth, aspect ratio, radius of curvature, relative curvature, and migration rate of bends, take a particular period to be responded to other than the period of the offtake evolution.

The discharge of the Arial Khan River had followed a specific pattern throughout the study period. An increasing pattern prevailed from 1972 to 1999, and then the trend had

been successively dropped down till 2017. In recent years, increased discharges have been found again. But the suspended sediment concentration in flow has been lowering successively since 1990 (Zheng et al., 2021). Hence, the river exhibits year-to-year variations in planform and bend geometry and migration. The summary of the findings from the time-scale analysis of the river is given in Table 5.12.

Table 5.12: Values of the parameters for the years of 1972, 1980, 1988, 1999, 2007, 2017 and 2021.

Parameters	1972	1980	1988	1999	2007	2017	2021
Length (km)	109.00	100.70	105.90	105.20	108.60	110.70	114.60
Sinuosity	1.87	1.62	1.69	1.79	1.72	1.88	1.95
Width (km)	324.25	294.25	349.42	306.42	264.00	210.25	221.58
Bend cutoff	-	3	1	1	1	-	-
Average radius of curvature (m)	833	832	747	993	1086	1045	1002
Relative curvature	2.66	3.05	2.32	3.75	4.57	5.38	5.31
Migration rate (m/y)	-	38 (1972-1980)	82 (1981-1988)	67 (1989-1999)	78 (2000-2007)	50 (2008-2017)	46 (2018-2021)

The average width of the river was higher (around 300 m) in 1972-1999. After that period the width had been decreasing till 2017 and in recent years width has started to increase again. From 1972 to 1988, the average depth of the river was below 3 m. After that period, depth had increased significantly and reached around 4 m in 1996. In recent years the depth has fallen below 3 m. The lowest value of 1.88 m was in 1981. Before the year 2000, the aspect ratio of the river was mostly above 100. From 2000 to 2019 the values remained below 100. The highest value was around 155 in 1981.

The radius of curvature of the river in the period of 1972-1999 was below the average value of 920 m, but after 2000 it was increased above the average value. The relative curvature of the river was 2.3-3.75 for all through 1972-1999, which is within the estimated range of 1.5-3.5 for the occurrence of maximum migration. This average relative curvature was within 3.7-5.4 during 2000-2021, which is above the estimated range of 1.5-

3.5. The average migration rate of the river is of the river was within 70-80 m/y from 1981 to 2007, which was within 40-50 m/y in the rest of the period.

Based on the pattern of discharge and migration parameters, two distinct periods of 1980-1999 and 2000-2021 are identified. The morphological responses of the Arial Khan River in terms of bend migration were relatively higher from 1980 through 1999 and lower between 2000 and 2021.

5.10.4 Natural and anthropogenic impact on bend-scale change of river

The factors of the natural systems within and around a river influence strongly the river planform changes, which include discharge, sediment supply, valley slope, bed-material type, and bank stress. Some factors act as a direct input to the river (discharge and sediment supply) and some factors act as a resisting force against the adjustment of the above-mentioned inputs, which are valley slope, bed-material type, and bank stress. It is difficult to identify the instantaneous impact of major flood events on morphological changes of the Arial Khan River. Because only one cutoff had occurred immediately after the major flood event of 1998. But, it has been found that the sinuosity of the river got changed to some extent immediately after the years (1988, 1998, and 2007) of the flood event. Other parametric changes due to the floods were so insignificant to be noticed separately.

In general, bank vegetation has an impact on channel geometry, as it provides a resistive force to the bank against flow stress. Different literatures have found out that, the rivers, which are narrower and comparatively deeper, achieve higher mean velocities with sufficient bank vegetation than the rivers with bare vegetation, though having the same bankfull discharges. The vast area around the offtake and R1 reach is loosely compacted char land of the Padma right bank and undergoes frequent erosion and deposition processes. The R1 and R2 reaches have plenty of distributaries and faced a high rate of channel migration and avulsion respectively. The entire region is in the absence of adequate and stable bank vegetation. But a different vegetation condition and relatively compacted soil than R1 and R2 have persisted on the banks of the R3 reach. Here, migration is self-controlled, occurred at an intake bank and in the same direction as that of previous years to most of the bends. Being a wider and shallower channel in R1, the W/D

and migration rate successively decrease from the offtake to R3; R3 is the deepest channel with the moderate migration rate.

Worldwide climate changes confer regional and local scale significant abnormality or sudden alteration into the diverse system of the environment. The Padma River catchment covers a vast area that includes the upstream of both the Ganges and the Brahmaputra River. For example, Zheng et al (2021) have described the La Nina period had persisted after 2010; heavy rains in the Padma River catchment had rendered an increased total suspended matter to discharge during that period.

The reaches R1 and R2 have river control structures, such as 1.44 km long right and 1.08 km long left bank protection for Dhaka-Mawa-Bhanga national highway adjacent to Haji Shariatullah Bridge, and 2.11 km long Madaripur town protection project along the right bank of the Arial Khan River, which restrict the free adjustment of these reaches. The interventions of bank protection works may have an impact on the excessive migration to some unprotected bends just the downstream locations of interventions. On the other hand, the partially controlled river may sometimes exhibit unusual behavior which is inconsistent with the historical record. The study has predicted that future migration of bend near the Arial Khan Bridge will threaten the bridge in near future.

5.10.5 Bend migration prediction

Three critical bends based on locations and the high rates of migration have been selected for future migration prediction analysis for the year 2024 for bend B3 and 2025 for bend B17 and 2030 for bend B27. The years are selected based on consistency of the migration behavior of the bends in previous years. Through these analyses, the probable position and curvature of the bends are identified. The bend B3 has huge potential to bypass the Haji Shariatullah Bridge in near future and has a threat to the bank protection project of the Dhaka-Mawa-Bhanga national highway. The prediction of the bend B17 reveals that the curvature of the bend will increase to some extent, will cause erosion to a vast area at Baherchar Katla. The bend B27 is located in the lower reach of the river, where small-scale chute cutoff had occurred, and channel avulsion is absent. But the prediction analysis says there is a possibility of avulsion to take place in this bend in near future, by which a 10 km length of the river will abandon.

CHAPTER SIX

CONCLUSIONS AND RECOMMENDATIONS

6.1 Conclusions

As a connecting river, the Arial Khan is very important for the surrounding floodplain and other tributary and distributary rivers and canals. The planform study of the river covers river morphology and deals with some important hydro-morphological controlling parameters. The overall shifting of the alluvial meander river planform is the response of morphology of the river in bend-scale and occurs repeatedly within the adjacent floodplain. For the Arial Khan River, some shifting footprints still exist as meander scars and oxbow lakes. The study of this planform changes in time- and bend-scales reveals the migration characteristics of the river. The key conclusions of this study are drawn as follows:

1. The Arial Khan River has spatial variability in floodplain characteristics, discharge: several entries and exits of flow, and strengths of the bank: natural and artificial. The heterogeneity of the floodplain around the upper reach and to some extent to the middle reach is so explicit to be identified easily through the Google Earth images and field visits. This portion of the river has a relatively wide river valley with loosely compacted soil, extended point bars along the banks, several oxbow lakes and meander scars, thin and scattered vegetation, tributary and distributary rivers and khals, and some permanent interventions. The lower reach is in a more natural environment having dense vegetation, compacted soil, and comparatively fewer and insignificant confluences. Thus, it was worthy to divide the river into three reaches based on some common parametric dissimilarity. Again, the river has significant temporal variability in discharge and as a consequence of sinuosity, length, width, depth and other bend parameters. Thus, the time-series analysis by image processing with a selection of the appropriate years is one of the important tasks of the study.
2. The offtake of the Arial Khan River works as a strong controlling component of the hydro-morphology, as it influences the entry of discharge and sediment flow from the Padma River by diverting a certain quantity into the Arial Khan. The offtake morphology of the river has been adapting in such a way that increasing and

decreasing trends of flow for a certain period persist in the Arial Khan River. However, the parent River Padma does not follow any such trend. Thus, the offtake of the Arial Khan is considered as one of the important components for this study, which renders a specific profile of the river; especially the change of river length and sinuosity are precisely identified. During downward shiftings of the offtake from ultimate upward positions, river lengths have been increased to 6-10 km and the sinuosities on an average of 0.33. Though each time 4-6 km linear lengths have been cut off from the offtake due to this shifting. Hence, those years of the images are selected for the time-scale analysis when the offtake was positioned to extreme downward (south/southwest) and extreme upward (north/northeast) points. According to the offtake positions, the years 1972, 1980, 1999, 2007, and 2021 are the selected, when the offtake was in downward and upward points alternately. Additional two years 1988 and 2017 have been selected as interim years.

3. The analysis of the bends migration consists of some migration parameters such as the lifetime of bends, the radius of curvature and relative curvature, and most importantly the migration rate. Some parameters are evaluated in reach- and section-wise such as river width, aspect ratio, and bend cutoff location. Finally, the findings of the time- and bend-scale migration analysis of the river are represented in three reaches – upper, middle, and lower of consecutive bends and in six time periods of (1972-1980), (1981-1988) (1989-1999), (2000-2007), (2008-2017) and (2018-2021).
4. The change of the morphology of the Arial Khan in terms of bend migration can be expressed in three reaches chronologically as – upper reach > lower reach > middle reach. The parameters in the upper reach conserve the values in such a way that make the reach more dynamic and migration prone. The bends of this reach have the lowest lifetime of 18 years and radius of curvature of 775 m and highest migration rate of 108 m/y and bend cutoff no. of 4. The values of the lifetime, radius of curvature, migration rate, and bend cutoff no. for the lower reach are 32 years, 883 m, 46 m/y, and 1 respectively and for the middle reach are 25 years, 1127 m, 42 m/y, and 1 respectively. These values, more specifically the migration rate- less than half to that of upper reach demonstrated lower two reaches more stable than upper reach. Again, the range of relative curvature value of the Arial Khan is established in this study as 1.50-3.50 with a peak ~ 3.00, for which the consecutive bends exhibit the highest

migration. For the upper and lower reach, the values are 3.5 and 3.1; remain within the established range. But, for the middle reach relative curvature is 4.8, which is above the range. The relative curvature values of three reaches also express the chronological bend migration position of the reaches.

5. From time-scale analysis, the change of the morphology of the Arial Khan in terms of bend migration can be expressed in the time periods as 1972-1999 > 2000-2021. The parameters which have relationships to bend migration show higher values in the period of 1972- 1999 and lower values in the period of 2000-2021. During 1972-1999, total bend cutoff occurred 5 out of 6; the radius of curvature values were below the average value of the river of 920 m; relative curvature value of 2.32-3.75, almost in the estimated range of 1.5-3.5; and the migration rate was in increasing trend. On the other hand, from 2000 to 2021, total bend cutoff no. was 1 out of 6; the radius of curvature values were above the average value of the river of 991 m; relative curvature value of 4.57-5.38, remained beyond the estimated range of 1.5-3.5; and the migration rate was in decreasing trend.
6. The average width and depth of the river reaches are in an order of lower reach > middle reach > upper reach. The time-scale analysis shows that the overall trends of width, depth, aspect ratio, and bend migration rate decline with time. Most of the bends of the river in recent years are changing their shapes by going through either an expansion or a contraction process; the tendency of downstream migration occurrence is low. The river is not facing any type of bend cutoff for the last 17 years. Again, the trend of sinuosity continuously climbs up. All the characteristics indicate the river adjustment. This adjustment may be interrupted by an unusual flow variation in the future.
7. The migration prediction analysis for three bends of B3, B17, and B27 demonstrates probable physical conditions and future threats of the bends. The high rate of migration and the direction of migration in the B3 bend create the possibility of bypassing the permanent bank protection measures at its downstream location. Prediction on bend B17 migration reveals expansion of the bend; hence, erosion will spread along a longer length of the bend. A probable avulsion of a 10 km long

channel has been predicted in bend B27. Necessary attempts will be taken to resolve the problem based on this prediction.

8. In this study, an empirical analysis approach has been used where different methods and techniques have been integrated from the well-established theories and empirical relationships of hydrological and morphometric parameters. The absence of sediment and local discharge data are the downstream were the major limitations of this study. Otherwise, this study can be considered as a milestone of multiple time- and bend-scale analysis of a meander river of Bangladesh.

6.2 Recommendations

The morphological study of a river covers vast areas and knowledge of different components and issues from the local bend-scale to a whole river system. The individual component has its influence on morphometric changes of the river as a whole. During the study, all parameters/ components could not be incorporated due to the unavailability of data and information. Thus, the following recommendations are made based on experiences of this study:

1. The bend-scale analysis for others meander rivers is in need to develop a river database on the morphological behavior of the rivers. This study will be an initiation of that attempt; the methodology and the analysis technique can be incorporated for studying other meander rivers.
2. The rivers having several tributaries and distributaries should have more than one discharge data.
3. The tidal influence, especially in the downstream reaches of meander rivers, should be considered.
4. The dominant water level, discharge, and hydraulic geometry are very important parameters, which are generally defined as the bankfull condition of the specific river and should be incorporated in the right way.

5. Different components of the floodplain geology are important parameters for the migration process, should be considered.
6. The influence of vegetation cover on planform changes of the Arial Khan River is significant, should be studied in detail.
7. The impact of several tributaries and distributary on local bend migration could be another topic for future study, which is important, especially for the flow diversion projects from the Arial Khan River.
8. The interventions, especially the permanent ones, should be carefully made after rigorous study on river bend migration.
9. The temporary protection work should be done with proper design and plan. The scattered unplanned dumping of the geobag is not only a waste of money but also hostile to nature.

REFERENCES

- Akhter, S., Eibek, K. U., Islam, S., Islam, A. R. M. T., Chu, R., and Shuanghe, S. (2019). Predicting spatiotemporal changes of channel morphology in the reach of Teesta River, Bangladesh using GIS and ARIMA modeling. *Quaternary International*, 513, 80–94. <https://doi.org/10.1016/j.quaint.2019.01.022>
- Akter, J., Sarker, M. H., and Haque, P. (2013). Morphological processes and effective river erosion management: a case study of the Arial Khan River in Bangladesh. *Proceedings of 4th International Conference on Water and Flood Management*, 263–274.
- Allison, M. A. (1998). Historical changes in the Ganges-Brahmaputra delta front. *Journal of Coastal Research*, 14(4), 1269-1275.
- Arefin, R., Meshram, S. G., and Seker, D. Z. (2021). River channel migration and land-use/land-cover change for Padma River at Bangladesh: a RS- and GIS-based approach. *International Journal of Environmental Science and Technology*, 18, 3109–3126. <https://doi.org/10.1007/s13762-020-03063-7>
- Ashrafuzzaman, A. K. (1992). A study on the geometric aspects of the Arial Khan River. Master of Engineering (Water Resources) Thesis, Department of Water Resources Engineering, Bangladesh University of Engineering and Technology, Dhaka.
- ASPRS. (1990). ASPRS accuracy standards for largescale maps. http://www.asprs.org/a/society/committees/standards/1990_jul_1068-1070.pdf
- Bag, R., Ismail, M., and Bandyopadhyay, J. (2019). Assessing the oscillation of channel geometry and meander migration cardinality of Bhagirathi River, West Bengal, India. *Journal of Geographical Sciences*, 29(4), 613–634. <https://doi.org/10.1007/s11442-019-1618-z>
- Bagnold, R. A. (1960). Some aspects of the shape of river meanders. *U.S. Geological Survey Professional Paper 282-E*, U.S. Geological Survey, Washington, D. C., 135–144.

Banda, M. S., and Meon, I. G. (2018). *Morphological development of meandering rivers due to changing discharge regimes* [Post Doctoral dissertation, Technical University of Braunschweig, Germany].

Begum, M. (2018). *The effect of climate and anthropogenic change on the spatial variability of turbidity maxima in the southwest delta of Bangladesh*. [Master of Science Thesis, Department of Applied Physics, University of Cadiz, Spain].

Biswas, R. N., Islam, M. N., Islam, M. N., and Shawon, S. S. (2021). Modeling on approximation of fluvial landform change impact on morphodynamics at Madhumati River Basin in Bangladesh. *Modeling Earth Systems and Environment*, 7(1), 71–93. <https://doi.org/10.1007/s40808-020-00989-2>

Biswas, R. N., Mia, M. J., and Islam, M. N. (2018). Predictive dynamics of channel pattern changing trends at Arial Khan River (1977-2018), Bangladesh. *American Journal of Geoscience*, 8(1), 1–13.

Briaud, J. L., Chen, H. C., and Park, S. (2001). *Predicting meander migration: Evaluation of some existing techniques* (Report No. 2105-1). USA: Texas Department of Transportation (pp. 1061-1080).

Brice, J. C. (1974). Evolution of meander loops. *Geological Society of America Bulletin*, 85, 581–586.

Brice, J. C. (1975). *Airphoto interpretation of the form and behavior of alluvial rivers*. (Final report). U. S. Army Research Office – Durham, USA.

Callander, R. A. (1969). Instability and river channels. *Journal of Fluid Mechanics*, 36(3), 465–480. <https://doi.org/https://doi.org/10.1017/S0022112069001765>.

Chang, H. H. (1992). *Fluvial Processes in river engineering*. Krieger Publishing, Malabar, Florida.

Chitale, S. V. (1970). River channel patterns. *Journal of Hydraulic Engineering*, 96, 201–221. <https://doi.org/10.1061/JYCEAJ.0002261>

Coleman, J. M. (1969). Brahmaputra River: channel processes and sedimentation. *Sedimentary Geology*, 3, 139–239. [http://dx.doi.org/10.1016/0037-0738\(69\)90010-4](http://dx.doi.org/10.1016/0037-0738(69)90010-4)

Constantine, J. A., Dunne, T., Ahmed, J., Legleiter, C., and Lazarus, E. D. (2014). Sediment supply as a driver of river meandering and floodplain evolution in the Amazon Basin. *Natural Geoscience*, 7, 899–903. <https://doi.org/10.1038/ngeo2282>

Deb, M., and Ferreira, C. (2015). Planform channel dynamics and bank migration hazard assessment of a highly sinuous river in the north-eastern zone of Bangladesh. *Environmental Earth Sciences*, 15(10), 6613–6623.

Dewan, A., Corner, R., Saleem, A., Rahman, M. M., Haider, M. R., Rahman, M. M., and Sarker, M. H. (2017). Assessing channel changes of the Ganges-Padma River system in Bangladesh using Landsat and hydrological data. *Geomorphology*, 276, 257–279. <https://doi.org/10.1016/j.geomorph.2016.10.017>.

Dietrich, W. E., and Smith, J. D. (1983). Influence of the point bar on flow through curved channels. *Water Resources Research*, 19(5), 1173–1192.

Donovan, M., Belmont, P., and Sylvester, Z. (2021). Evaluating the relationship between meander-bend curvature, sediment supply, and migration rates. *Journal of Geophysical Research: Earth Surface*, 126(3). <https://doi.org/10.1029/2020JF006058>

Duan, J. G., and Julien, P. Y. (2010). Numerical simulation of meander evolution. *Journal of Hydrology*, 391(1–2), 34–46. <https://doi.org/doi:10.1016/j.jhydrol.2010.07.005>.

Ferguson, R. I. (1975). Meander irregularity and wavelength estimation. *Journal of Hydrology*, 26, 315–333. [https://doi.org/10.1016/0022-1694\(75\)90012-8](https://doi.org/10.1016/0022-1694(75)90012-8)

Finotello, A., Lanzoni, S., Ghinassi, M., Marani, M., Rinaldo, A., and D'Alpaos, A. (2018). Field migration rates of tidal meanders recapitulate fluvial morphodynamics. *Proceedings of the National Academy of Sciences*, 115(7), 1463-1468.

Gautam, V. K., Gaurav, P. K., Murugan, P., and Annadurai. (2015). Assessment of surface water dynamics in Bangalore using WRI, NDWI, MNDWI, supervised classification and KT transformation. *Aquatic Procedia*, 4, 739–746.

Gazi, M. Y., Hossain, F., Sadeak, S., and Uddin, M. M. (2020). Spatiotemporal variability of channel and bar morphodynamics in the Gorai-Madhumati River, Bangladesh using remote sensing and GIS techniques. *Frontiers of Earth Science*, 14(4), 828–841.

Ghosh, B., and Mukhopadhyay, S. (2021). Channel planform dynamics, avulsion and bankline migration: A study in the monsoon-dominated Dwarkeswar River, Eastern India. *Arabian Journal of Geosciences*, 14(10) 1–16.

<https://doi.org/https://doi.org/10.1007/s12517-021-07270-5>.

Goodbred Jr., S. L., and Kuehl, S. A. (1999). Holocene and modern sediment budgets for the Ganges-Brahmaputra River system: Evidence for high storage and dispersal to flood-plain, shelf, and deep-sea depocenters. *Geology*, 27(6), 559–562.

Guo, X., Gao, P., and Li, Z. (2021). Morphological characteristics and changes of two meandering rivers in the Qinghai-Tibet Plateau, China. *Geomorphology*, 379, 1–11. <https://doi.org/https://doi.org/10.1016/j.geomorph.2021.107626>

Halder, A. and Chowdhury, R. M. (2021). Evaluation of the river Padma morphological transition in the central Bangladesh using GIS and remote sensing techniques. *International Journal of River Basin Management*, 1–15.

<https://www.tandfonline.com/loi/trbm20>

Harvey, M. D. (1988). *Meander belt dynamics of the Sacramento River, California*. Proceedings of the California Riparian Systems Conference, September 22–24, Davis, CA. USDA Forest Service General Technical Report, PSW-110, 54– 59.

Heo J., Duc, T. A., Cho, H. S., and Choi, S. U. (2009). Characterization and prediction of meandering channel migration in the GIS environment: A case study of the Sabine River in the USA. *Environmental Monitoring and Assessment*, 152(1), 155–165.

Hickin, E. J., and Nanson, G. C. (1975). The Character of channel migration on the Beatton River, Northeast British Columbia, Canada. *Geological Society of America Bulletin*, 86(4), 487–494.

Hickin, E. J., and Nanson, G. C. (1984). Lateral migration rates of river bends. *Journal of Hydraulic Engineering*, 110(11), 1557–1567.

[https://doi.org/10.1061/\(asce\)0733-9429\(1984\)110:11\(1557\)](https://doi.org/10.1061/(asce)0733-9429(1984)110:11(1557)).

Hooke, J. M. (1987). *Changes in meander morphology*. International Geomorphology, 1986: Proceedings of the First International Conference on Geomorphology, Chichester: John Wiley and Sons, 1, 591-609.

Hooke, J. M. (1977). Distribution and nature of changes in river channel pattern: The example of Devon. *River Channel Changes (British Geomorphological Research Group)*, John Wiley and Sons, 265-279.

Hooke, J. M. (2004). Cutoffs galore!: Occurrence and causes of multiple cutoffs on a meandering river. *Geomorphology*, 61(3-4), 225 – 238.

<https://doi.org/10.1016/j.geomorph.2003.12.006>

Hooke, J. M. (2006). Hydromorphological adjustment in meandering river systems and the role of flood events. *Iahs- Aish Publication*, 306, 127–135.

Hooke, J. M., and Yorke, L. (2010). Rates, distributions and mechanisms of change in meander morphology over decadal timescales, River Dane, UK. *Earth Surface processes and Landform*, 35(13) 1601–1614. <https://doi.org/10.1002/esp.2079>

Hossain, M. M., Islam, M. Z., Ferdousi, S., Kabir, M. M., and Rahman, K. M. (2007). *Morphological characteristics of Arial Khan River in the vicinity of Arial Khan Bridge in*

Bangladesh. Proceedings of International Conference on Institute of Water and Flood Management, BUET, 241–248.

Howett, Julia. (2017). *Meander belt delineation: Developing a predictive model for meander belt width*. [Master of Science Thesis, the University of Western Ontario, London, Ontario, Canada. 4915. <https://ir.lib.uwo.ca/etd/4915>

Hudson, P. F., and Kesel, R. H. (2000). Channel migration and meander-bend curvature in the lower Mississippi River prior to major human modification, *Geology*, 28(6), 531-534. [https://doi.org/10.1130/0091-7613\(2000\)28<531](https://doi.org/10.1130/0091-7613(2000)28<531)

Hussain, M. T., Uddin, M. M., Munna, G. M., Sanzida, R., and Choudhury, T. P. (2021). Assessment of bank erosion-deposition and bankline shifting of Padma River at Chapainawabgonj district in Bangladesh using RS and GIS technique, *International Journal of Scientific and Technology Research*, 10(4), 376-381.

Ikeda, S., Parker, G., and Sawai, K. (1981). Bend theory of river meanders. Part 1: Linear development. *Journal of Fluid Mechanics*, 112, 363–377.

Islam, A. R. M. T. (2016). Assessment of fluvial channel dynamics of Padma River in northwestern Bangladesh. *Universal Journal of Geoscience*, 4(2), 41–49. <https://doi.org/10.13189/ujg.2016.040204>

Julien, P. Y. (2018) *River Mechanics (2nd Ed.)*. Cambridge University Press. <https://doi.org/DOI:10.1017/9781316107072>

Lagasse, P. F., Spitz, W. J., Zevenbergen, L. W., and Zachmann, D. W. (2004). *Handbook for predicting stream meander migration and supporting software*. National Cooperative Highway Research Program, Transportation Research Board, Washington, D.C. <https://doi.org/10.17226/23346>

Langbein, W. B., and Leopold, L. B. (1966). River meanders and the theory of minimum variance. *United States Geological Survey, Professional Paper 442-H*, 1-15.

Leopold, L. B. (1972). River channel change with time: An example. *Geological Society of America Bulletin*, 84(6), 1845–1860.

Leopold, L. B., and Maddock, T. (1953). *The hydraulic geometry of stream channels and some physiographic implications (Vol. 252)*. US Government Printing Office.

Leopold, L. B., and Wolman, M. G. (1957). *River channel patterns: braided meandering and straight*. Geological Survey of Professional Papers, 282-B, 39–85.

Leopold, L. B., and Wolman, M. G. and Miller, J. P. (1964). *Fluvial processes in geomorphology*. San Francisco, W. H. Freeman and Co.

Mamun, M. Y. (2008). *Study of offtake morphology and conveyance characteristics of Arial Khan River*. [Master of Engineering (Water Resources) Thesis, Department of Water Resources Engineering, Bangladesh University of Engineering and Technology, Dhaka].

Mason, J., and Mohrig, D. (2019). Differential bank migration and the maintenance of channel width in meandering river bends. *Geology*, 47(12), 1136–1140.
<https://doi.org/https://doi.org/10.1130/G46651.1>

Mcfeters, S. K. (1996). The use of the normalized difference water index (NDWI) in the delineation of open water features. *International Journal of Remote Sensing*, 17, 1425–1432.

Mirzaee, S., Yousefi, S., Keesstra, Saskia Pourghasemi, Hamid Reza Cerdà, A., and Fuller, I. C. (2018). Effects of hydrological events on morphological evolution of a fluvial system. *Journal of Hydrology*, 563, 33–42. <https://doi.org/10.1016/j.jhydrol.2018.05.065>

Morais, E. S., Rocha, P. C., and Hooke, J. (2016). Spatiotemporal variations in channel changes caused by cumulative factors in a meandering river: the lower Peixe River, Brazil. *Geomorphology*, 273, 348–360.

- Mukherjee, N. R., and Samuel, C. (2016). Assessment of the temporal variations of surface water bodies in and around Chennai using Landsat imagery. *Indian Journal of Science and Technology*, 9(18), 1–7. <https://doi.org/10.17485/ijst/2016/v9i18/92089>
- Nanson G.C. and Hickin E.J. 1986. A statistical analysis of bank erosion and channel migration in western Canada. *Geological Society of America Bulletin*, 97(4), 497–504.
- Nicoll, T. J., and Hickin, E. J. (2010). Planform geometry and channel migration of confined meandering rivers on the Canadian prairies. *Geomorphology*, 116(1–2), 37–47.
- Nippon Koei Co., Ltd. and Construction Project Consultants, Inc. (2005). *The Feasibility Study of Padma Bridge in the People's Republic of Bangladesh*(Final Report, volume 5). River Studies, Japan International Cooperation Agency (JICA) and Jamuna Multipurpose Bridge Authority (JMBA).
- Ophra, S. J., Begum, S., and Islam, R. (2018). Assessment of bank erosion and channel shifting of Padma River in Bangladesh using RS and GIS techniques. *Spatial Information Research*, 26, 599–605.
- Prosoil Foundation Consultant (2016). *Classification of wetlands of Bangladesh*(Main Report, Volume 1). Department of Bangladesh Haor and Wetland Development, Ministry of Water Resources, Government of the People's Republic of Bangladesh, Dhaka.
- Parish Geomorphic (2004). *Belt width delineation procedures* (Report 98-023). Toronto and Region Conservation Authority.
<http://sustainabletechnologies.ca/wp/wp-content/uploads/2013/01/Belt-Width-Delineation-Procedures.pdf>
- Rhoads, B. L. (2020). *River dynamics: Geomorphology to support management*. Cambridge University Press. <https://doi.org/10.1017/9781108164108>
- Rosgen, D. L. (1994). A classification of natural rivers. *Catena*, 22(3), 169–199. [https://doi.org/10.1016/0341-8162\(94\)90001-9](https://doi.org/10.1016/0341-8162(94)90001-9)

Roy, B., Khan, M. S. M., Saiful Islam, A. K. M., Khan, M. J. U., and Mohammed, K. (2021). Integrated flood risk assessment of the Arial Khan River under changing climate using IPCC AR5 risk framework. *Journal of Water and Climate Change*, 12(7), 3421-3447.

Park C. C. (1977). World-wide variations in hydraulic geometry exponents of stream channels – an analysis and some observations. *Journal of Hydrology*, 33, 133–146.

Sarker, M. H. (2008). *Morphological response of the Brahmaputra–Padma–Lower Meghna River system to the Assam earthquake of 1950*. [Doctoral thesis, University of Nottingham].

Sarker, M. H., Akter, J., and Rahman, M. (2013). *Century-scale dynamics of the Bengal delta and future development*. Proceedings of 4th International Conference on Water and Flood Management, Institute of Water and Flood Management, BUET, 91–104. <https://www.researchgate.net/publication/263125663>

Schumm, S. A. (1968). River adjustment to altered hydrologic regimen, Murrumbidgee River and paleochannels, Australia. *Geological Survey of Professional Papers*, US Government Printing Office, 598, 1-65.

Schumm, S. A. (1977). *The fluvial system*. John Wiley and Sons, New York.

Schumm, S. A., and Thorne, C. R. (1989). *Geologic and geomorphic controls on bank erosion*. In M. A. Port (ed), Proceedings of the 1989 National Conference on Hydraulic Engineering, Ports, M. A. (ed.), Hydraulic Engineering, New York, 106–111.

Seminara, G., and Tubino, M. (1989). Alternate bars and meandering: Free, forced and mixed interactions. *Water Resources Monograph*, 12, 267–320.

Shen, H. W. (1971). Stability of alluvial channels. *Water Resource Publications, Fort Collins, CO*, 1, 16–33.

Shen, H. W., Schumm, S. A., Doehring, D., and State, C. (1979). Stability of stream channel patterns. *Committee on Hydrology, Hydraulics, and Water Quality*, 22–28.

Sylvester, Z., Durkin, P., Covault, J. A., and Sharman, G. R. (2019). High curvatures drive river meandering. *Geology*, 47, 263–266. <https://doi.org/10.1130/G45608.1>

Thorne, C. R. (1992). Bend scour and bank erosion on the meandering Red River, Louisiana. *Lowland Floodplain Rivers: Geomorphological Perspectives*, John Wiley and Sons, New York, 95–115.

Uddin, M., Deb, M., and Das, D. (2012). Remote sensing-based analysis of critical bends of Kushiyara River in Bangladesh. *Space Science and Technology*, 1(3), 1–12.

Winkley, B., Leslighter, E. J., and Cooney, J. R. (1994). Instability problems of the Arial Khan River, Bangladesh, *The variability of large alluvial rivers*, 269–284.

Yousefi, S., Pourghasemi, H.R., Rahmati, O., Keesstra, S., Emami, S. N., and Hooke, J. (2021). Geomorphological change detection of an urban meander loop caused by an extreme flood using remote sensing and bathymetry measurements: A case study of Karoon River, Iran. *Journal of Hydrology*, 597, 1–31.

Zheng, Z., Wang, D., Gong, F., He, X., and Bai, Y. (2021). A study on the flux of total suspended matter in the Padma River in Bangladesh based on remote-sensing data. *Water*, 13(17), 2373.

APPENDIX A
DATA OF BEND GEOMETRY AND RIVER PLANFORM OF DIFFERENT
YEARS

Table A1: Bend ID, coordinate, river width and amount of migration of each bend (1972 - 1980).

Bend ID	Latitude (Degrees Minutes)	Longitudes (Degrees Minutes)	R _c (m)	Width (m)			Migration	
				Crossing 1	Apex	Crossing 2	Lateral	Downstream
B1	23° 26.616'	90° 6.438'	426	388	387	148.3	16	410
B2	23° 25.559'	90° 4.186'	331	249	246	161	8	185
B5	23° 23.634'	90° 3.570'	218	157	382	135	Neck Cutoff (1978)	
B11	23° 17.652'	90° 5.501'	432	201	199	154	Chute Cutoff (1976)	
B12	23° 17.014'	90° 8.167'	802	251	134	140	352	-68
B13	23° 14.849'	90° 7.816'	391	141	210	248	240	104
B16	23° 11.005'	90°12.742'	752	380	288	287	217	204
B17	23° 11.271'	90°14.363'	888	359	375	381	172	-173
B19	23° 7.505'	90°14.177'	547	369	353	265	188	73
B20	23° 7.574'	90°16.189'	2435	295	322	325	116	-35
B22	23° 6.649'	90°19.871'	804	359	279	358	41	41
B23	23° 5.029'	90°19.005'	881	458	287	320	89	144
B24	23° 4.317'	90°19.638'	768	320	349	446	14	52
B25	23° 3.169'	90°17.948'	1063	446	345	420	957	0
B28	23° 1.965'	90°19.811'	1160	420	315	419	369	97
B29	22° 59.973'	90°18.968'	1011	554	397	361	77	95
B31	22° 59.238'	90°20.018'	1270	361	320	462	26	186

Table A2: Bend ID, coordinate, river width and amount of migration of each bend (1980 - 1988).

Bend ID	Latitude (Degrees Minutes)	Longitudes (Degrees Minutes)	R _c (m)	Width (m)			Migration (m)	
				Crossing 1	Apex	Crossing 2	Lateral	Downstream
B1	23° 26.616′	90° 6.438′	494	170	182	177	Neck cutoff (1988)	
B3	23° 26.456′	90° 4.803′	1190	180	170	180	906	479
B2	23° 25.559′	90° 4.186′	324	170	480	180	457 (Straight)	
B5a	23° 23.012′	90° 4.519′	407	158	360	180	113	732
B11a	23° 16.979′	90° 7.313′	443	180	255	217	442	1561
B12	23° 17.014′	90° 8.167′	549	217	300	180	643	170
B13	23° 14.849′	90° 7.816′	418	180	170	180	Avulsion	
B16	23° 11.005′	90°12.742′	675	370	300	365	66	370
B17	23° 11.271′	90°14.363′	685	403	350	420	392	-201
B19	23° 7.505′	90°14.177′	491	340	277	240	87	302
B20	23° 7.574′	90°16.189′	2385	240	300	315	416	-601
B22	23° 6.649′	90°19.871′	795	300	240	261	281	-57
B23	23° 5.029′	90°19.005′	848	440	300	240	204	179
B24	23° 4.317′	90°19.638′	669	240	300	300	437	-26
B25	23° 3.169′	90°17.948′	607	300	480	300	487	354
B28	23° 1.965′	90°19.811′	1544	300	300	300	1031	-290
B29	22° 59.973′	90°18.968′	1089	300	255	300	589	-54
B31	22° 59.238′	90°20.018′	1370	300	480	472	Avulsion	

Table A3: Bend ID, coordinate, river width and amount of migration of each bend (1988 - 1999).

Bend ID	Latitude (Degrees Minutes)	Longitudes (Degrees Minutes)	R _C (m)	Width (m)			Migration (m)	
				Crossing 1	Apex	Crossing 2	Lateral	Downstream
B1a	23° 26.658'	90° 5.665'	242	300	300	342	1027	512
B3	23° 26.456'	90° 4.803'	589	332	283	390	458	1985
B4	23° 23.968'	90° 5.468'	919	281	420	366	1010	242
B5a	23° 23.012'	90° 4.519'	786	319	404	217	96	-115
B6	23° 22.995'	90° 5.955'	1193	217	301	217	882	-742
B7	23° 21.671'	90° 7.582'	669	300	260	283	192	734
B8	23° 21.234'	90° 6.935'	769	283	505	258	66	1160
B11a	23° 16.979'	90° 7.313'	633	390	240	250	840	271
B12	23° 17.014'	90° 8.167'	449	270	240	150	125	-495
B16	23° 11.005'	90°12.742'	756	390	300	281	281	111
B17	23° 11.271'	90°14.363'	555	330	336	277	195	-535
B19	23° 7.5052'	90°14.177'	474	384	726	309	421	97
B20	23° 7.5747'	90°16.189'	1980	309	330	324	47	-72
B22	23° 6.649'	90°19.871'	642	390	558	277	128	624
B23	23° 5.029'	90°19.005'	857	277	510	330	952	311
B24	23° 4.317'	90°19.638'	436	330	362	361	320	841
B25	23° 3.169'	90°17.948'	685	420	450	300	12	231
B28	23° 1.965'	90°19.811'	725	270	300	296	208	219
B29	22° 59.973'	90°18.968'	832	391	420	336	455	751

Table A4: Bend ID, coordinate, river width and amount of migration of each bend (1999-2007).

Bend ID	Latitude (Degrees Minutes)	Longitudes (Degrees Minutes)	R _c (m)	Width (m)			Migration (m)	
				Crossing 1	Apex	Crossing 2	Lateral	Downstream
B1a	23° 26.658'	90° 5.665'	848	240	300	192	1155	-151
B3	23° 26.456'	90° 4.803'	461	234	300	322	481	840
B4	23° 23.968'	90° 5.468'	2078	200	254	224	1789	274
B5a	23° 23.012'	90° 4.519'	975	210	235	300	Neck Cutoff (2004)	
B6	23° 22.995'	90° 5.955'	780	300	192	240	708	283
B7	23° 21.671'	90° 7.582'	1030	257	240	235	81	1301
B8	23° 21.234'	90° 6.935'	639	235	270	192	456	695
B9	23° 19.895'	90° 7.657'	1301	192	420	240	847	568
B12	23° 17.014'	90° 8.167'	570	180	180	180	Channel Avulsion	
B14	23° 14.672'	90° 8.029'	347	137	190	128	101	126
B15	23° 13.233'	90° 13.268'	947	319	270	210	14	425
B16	23° 11.005'	90° 12.742'	1422	400	371	275	118	108
B17	23° 11.271'	90° 14.363'	633	212	277	228	276	-147
B18	23° 9.670'	90° 14.365'	1843	228	300	212	343	153
B20	23° 7.574'	90° 16.189'	2176	270	480	237	1130	932
B21	23° 6.649'	90° 19.871'	2094	338	270	210	104	207
B22	23° 5.029'	90° 19.005'	711	210	240	366	108	-32
B23	23° 4.684'	90° 18.453'	521	380	330	270	570	443
B24	23° 3.169'	90° 17.948'	686	390	270	270	37	151
B25	23° 7.505'	90° 14.177'	870	300	240	250	402	157
B26	23° 2.420'	90° 17.703'	410	243	330	270	439	3
B27	23° 2.849'	90° 18.322'	1713	270	360	265	20	1398
B28	23° 1.965'	90° 19.811'	769	265	300	270	98	140
B29	22° 59.574'	90° 18.570'	558	390	390	210	13	180

Table A5: Bend ID, coordinate, river width and amount of migration of each bend (2007-20017).

Bend ID	Latitude (Degrees Minutes)	Longitudes (Degrees Minutes)	R _c (m)	Width (m)			Migration (m)	
				Crossing 1	Apex	Crossing 2	Lateral	Downstream
B1a	23° 26.658'	90° 5.665'	2197	261	180	180	382	-333
B3	23° 24.648'	90° 4.445'	947	220	210	180	155	2141
B4	23° 23.870'	90° 6.052'	1301	210	270	180	671	-451
B5b	23° 23.005'	90° 6.034'	817	180	408	210	Straight	
B6	23° 22.942'	90° 6.935'	640	210	235	240	Straight	
B7	23° 20.573'	90° 7.456'	627	210	300	180	Straight	
B8	23° 20.081'	90° 6.903'	386	180	270	180	Straight	
B9	23° 19.259'	90° 7.99'	929	300	270	180	338	1021
B14	23° 14.672'	90° 8.029'	362	210	242	177	609	-378
B15	23° 13.233'	90° 13.268'	1165	350	210	235	387	225
B16	23° 11.005'	90° 12.742'	2013	223	418	166	42	152
B17	23° 11.271'	90° 14.363'	621	220	188	172	110	-104
B18	23° 9.670'	90° 14.365'	3246	172	240	258	64	36
B19a	23° 7.542'	90° 15.291'	1136	210	180	276	269	368
B20	23° 7.574'	90° 16.189'	995	276	210	205	303	-335
B21	23° 6.649'	90° 19.871'	2447	205	240	240	295	564
B22	23° 5.029'	90° 19.005'	676	240	243	192	89	-46
B23	23° 4.684'	90° 18.453'	1152	192	443	218	820	255
B24	23° 3.169'	90° 17.948'	809	218	360	370	53	80
B25	23° 7.505'	90° 14.177'	791	420	210	240	227	19
B26	23° 2.420'	90° 17.703'	426	240	255	180	228	507
B27	23° 2.849'	90° 18.322'	660	180	360	235	125	-159
B28	23° 1.965'	90° 19.811'	738	235	330	254	118	69
B29	22° 59.574'	90° 18.570'	649	282	322	253	154	246
B30	22° 59.564'	90° 19.570'	1408	253	360	256	126	-309

Table A6: Bend ID, coordinate, river width and amount of migration of each bend (2017-2021).

Bend ID	Latitude (Degrees Minutes)	Longitudes (Degrees Minutes)	R _c (m)	Width (m)			Migration (m)	
				Crossing 1	Apex	Crossing 2	Lateral	Downstream
B1a	23° 26.658'	90° 5.665'	2222	91	190	147	201	-65
B3	23° 24.648'	90° 4.445'	597	191	90	150	469	692
B4	23° 23.870'	90° 6.052'	867	150	180	96	99	41
B9	23° 19.259'	90° 7.990'	620	255	210	180	28	109
B10	23° 18.161'	90° 6.970'	1383	180	164	180	439	-121
B14	23° 14.672'	90° 8.029'	677	217	150	131	35	9
B15	23° 13.233'	90° 13.268'	855	215	180	151	223	108
B16	23° 11.005'	90° 12.742'	1880	313	173	198	3	4
B17	23° 11.271'	90° 14.363'	652	198	240	123	14	-16
B18	23° 9.670'	90° 14.365'	3220	123	210	222	181	18
B19a	23° 7.542'	90° 15.291'	766	240	150	360	91	116
B20	23° 7.574'	90° 16.189'	656	360	170	219	147	76
B21	23° 6.649'	90° 19.871'	1298	311	180	270	54	268
B22	23° 5.029'	90° 19.005'	632	300	120	144	52	0
B23	23° 4.684'	90° 18.453'	705	144	240	242	260	224
B24	23° 3.169'	90° 17.948'	891	242	270	152	33	66
B25	23° 7.505'	90° 14.177'	1106	276	150	150	16	4
B26	23° 2.420'	90° 17.703'	982	240	206	240	85	-196
B27	23° 2.849'	90° 18.322'	627	240	240	201	117	71
B28	23° 1.965'	90° 19.811'	684	389	180	210	201	75
B29	22° 59.574'	90° 18.570'	511	270	180	242	111	126
B30	22° 59.564'	90° 19.570'	1161	242	330	296	9	-38

Table A7: River width in different years and sections, measured at 1.5 km intervals.

River Reach	Section (BWDB)	1972	1980	1988	1999	2007	2017	2021	Average
R1	AKU1+AKU2	242	233	354	250	210	156	169	231
	AKU3	233	245	305	250	207	153	148	220
	AKU4	235	260	290	289	284	159	220	248
	AKU5+AKU6	198	212	319	333	255	185	233	248
Average		227	238	317	281	239	163	193	237
R2	AKU7 +AKU8	249	245	278	349	288	193	179	254
	AKU9+AKU10	371	320	319	306	229	200	200	278
	AKU11+AKU12	384	295	386	307	253	241	232	300
Average		335	287	328	321	257	211	204	277
R3	AK7	330	304	444	314	263	231	254	306
	AK8	404	334	367	290	314	250	258	317
	AK9	424	380	392	301	259	232	260	321
	AK10	430	383	367	320	320	263	260	335
	AK11	391	320	372	368	286	260	246	320
Average		324	294	349	306	264	210	222	320

Table A8: River length (Lr), valley length (Lv) in meter and sinuosity (SI) of the three reaches R1, R2, R3 and the entire river for different years.

Year	R1			R2			R3			Total River		
	Lr	Lv	SI	Lr	Lv	SI	Lr	Lv	SI	Lr	Lv	SI
1972	47.64	20.77	2.29	36.22	25.14	1.44	25.15	16.32	1.54	109.01	62.23	1.87
1980	38.19	24.63	1.55	36.95	25.21	1.47	25.58	15.94	1.60	100.72	65.78	1.62
1988	40.25	25.97	1.55	39.30	25.31	1.55	26.35	14.03	1.88	105.90	65.31	1.67
1999	33.87	22.04	1.54	41.77	25.40	1.64	29.69	13.74	2.16	105.33	61.18	1.79
2007	38.00	27.77	1.37	39.51	26.37	1.50	31.04	13.65	2.27	108.55	67.79	1.72
2017	37.23	23.10	1.61	40.28	26.62	1.51	33.21	13.52	2.46	110.72	63.24	1.88
2021	39.22	22.62	1.73	40.98	26.80	1.53	34.40	13.56	2.54	114.60	62.98	1.95
Average SI			1.60			1.54			2.11			1.78

Table A9: Water depth in meter of the river in different years and sections.

Section	1973	1981	1988	1996	1999	2005	2009	2019	Avg. D
AKU1	-	Dry channel	-	3.96	0.93	Dry channel	2.64	2.09	2.41
AKU2	-	0.84	3.43	2.96	2.18	3.5	1.67	4.28	2.69
AKU3	4.45	1.22	4.29	3.01	4.25	0.81	1.01	1.28	2.54
AKU4	1.13	1.47	3.64	4.11	3.71	3.03	2.54	1.33	2.62
AKU5	2.17	1.41	2.41	3.38	3.44	3.14	2.31	2.6	2.61
AKU6	1.66	3.53	2.75	3.96	4.69	2.94	3.03	2.37	3.12
AKU7	3.57	1.97	3.51	6.1	4.1	2.96	7.27	3.1	4.07
AKU8	1.55	1.16	3.12	4.03	3.42	3.5	4.51	3	3.04
AKU9	2.18	0.95	1.37	4.97	2.34	3.59	4.58	2.7	2.84
AKU10	1.08	2.44	2.61	4.19	3.33	4.2	3.8	2.26	2.99
AKU11	1.24	4.24	2.05	3.62	4.9	4.36	3	5.27	3.59
AKU12	1.38	1.5	1.41	3.24	2.9	3.1	5.44	5.33	3.04
AK8	-	-	-	-	-	-	-	5.1	5.10
AK9	-	-	-	-	-	-	-	3.78	3.78
AK10	-	-	-	-	-	-	-	7.27	7.27
AK11	-	-	-	-	-	-	-	7.92	7.92
AK12	-	-	-	-	-	-	-	5.03	5.03
Avg. D	2.04	1.88	2.78	3.96	3.35	3.19	3.48	2.44	3.50

Table A10: Average water depth, width, and aspect ratio of different sections. Here widths are collected by image processing of different years.

Reach	Section	Column1	Avg. W (m)	Avg. D (m)	Average W/D
R1	AKU1+AKU2		230.57	2.55	90.42
	AKU3		220.14	2.54	86.67
	AKU4		248.14	2.62	94.71
	AKU5+AKU6		247.86	2.86	86.66
Average			236.68	2.64	89.62
R2	AKU7 +AKU8		254.43	3.55	71.59
	AKU9+AKU10		277.86	2.91	95.42
	AKU11+ AKU12		299.71	3.31	90.52
Average			277.33	3.26	85.84
R3	AK7		305.71	3.22	94.94
	AK8		316.71	5.10	62.10
	AK9		321.14	3.78	84.96
	AK10		334.71	7.27	46.04
	AK11		320.43	7.92	40.46
Average			319.74	5.46	65.70

Table A11: Average water width depth, and aspect ratio of the river in different years. Both width and depth are field measured data of BWDB.

Parameter	1973	1981	1988	1996	1999	2005	2009	2019	Average
W	240.34	290.57	270.96	290.42	403.10	296.14	308.17	206.94	288.33
D	2.04	1.88	2.78	3.96	3.35	3.19	3.48	2.44	2.87
W/D	117.75	154.19	97.44	73.32	120.36	92.73	88.47	84.96	100.64

APPENDIX B
DEVELOPMENT OF RATING CURVE

Rating Curve:

Water level and discharge data of five months (June-October) of the year of 2010 is used here. The general equation for rating curve relating to Q and WL is as follows:

$$Q = C_r(G - a)^\beta$$

$$C_r = \log^{-1}\left(\frac{\sum Y - \beta \sum X}{N}\right)$$

$$\beta = (N \sum(XY) - \sum X \sum Y) / (N \sum X^2 - (\sum X)^2)$$

where, $X = \log(G - a)$, $Y = \log Q$. Q is estimated discharge (m^3/s) for the gauge reading G (m) of WL and “a” is the value of G (m) corresponding to $Q = 0$. G1, G2 and G3 values corresponding to Q1, Q2 and Q3 values are: 3.8, 4.75 and 5.95; selected such a way that $Q1/Q2 = Q2/Q3$ in the Figure B1. The “a” is calculated by following equation:

$$a = \frac{G1G3 - G2^2}{(G1 + G3) - 2G2}$$

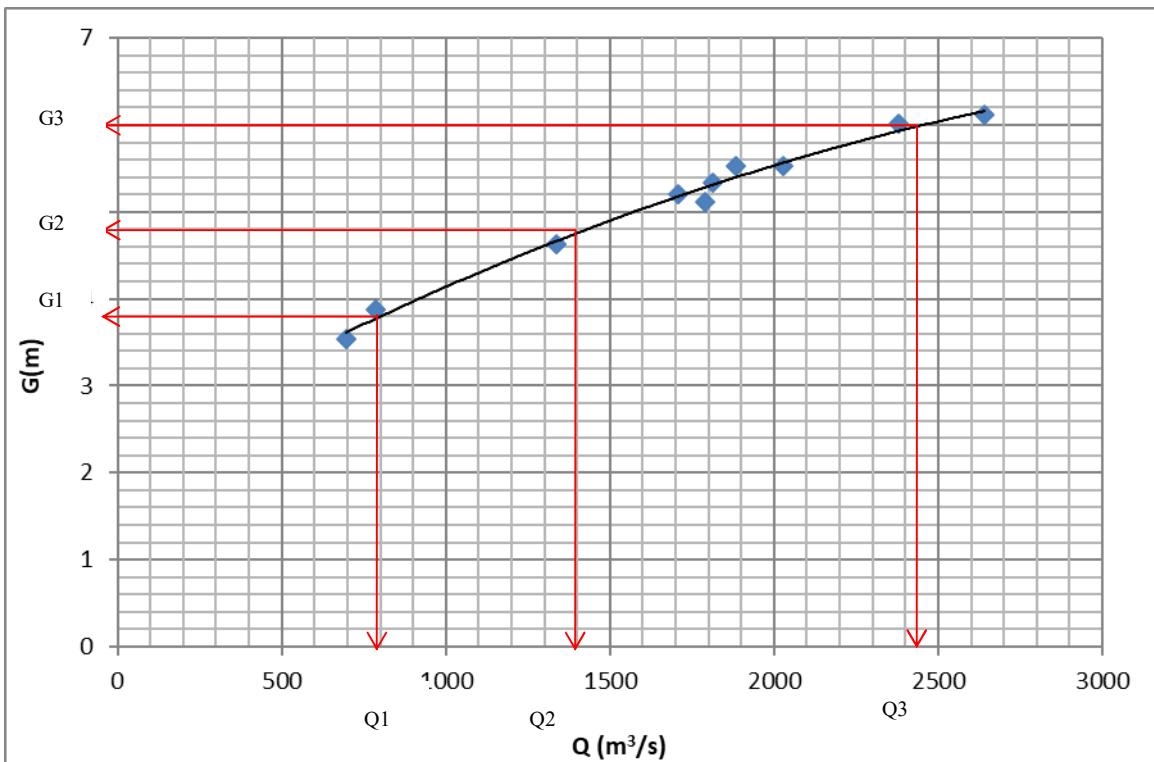


Figure B1: G1, G2 and G3 points from the relationship of Q and WL of gauge reading.

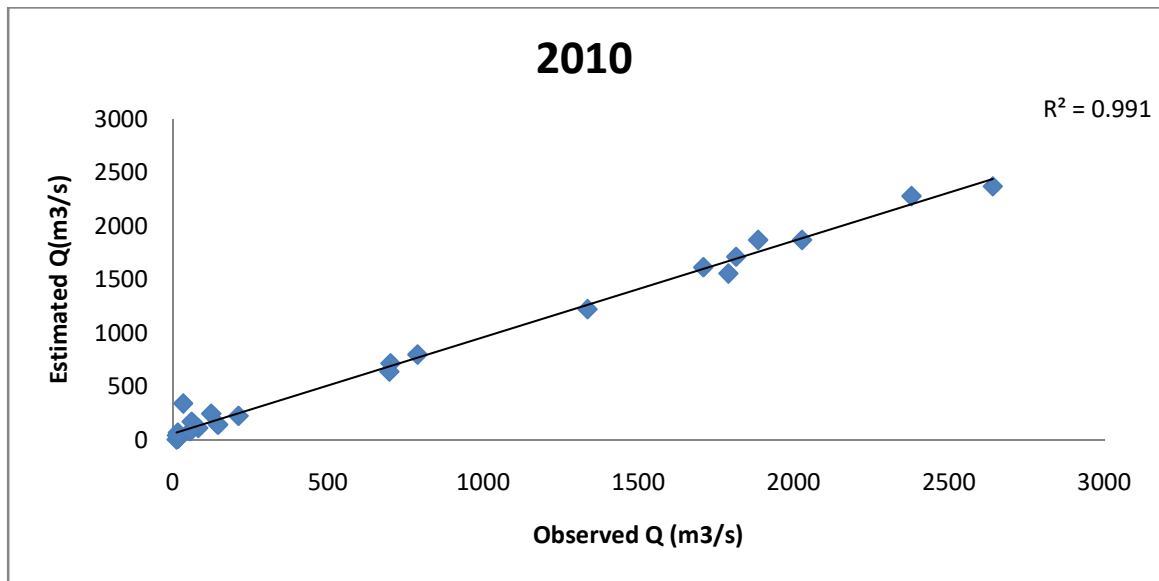


Figure B2: Relationship between estimated and observed Q for the year of 2010.

The discharge for a certain water level G:

$$Q = 39.72(G - 0.50)^{2.34}$$

Table B1: Mean G, (G-a) and corresponding Q for 22 days of January 2010.

Date	G(mean) (m)	G-a (m)	Q (m3/s)	Date	G(mean) (m)	G-a (m)	Q (m3/s)
01-01-10	0.78	0.59	11.55	11-01-10	0.63	0.44	5.66
02-01-10	0.84	0.65	14.49	12-01-10	0.58	0.39	4.38
03-01-10	0.89	0.70	17.24	13-01-10	0.56	0.37	3.75
04-01-10	0.94	0.75	19.94	14-01-10	0.54	0.35	3.40
05-01-10	0.94	0.75	19.94	15-01-10	0.56	0.37	3.88
06-01-10	0.89	0.70	17.24	16-01-10	0.64	0.45	6.13
07-01-10	0.83	0.64	13.72	17-01-10	0.67	0.48	7.13
08-01-10	0.76	0.57	10.44	18-01-10	0.73	0.54	9.39
09-01-10	0.72	0.53	8.79	19-01-10	0.79	0.60	12.02
10-01-10	0.67	0.48	7.13	20-01-10	0.87	0.68	15.83

APPENDIX C
CALCULATION OF BEND MIGRATION

Migration Rate

$$\text{Migration rate (m/y), } M_r = \frac{\sqrt{Mt^2 + M_x^2}}{\text{no. of years (Y2-Y1)}}$$

where,

$$Mt = \sqrt{(x_2 - x_1)^2 + (y_2 - y_1)^2}$$

$$M_x = R_{C2} - R_{C1}$$

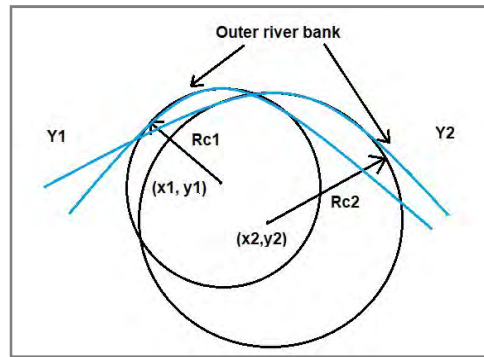


Figure C1: Migration of bend from initial year (Y1) to final year (Y2)

Here, $(x_1, y_1) = (100, 100)$ and $(x_2, y_2) = (150, 60)$; $Y_1 = 2007$ and $Y_2 = 2021$, $R_{C1} = 950$ m and $R_{C2} = 1050$ m.

$$Mt = \sqrt{(150 - 100)^2 + (60 - 100)^2} = 64 \text{ m}$$

$$M_x = 1050 - 950$$
$$M_r = \frac{\sqrt{64^2 + 100^2}}{14 (Y_2 - Y_1)} = 8.48 \text{ m/y}$$

APPENDIX D
PHOTOS OF FIELD VISIT AND SOME RELATED FEATURES



Photo D1: Photo showing location detection by using GPS along the outer bank of the river bend B3.



Photo D2: Photo showing insignificant bank erosion at the location of far upstream of the bend apex of the bend B3.



Photo D3: Photo showing the upstream of the bend apex where deposition has taken place at B3 bend.



Photo D4: Photo showing long and extended mid-channel bar at upper reach near the bend B3.



Photo D5: View of river navigation improvement by dredging project at the upper reach of the Arial Khan River.



Photo D6: Photo represents the oxbow lake (Chanda khal, N=23°22.967', E =90°04.692') at the floodplain of the upper reach.

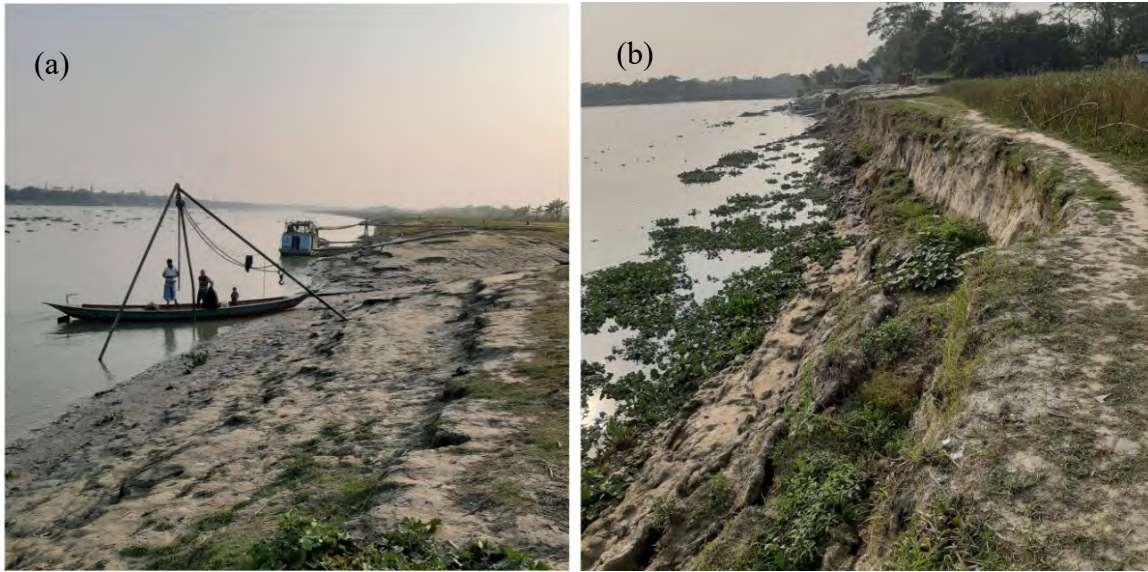


Photo D7: Views of erosion condition of the bend B17 at Bahir Char Katla, Madaripur Sadar, Madaripur. Left photo - insignificant erosion at upstream of apex, right Photo - massive erosion at downstream of bend apex.



Photo D8: Photo showing the measurement of the height of cut-bank near downstream of bend apex, Bahir Char Katla (N=23°12.055', E =90°14.571') of bend B17.



Photo D9: View of the Madaripur town protection work.



Photo D10: Photo showing ineffective temporary river protection- unplanned dumping of geobag at erosion prone bank.



Photo D11: View of the confluence point of the Arial Khan and Lower Kumar River.



Photo D12: Photos represent the inspection of unprotected and protected banks of bend B22 at Khasherhat Bazar at Kalkini Upazila, Madaripur. Left photo - erosion by mass failure, right photo-Khasherhat Bondor protection project.



Photo D13: View showing massive erosion adjacent to the brick-soling road at the bend 22.



Photo D14: Photo showing the height of cut-bank of bend B22 at Kanurgau village near Khasherhat bazaar, Kalkini Upazila (N=23°06.006', E =90°20.045')